University of Technology, Sydney

Developing a Migraine Attack Prediction System using Resting-state EEG

Zehong Cao

A Thesis Submitted for the Degree of

Doctor of Philosophy

Faculty of Engineering and Information Technology

University of Technology, Sydney

November 2017

Copyright © 2017 by Zehong Cao. All Rights Reserved.

Certificate of Authorship/ Originality

This thesis is the result of a research candidature conducted jointly with another university as part of a collaborative doctoral degree. I certify that the work in this thesis has not previously been submitted for a degree nor has it been submitted as part of requirements for a degree except as part of the collaborative doctoral degree and/or fully acknowledged within the text.

I also certify that the thesis has been written by me. Any help that I have received in my research work and the preparation of the thesis itself has been acknowledged. In addition, I certify that all information sources and literatures used are indicated in the thesis.

Signature of Candidate

Production Note:
Signature removed prior to publication.

Acknowledgements

First and foremost, I would like to express sincere gratitude to my supervisor, Prof. *Chin-Teng Lin*, who not only offered me a unique opportunity to study in UTS, but also provided tremendous guidance and supported for my research and life in my joint Ph.D. program. His enthusiasm for research and the excellent examples provided as a successful researcher were so motivational, has become my life treasure. I also would like to thank Dr. *Michael Chuang* for his academically and emotionally support through the road to finish my Ph.D. degree. Their respectful personality and precise academic attitude have benefited me so much. I really appreciate all the kind help from them.

My experience at the Computational Intelligence and Brain Computer Interface (CI-BCI) Lab in the Centre for Artificial Intelligence (CAI), has been more than amazing. The great lab members of mine have contributed immensely to my professional and personal time at UTS. I would like to thank all the friends that provide me with kind support during my PhD study. Addition to this, as a joint-degree Ph.D. student, I would like to express my warm thanks to all of members in Brain Research Centre, National Chiao Tung University (NCTU), Taiwan. I also would like to express my earnest thanks to Dr./ Prof. *Shuu-Jiun Wang*, who gave me an enormous amount of help and support since the year 2014. Thanks for all their support and help.

I gratefully acknowledge the funding sources that made my research possible. Special thanks go to UTS president plus joint-degree Scholarship cover my tuition fee and living cost in Sydney. Furthermore, thanks to CAI Travel Fund and FEIT Travel Fund for providing me with financial support for international conferences travelling. I also would like to express my sincerely thanks to proofreading editors for helping me to correct English presentation problems in my publications.

Last but not least, I would like to thank my family members for their continuous support during my Ph.D. study. I have amazing parents, who have provided me with unconditional support and encouragement all these years. I am also grateful to thank my wife - Jiaying Chen. Your patience, care and love encourage me to finish Ph.D. study. My family is the energy source and harbour of my heart. I love both of you, Mom and Dad, and Jiaying.

Zehong Cao

July 2017 at Sydney

Abstract

Migraine is a common episodic neurological disorder with complex pathophysiology that is characterised by recurrent headaches during a set period, such as one month. A small group of migraine patients (13-31%) experience transient neurological symptoms (most frequently visual aura) prior to headache onset, while the majority of patients do not possess any premonitory symptoms. This study explored neurophysiological evidence of the resting-state electroencephalogram (EEG) power, coherence and entropy to support the cortical signals that relate to different migraine phases, and then used this to develop an EEG-based system for predicting migraine attacks. First, we investigated EEG devices, pre-processing and artefact removal methods, and feature extraction technologies, including power, coherence and entropy analysis. Next, we discovered the cyclic EEG dynamics of migraine on a cross-sectional basis. The results indicated that EEG power spectral and coherence were significantly increased in the pre-ictal group, relative to EEG data obtained from the inter-ictal group. Inter-ictal patients had decreased EEG power and connectivity relative to healthy controls, which were "normalised" in the pre-ictal patients. Furthermore, using longitudinal design, we utilised a wearable EEG device to estimate brain dynamics before migraine attacks. The results showed the EEG entropy of individual patients in the pre-ictal phase, resembling normal control subjects, was significantly higher than that in their inter-ictal phase in prefrontal area. That is, the entropy measures identified enhancement or "normalisation" of frontal EEG complexity in pre-ictal phase. Finally, based on these neuroscience discovery of inter- and pre-ictal EEG entropy in individuals, this study proposed a support vector machine (SVM) based system with 76% accuracy to predict migraine attacks. The prediction system characterised the EEG entropy of a single (prefrontal) area and favoured the application of brain-computer interface in migraine.

Table of Contents

Certificate of authorship/originality..... i
Acknowledgements……..... ii
Abstract..... iii
Table of Contents..... iv
List of Tables..... vii
List of Figures..... viii

Chapter 1 INTRODUCTION..... 9
1.1 Motivation..... 9
1.2 Background 10
1.3 Statement of the Problem..... 12
1.3.1 Resting-state EEG methodology remains challenging……..... 12
1.3.2 Migraine phases correlate of EEG signatures remain unknown... 13
1.3.3 Migraine attack prediction remains unseen..... 13
1.4 Research Significance…… 15
1.5 Hypotheses of the Study..... 15
1.6 Aims of the Study..... 16
1.7 Organization of the Thesis..... 17

Chapter 2 LITERATURE REVIEW..... 19
2.1 Migraine Headache……..……..…..... 19
2.2 EEG Methodology……..……..... 20
2.3 EEG Dynamics relates to Migraine……..... 23

Chapter 3 METHODOLOGY IN RESTING-STATE EEG ANALYSIS..... 25
3.1 EEG Devices……..... 25
3.2 EEG Pre-processing ……..……..... 26
3.2.1 Artefact handling and filtering……..……..... 27
3.2.2 Choices of frequency bands……..……..... 29
3.3 EEG Feature Extraction……..……..... 30

3.3.1 Power measures..... 30
3.3.2 Coherence measures..... 30
3.3.3 Entropy measures..... 32
3.4 Conclusion……..... 47

Chapter 4 EEG POWER, COHERENCE, AND ENTROPY CHANGES IN MIGRAINE……..... 48
4.1 Experimental Materials..... 48
4.1.1 Subjects……..……..... 49
4.1.2 Experimental design…….....……..... 50
4.2 Data Analysis……..... 51
4.2.1 EEG processing and measurements..... 51
4.2.2 Statistical analysis..... 53
4.3 Results..... 54
4.3.1 Demographic and clinical characteristics..... 54
4.3.2 Comparisons of resting-state EEG dynamics between migraine patients and healthy controls..... 55
4.3.3 Comparisons of resting-state EEG dynamics across migraine phases..... 60
4.4 Discussion..... 59
4.4.1 Abnormal resting-state EEG activity in migraine..... 64
4.4.2 Strength and weakness of EEG coherence..... 67
4.4.3 Limitations..... 67
4.5 Conclusion..... 69

Chapter 5. EEG-BASED MIGRAINE ATTACKS PREDICTION…… 70
5.1 Experimental Materials..... 70
5.1.1 Participants..... 71
5.1.2 Experimental paradigm..... 72
5.2 Data Analysis..... 73
5.2.1 EEG processing and measurements..... 75
5.2.2 Individualized prediction models..... 76
5.2.3 Statistical analysis..... 87
5.3 Results..... 87

5.3.1 Demographic and clinical characteristics..... 87
5.3.2 Comparisons of EEG dynamics between healthy controls and inter-ictal or pre-ictal patients……...……..… 90
5.3.3 Comparisons of EEG dynamics between inter-ictal and pre-ictal phases..... 92
5.3.4 Performance of the EEG prediction model..... 95
5.4 Discussion..... 96
5.4.1 Prefrontal EEG complexity in migraine patients..... 96
5.4.2 EEG complexity normalization in pre-ictal phase..... 97
5.4.3 EEG-based migraine phase classification..... 97
5.4.4 Results of 48-hour and 36-hour criteria..... 99
5.4.5 Limitations..... 100
5.5 Conclusion..... 101

Chapter 6 SUMMARY AND FUTURE WORKS..... 102
6.1 Summary..... 102
6.2 Future works..... 104

References..... 106
Appendix..... 123
Publication..... 132

List of Tables

Table 3-1. Comparisons of EEG devices……..... 21
Table 3-2. Overview of different EEG coherence measures..... 26

Table 4-1. Comparisons of demographics, headache profiles, and psychological characteristics……..... 49

Table 5-1. The statistics of EEG examinations..... 83
Table 5-2. Demographics, headache profile and psychological characteristics……..... 84
Table 5-3. The performance of various predictors..... 90

List of Figures

Figure 1-1. Migraine cycle…… 17

Figure 3-1. EEG preprocessing produce to remove eyes contaminations…… 31
Figure 3-2. Flowchart of the Inherent Fuzzy Entropy algorithm……..... 35
Figure 3-3. EMD processing and reconstruction of EEG signals..... 37
Figure 3-4. The analytical procedures: EEG recording, EEG processing and entropy evaluation..... 41
Figure 3-5. The EEG dynamic complexity by ApEn, SampEn, FuzzyEn and Inherent FuzzyEn evaluations..... 44
Figure 3-6. Complexity evaluation using RMSD in EO and EC conditions..… 45

Figure 4-1. Analytical procedures..... 51
Figure 4-2. EEG power differences between migraine patients in different migraine phases and HCs..... 56
Figure 4-3. EEG coherence differences between migraine patients in different migraine phases and HCs..... 59
Figure 4-4. EEG entropy differences between patients in different migraine phases and HCs, as well as between migraine patients in each of the four phases of the migraine cycle..... 59
Figure 4-5. EEG power differences between migraine patients in each of the four phases of the migraine cycle..... 61
Figure 4-6. EEG coherence differences between migraine patients in each of the four phases of the migraine cycle..... 63

Figure 5-1. Experimental procedures……..……..... 72
Figure 5-2. Data analysis……..……..……..... 74
Figure 5-3. LDA projection……..……..……..... 78
Figure 5-4. KNN algorithm……..……..……..... 81
Figure 5-5. A multilayer perception ……..……..……..……..... 83
Figure 5-6. Hyper-plane and two classes of data……..……..... 86
Figure 5-7. Comparisons of prefrontal EEG entropy for inter-ictal or pre-ictal phase vs. controls ……..……..... 91
Figure 5-8. Comparisons of prefrontal EEG entropy for inter-ictal vs. pre-ictal phases..... 93

Chapter 1 INTRODUCTION

1.1 Motivation

Migraine is a common and potentially disabling neurological disorder that affects about 11% of people worldwide [1], including 11.5% [2] and 9.1% [3] in Australia and Taiwan, respectively. A minority of migraine patients (13-31%) experience aura symptoms prior to headache onset [4, 5], however the majority of migraine patients have migraine without aura (MO). Taking abortive medications during the early stages of a migraine attack increases medication efficacy and reduces recurrence [6]. However, MO patients do not exhibit prodromal symptoms with aura [4], so their migraine attacks are generally unpredictable [7].

Migraine refers to a cyclic disorder with an inclusion of four phases (inter-ictal, pre-ictal, ictal, and post-ictal), so the cyclic neurophysiological patterns of migraine can be discovered by neuroimaging methodology [8]. It is generally believed that the mechanisms of the primary brain dysfunctions leading to the onset of a migraine attack may depend on the activation and sensitisation of the trigeminovascular pain pathway [9, 10]. If dysfunction of neural dynamics plays an important role in the pathophysiology of migraine, effective ways of evaluating the change of neurophysiologic signals are crucial to study the transition. Therefore, pre-emptive identification of pre-attack migraine signatures might contribute to develop a headache prediction system for migraine patients.

1.2 Background

Migraine is a disabling disorder, characterized by recurrent headaches, particularly prevalent in developed countries [11]. When the headache attacks, patients have difficulty in maintaining concentration, attention and daily activities, resulting in considerable economic losses. Most EEG studies of migraine describe functional changes during attacks, including hyperresponsivity to repeated sensory stimuli with abnormal temporal processing, the malfunctioning sequential recruitment of neuronal networks, and impaired habituation.

In recent years, there has been growing interest in characterising the neurophysiology of the brain "at rest". This so-called resting-state paradigm is thought to reflect the default activity of the brain [12], which may reveal valuable information about issues from brain cortical activities to hypothalamus functions. This paradigm has been linked to fluctuations in neural activity in cognitive neuroscience and diseases. In migraine, resting-state experiments, in which additional cortical activations are not induced, are more convenient and comfortable for patients than stimulation-related tasks. Acquisition of physiological signals in resting-state conditions is a relatively novel tool which explores brain dynamics, such as functional links in brain regions. The use of this technique has allowed the identification, at rest, of the main brain functional networks without requiring subjects to perform specific active tasks.

Non-invasive neurophysiological methods are well suited to study the pathophysiology of migraine. Currently, there exist several neuroimaging technologies to

explore brain function, including magnetoencephalography (MEG), electroencephalography (EEG), near-infrared spectroscopy (NIRS), functional magnetic resonance imaging (fMRI), and positron emission tomography (PET). EEG is an electrophysiological monitoring method used to record the electrical activity of the brain, and possesses the advantages of high temporal resolution, good mobility and low cost [13]. EEG is typically noninvasive and involves electrodes placed along the scalp that measures voltage fluctuations resulting from ionic currents within the neurones of the brain [14]. In a clinical context, EEG refers to the recording of the brain's spontaneous electrical activity over a period of time [14], as logged by multiple electrodes placed on the scalp.

The abnormal functioning of the migrainous brain between, before and during attacks, reflected by EEG patterns, facilitates the detection of imminent migraine headaches hours in advance and helps in monitoring the effects of therapeutic interventions. An effective treatment for migraine attacks is to take preventive medications. The severity of headaches can be significantly reduced and their duration shortened by the use of preventive medications before attacks. Therefore, investigating the fundamental patterns that can be used to distinguish the EEG activity of the inter-ictal phase from that of the pre-ictal phase is critical.

1.3 Statement of the Problem

1.3.1 Resting-state EEG methodology remains challenging

Commonly, subjects are asked to open and close the eyes alternately during a resting state experiment. Even when the same guidelines were given to subjects, the individual differences still were presented on account of the subjective experience. Also, brain dynamics were influenced by the cognitive state before the EEG recording. Interestingly, a prior study described the heterogeneous experience of subjects in the resting-state condition [15], indicating the brain "at rest" may not look as simple as it seems. Previous migraine studies were conducted with visual stimulus designs, which showed the hyper- or hypo-excitability in migraine patients [16], such as lack of habituation in the inter-ictal phase [17] and normalisation in the pre-ictal phase (Sand and Vingen, 2000) in the occipital area. To reduce the induced cortical abnormal activation in migraine, a better approach is to explore EEG dynamics in the resting-state condition.

On the other hand, our review of EEG power and coherence analysis methods can be considered a reflection of the current state of the field, as a few methodological studies have systematically addressed resting-state EEG research. Moreover, there has been little research linked to EEG complexity; therefore, our study aimed to improve the assessment of brain complexity associated with entropy methodological issues [18].

1.3.2 Migraine phases correlate of EEG signatures remain unknown

Resting-state cortical activities, such as EEG power density, coherence, and entropy, have not been the focus of substantial research in relation to specific migraine phases. To our knowledge, only two studies have analysed the period before and/or after the attack specifically with resting-state EEG power. Only one of these studies compared both the pre- and post-ictal intervals with an inter-ictal interval, and both studies used relatively wide intervals in the definition of the pre (post)-ictal phase. Furthermore, few studies have investigated EEG connectivity or complexity for migraine patients, so our resting-state study can provide evidence for the possible application of coherence and entropy analysis methods in understanding both brain connectivity and complexity in migraine.

1.3.3 Migraine attack prediction remains unseen

As shown in Fig. 1-1, migraine cycle is classified into four potential phases: pre-ictal (the period of 36-72 hours before a headache attack), ictal (headache attack), post-ictal (the period of 36-72 hours after a headache attack), and inter-ictal (the period between the post-ictal phase and the pre-ictal phase). To avoid the headache attack, predicting the changed EEG dynamics from the inter-ictal phase to the pre-ictal phase is desirable.

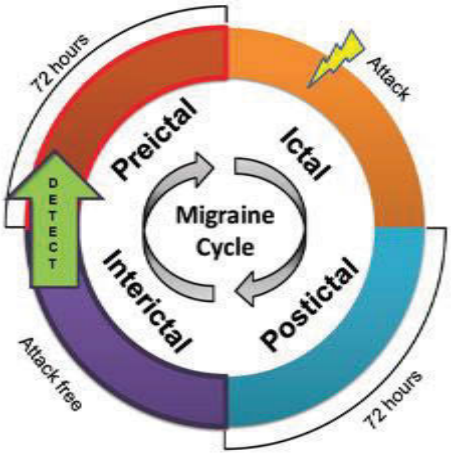

Fig. 1-1 Migraine cycle.

Prior studies have investigated cyclic EEG patterns in the cross-sectional study, but have not yet replicated this on the individual basis. To develop a prediction system, EEGs of individual migraine patients should be recorded in multiple examinations, to investigate personalised EEG patterns of different migraine phases. If the migraine pre-attack signatures have been identified on an individual basis, it is feasible to build an EEG-based system to predict migraine attacks. Using a wireless and wearable EEG device could feasibly support at-home healthcare through monitoring EEG patterns of migraine.

1.4 Research Significance

This research addresses the important issues of cutting-edge EEG processing technology, significant EEG-based signatures in different migraine phases, and solves the challenges of predicting migraine attacks in individuals. The specific significance describes as follows:

Significance 1: This study provides wireless EEG devices, and extracts reliable EEG features by advanced EEG analysis methods (Question1).

Significance 2: This study reveals dynamic resting-state EEG changes (e.g. power spectral, connectivity and complexity) across different migraine phases, providing an opportunity to predict migraine attacks in a generalized or personalised group (Question 2).

Significance 3: This study develops a wireless EEG-based migraine detection system by training discriminative EEG-based signatures (Question 3).

1.5 Hypothesis of the Study

Migraine attacks have been hypothesized to start at the cortical level [19-21], so EEG device is a reliable tool to acquire cortical signals. Previously, the synchronization levels of cortical activity during visual stimulation in migraine patients have been shown to differ from those in healthy controls [22, 23]. Some prior resting-state EEG studies demonstrated cortical activity differences between adjacent migraine phases in resting-station conditions [24, 25].

Thus, we hypothesise that cortical abnormalities during a resting state as detected by EEG power spectra and coherence analyses.

In terms of characterizing complex temporal dynamics, entropy approaches have revealed novel insights into a wide range of physiological systems [26]. Generally, entropy is an objective measure of the complexity of physiological signals, and represents the robustness of the system involved. Diseased systems usually show reduced entropy values compared to those of healthy systems, such as decreased entropy of heart rate variability in patients with heart failure [27], and decreased EEG entropy in patients with dementia [28]. Thus, we hypothesise that the EEG complexity in migraine is lower than that in healthy controls.

1.6 Aims of the Study

Migraine refers to a cyclic disorder with an inclusion of four phases (inter-ictal, pre-ictal, ictal, and post-ictal), but few state-of-the-art analysis approaches have been applied to explore the cyclic resting-state EEG patterns in migraine. In this thesis, the analysis methods (power, coherence and entropy) are presented with the aim of highlighting the challenges and opportunities that are encountered when performing in resting-state EEG research. Then, the resting-state EEG power, coherence and entropy changes that correlate with different migraine phases are examined in a cross-sectional and controlled study. Finally, the identified EEG

signatures on an individual basis contribute to developing an EEG-based system for predicting migraine attacks.

More specifically, the thesis would thoroughly elucidate how the transition of migraine phases affects EEG dynamics in the resting-state condition. At the beginning, the aim is to review power, coherence and entropy analysis methods that can be considered as a reflection of the current resting-state EEG research, as well as to explore a modified entropy approach to performing EEG complexity with excellent reliability. Then, EEGs will be collected on four subgroups of migraine patients with a cross-sectional design. The aim is to assess the EEG dynamics in each group by power, coherence, and entropy analysis, as well as the possible diversity relative to healthy controls. Furthermore, multiple EEG examinations will be collected on the basis of individual migraine patients. By measuring the distinguished pre-attack EEG signatures in individuals, it is feasible to develop a personalised EEG-based prediction system for migraine patients.

1.7 Organisation of the Thesis

The thesis is organised into distinct sections as described here. In Chapter 2, methodological opportunities and challenges were reviewed in resting-state EEG research, including power spectral, coherence and entropy analysis methods. In particular, a modified entropy algorithm was proposed to improve the reliability of complexity in realistic EEG

application. In Chapter 3, one cross-sectional study investigated resting-state EEG power, coherence and entropy variations between migraine phases. In Chapter 4, another longitudinal study of individuals was conducted to estimate personalised EEG dynamics that can contribute to developing an EEG-based migraine prediction system. Finally, a summary, limitations of this study and future works were described in Chapter 5.

Chapter 2 LITERATURE REVIEW

2.1 Migraine Headache

Migraine is a leading cause of disability worldwide, with a prevalence of 10–15% (1). In a subset of patients with migraine, episodic migraine (EM) is characterized by those with migraine who have 1-15 headache days per month, while chronic migraine (CM) is characterized by over 15 headache days per month. Specifically, revised International Classification of Headache Disorders (ICHD-2) criteria define CM as headache on 15 or more days per month for 3 or more months, of which 8 or more days meet criteria for migraine without aura and/or respond to migraine-specific treatment, occurring in a patient with a lifetime history of at least five prior migraine attacks not attributed to another causative disorder and no medication overuse [29].

Migraines are believed to be due to a mixture of environmental and genetic factors [30]. About two-thirds of cases run in families. Changing hormone levels may also play a role, as migraines affect slightly more boys than girls before puberty and two to three times more women than men. The risk of migraines usually decreases during pregnancy. The underlying mechanisms are not fully known. It is, however, believed to involve the nerves and blood vessels of the brain. Initial recommended treatment is with simple pain medication such as ibuprofen and paracetamol (acetaminophen) for the headache, medication for the nausea, and the avoidance of triggers [31]. Specific medications such as triptans or ergotamines may be

used in those for whom simple pain medications are not effective. A number of medications are useful to prevent attacks including metoprolol, valproate, and topiramate [32].

Because there are no biological markers for migraine, diagnosis is based on clinical history and the exclusion of other headache disorders. Health care professionals apply clinical criteria to guide diagnoses and subsequent treatment. The definition of migraine without aura from the second edition of the ICHD-2 requires all of the following symptoms: a) recurrent headaches (at least 5 lifetime attacks); b) untreated or unsuccessfully treated headache duration of 4 to 72 h; and c) at least two of the following pain characteristics: unilateral, pulsating, moderate or severe intensity, or aggravated by routine physical activity. In addition, the migraine attacks are associated with at least one of nausea/ vomiting, photophobia, or phonophobia. Finally, other causes of headache must be excluded.

2.2 EEG Methodology

In the last decade, the number of different neuroimaging analysis approaches has been expanded, corresponding with rising interest in neuroscience and clinical studies. For instance, EEG power and EEG coherence studies have gained considerable interest, resulting in yearly increases in the number of published studies [24, 25, 33]. These studies have provided valuable information on the deviant organisation in the diseased brain and in the healthy brain related to topics such as migraine. In addition to power and coherence analyses in EEG research, entropy-

based algorithms underline brain complexity, which can help us better understand complex brain systems [34]. The concept of brain complexity has been applied in some clinical solutions [35], and has demonstrated potential for applications in migraine prediction.

Using power spectral analysis, prior migraine studies have shown abnormal cortical evoked potentials [16, 20] in different stimulus models of migraine, such as lacking habituation of visual and auditory cortex excitability [36] and reduced motor and visual cortical thresholds [37]. Specifically, compared to controls, migraine patients showed increased phase synchronisation after stimulation during the migraine-free inter-ictal phase (the period that exists between episodes of migraine) [22, 23]. Furthermore, in the pre-ictal phase (within 72 hours before a migraine attack), migraine patients exhibited normal habituation of visually-evoked and auditory-evoked potentials [38], but decreased motor cortex activity [39].

EEG coherence, which involves cross-correlation between signals in the frequency domain to reveal interrelationships of EEG signals, is a widely used measure of functional and effective connectivity [40]. High-level coherence between two EEG signals reflects synchronised neuronal oscillations, whereas low-level coherence suggests desynchronized neural activity. When performing an EEG coherence analysis [41], there are several assumptions and different choices of coherence methods that may influence the results. Of note, classical coherence analysis has disadvantages such as volume conduction and influences from common sources or indirect connections [41]. These problems are typical when bivariate

approaches are used instead of multivariate approaches. To solve these inherent problems, we have proposed a new connectivity measurement, such as isolated effective coherence (iCoh) [42], designed to render more accurate interactions among the cerebral regions. Although EEG coherence analysis has been applied to study migraine-related neural abnormalities in stimulation tasks [22, 23], resting-state EEG coherence in different phases of migraine has not yet been examined. The notion of EEG-detected connectivity is supported by resting-state functional MRI studies that show significant network changes in migraine [43, 44]. In addition, this study identified and investigated brain networks between migraine patients and healthy controls in flash stimulus tasks [22, 23].

While EEG usually exhibits complex fluctuations, uncertain disturbance and high levels of nonlinearity and nonstationarity, it also contains abundant dynamic information [45]. There has been a rapid development of entropy techniques, and these methods have been applied for measuring such dynamic complexity [18]. Entropy approaches characterising complex temporal dynamics have revealed novel insights into a wide range of physiological systems. The brain activities of neural networks can be represented as a nonlinear dynamic approach by multiple couplings and feedback loops within and across multiple neuronal populations [26]. The notion of complexity is not precisely delineated, yet time series of dynamic complexity have been investigated via several entropy measures, e.g., approximate entropy [46], sample entropy [27, 47] and fuzzy entropy [34]. Since entropy approaches to

characterising complex temporal dynamics have revealed novel insights into a wide range of physiological systems [26], the EEG entropy analysis method is therefore a feasible approach to estimate brain cortical complexity. There is a growing body of literature reporting entropy analyses with applications to disorders such as higher complexity in schizophrenia [26] and less complexity in Alzheimer's disease [28], but not in migraine patients.

2.3 EEG Dynamics relates to Migraine

Previous EEG studies have addressed the correlations between migraine attacks and EEG signals [48, 49]. Of particular interest is a study demonstrating the prefrontal dysfunction with ineffective inhibitory capability [50] and another showing reduced P3a amplitude [51] during a migraine head-free period. Moreover, the occipital region presents a hyperexcitability [16] or a lack of habituation [17] in migraine patients, and these states are generally associated with headache attacks. In the period before migraine attacks (within 36-72 hours), prior studies have indicated "normalisation" performance [38, 52-54], most abnormalities in CNV [55], changes in event-related P300 [56] and sleep quality [57], relative to healthy controls.

These findings support the theory of a fluctuating cortical dysfunction that may hit a significant degree within the few days before a migraine attack. It is thought that the cortical dysfunction might stem from the subcortical cholinergic dysregulation in the mesencephalic reticular substance and basal forebrain [58]. Thalamocortical dysfunction may also contribute

to the changed EEG dynamics in the pre-ictal phase [59]. Additionally, the abnormality of the trigeminovascular pain pathway following primary brain dysfunction leads to the onset of a migraine attack [9, 10]. Therefore, it should be of interest to examine the EEG dynamics in closer proximity to the migraine attacks.

Patients with MO develop episodes of unpredictable headache with relation to behavioural patterns [60]. Therefore, identifying EEG dynamics before a migraine attack is a critical point to detect the onset of a headache. By developing predictors through measuring the identified EEG dynamics and using machine-learning techniques, this study developed a migraine attack prediction system by monitoring EEG dynamics in the real world.

Chapter 3 METHODOLOGICAL CHALLENGES IN RESTING-STATE EEG RESEARCH

3.1 EEG Devices

In the thesis, three types of EEG devices were chosen for EEG recordings (Table 3-1). The Compumedical NeuroScan is a popular EEG recording product that uses Ag/AgCl electrodes attached to a 32-128 channel Quik-Cap. In our study, electrodes were arranged according to a modified International 10-20 system, and two reference electrodes were placed on both mastoid bones. The skin under the reference electrodes was abraded using Nuprep (Weaver and Co., USA) and was disinfected with a 70% isopropyl alcohol swab before calibration. The impedance of the electrodes was calibrated under 5 kΩ using an NaCl-based conductive gel (Quik-Gel, Neuromedical Supplies®). The EEG signals from the electro-cap were amplified using the Scan NuAmps Express system (Compumedics Ltd., VIC, Australia) and were recorded at a sampling rate of 500 Hz with 16-bit quantisation.

Table 3-1. Comparisons of EEG devices.

Name	NeuroScan	Nicolet EEG	MINDO
Exterior			
Company	Compumedics	Natus	Brain Rhythm Inc.
Nationality	US	US	Taiwan
Sensor	Wet sensor	Wet sensor	Dry sensor
Volume	Big	Big	Small
Channels	32-128	32-64	4-64
Transmission	Cable	Cable	Bluetooth
Saving	SD card	SD card	Cloud and SD card

The Nicolet EEG machine is a commercial product and is frequently used in clinical settings throughout the world. This machine provides various options for EEG amplifiers ranging from 32-channel to 64-channel. The amplifier thus allows one to flexibly apply additional channels other than the 10-20 system, such as EOG (electrooculogram), ECG (electrocardiogram), and EMG (electromyogram), during EEG recording. In our study, we applied the conventional 10-20 EEG system only (19 channel placement: Fp1, Fp2, F7, F3, Fz, F4, F8, T3, C3, Cz, C4, T4, T5, P3, Pz, P4, T6, O1, and O2), as in our routine clinical EEG examinations. We also followed the guidelines of the American Clinical Neurophysiology Society: A proposal for standard montages to be used in clinical EEG, in which montages are

designed based on 16, 18 or 20 channels. We used the 16-channel montage with Fz as the reference channel.

MINDO offers numerous advantages in terms of convenience and comfort for 4- to 64-channel EEG recordings (developed by Prof. Chin-Teng Lin in UTS & NCTU). First and foremost, the data quality is comparable to that obtained with wet-electrode systems but without the need for skin abrasion or preparation or the use of gels. Second, the headset is very easy to wear and remove, which even allows trained users to place it on themselves in very little time. Third, users invariably report that MINDO is very comfortable, and if they have had any wet electrode experience, they praise the lack of gels. Fourth, MINDO is wireless and thus allows recordings without being tethered to a computer, and subjects are able to move freely around the room/office. MINDO includes wearable, wireless dry electrodes that allow high-temporal-resolution EEG monitoring in realistic operational environments and electronics for biologically inspired information management.

3.2 EEG Pre-processing

3.2.1 Artefact handling and filtering

The resting-state experiment is greatly influenced when recording in an eyes-open or eyes-closed condition. Power spectral and connectivity measurements have revealed differences between eyes-open and eyes-closed [61]. Eyes blinks are more prevalent during

eyes open condition, whereas rolling of the eyes might influence the eyes closed condition. Also, both eyes-open and eyes-closed conditions are associated with eye movements. Eye movements that are located at frontal area can affect further EEG analysis. Furthermore, combined with the strong effect in the alpha frequency band when eye is closed, it provides a good guide for choosing resting-state epochs.

To minimise the influence of eye contaminations of EEG signals, visual inspection and Independent Component Analysis (ICA) detection of artefacts are often used to remove eye contaminations. In our study, the preprocessing produced in EEGLAB [62] is used to eliminate the noises contaminated by eye movements and blinks. As shown in the Fig. 3-1, firstly, we manually removed some apparent eye contaminations in EEG signals by visual inspection using "reject continuous data by eyes" function in EEGLAB (Fig. 3-1a). Secondly, we applied ICA to the EEG signals and rejected the components responsible for the eye movements and blinks (Fig. 3-1b). Then, we reconstructed the EEG signals without these components using the back-projection method (Fig. 3-1c). Finally, the reconstructed EEG signals were inspected again using the "Automatic Channel Rejection (ACR)" function with Kurtosis measurement and Z-score threshold of 5 in EEGLAB (Fig. 3-1d) to remove noisy channels. After the above three steps for artefact rejections, eye contaminations were largely removed in the EEG signals.

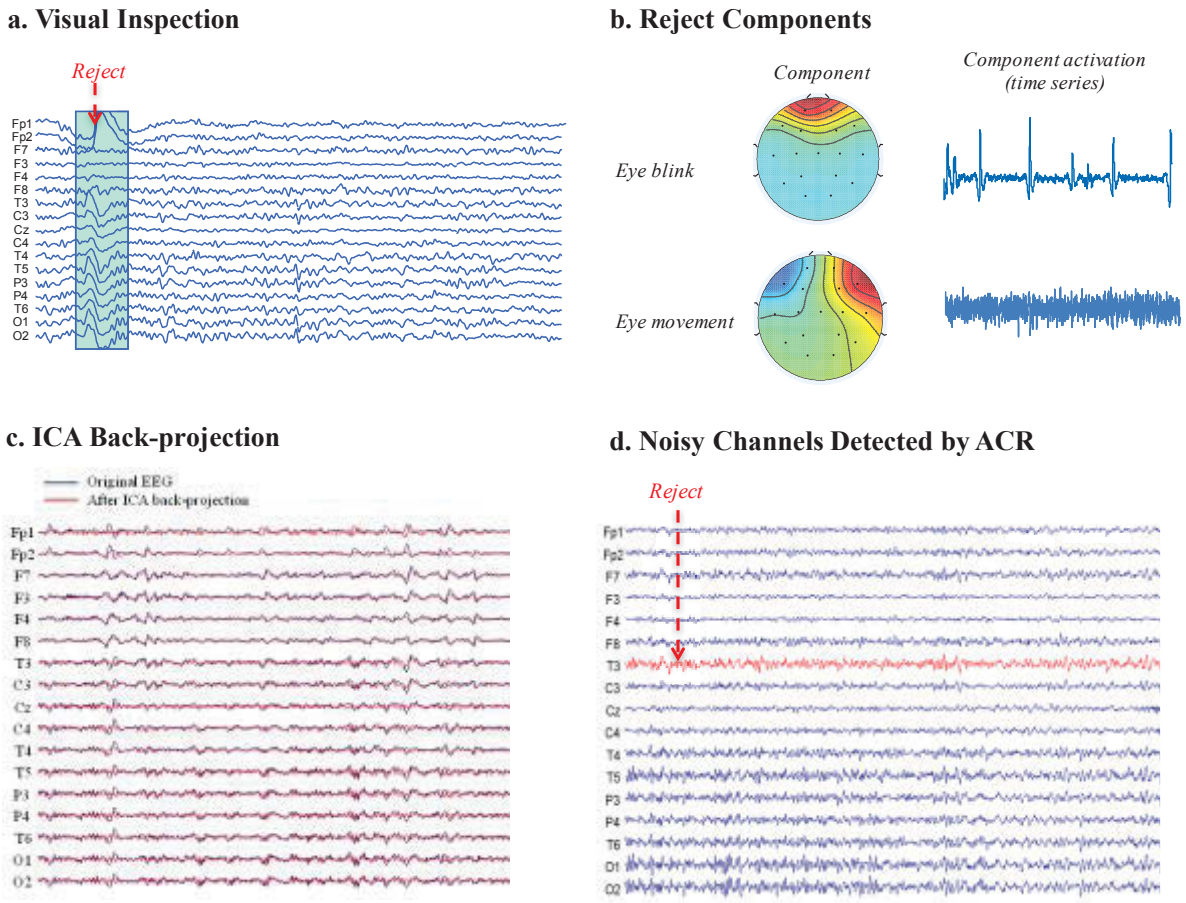

Figure 3-1. EEG preprocessing produce to remove eyes contaminations.

3.2.2 Choice of frequency bands

Before the selection of frequency bands, the raw EEG recordings were preprocessed using a digital band-pass filter (1-30 Hz) to remove line noise. In our study, delta (δ: 1–3.5 Hz), theta (θ: 4–7.5 Hz), alpha (α: 8–12.5 Hz), and beta (β: 13–30 Hz) bands were chosen after a Fast Fourier Transform (FFT).

3.3 EEG Feature Exaction

3.3.1 Power measures

To assess spectral amplitude perturbations in data recorded from single electrodes, the custom spectral decomposition techniques were employed in EEGLAB. Our primary measures were the baseline power spectrum measure: spectral perturbation measuring the changes in the power spectrum at a data channel. In specific, processed time-series data were transformed into the frequency domain by a n-point fast Fourier transform with Welch's method. Couples second spans of data were analysed with a m-point moving window with a k-point overlap. Windowed data were extended to m points by zero-padding to calculate power spectra, yielding an estimation of the power spectra from 1 to 30 Hz. Power spectra of these windows were averaged and converted to a logarithmic scale.

3.3.2 Coherence measures

In Table 3-2, we provided an overview of the currently most often used coherence measures, including their main advantages and disadvantages.

Table 3-2. Overview of different EEG coherence measures.

Connectivity Measure	Measured Property	Advantages	Disadvantages
Correlation [63]	The linear relation between the amplitude of two signals	Common; Straightforward method	No nonlinearity; No distinction between direct and indirect relations; Sensitive to volume conduction
Phase locking value [64]	Gives the modulus of the averaged instantaneous phase differences	Nonlinearity	No directionality of interaction; Included the size of the instantaneous phase difference; Sensitive to volume conduction
Granger causality [65]	The future of signal X can be predicted more precisely when the past of signal Y is included and vice versa	Estimates causal interaction; Directionality	No Nonlinearity; Actual causality influenced by many confounders volume conduction
Partial directed coherence [66]	Gives the causal relation between the outflow of node X towards node Y in the frequency domain based on Granger causality principle, normalised by all outflows from node X	Directionality of information flow; Insensitive to volume conduction	No nonlinearity; No distinction between direct and indirect relations; No conclusion about the strength of coupling
Generalised partial directed coherence [67]	Same as partial directed coherence	Directionality of information flow; Insensitive to volume conduction; Variance stabilisation	No nonlinearity; No distinction between direct and indirect relations; No conclusion about the strength of coupling
Isolated effective coherence [42]	Consists of estimating the partial coherence under a multivariate auto-regressive model, followed by setting all irrelevant associations to zero	Not affected by indirect relations; Insensitive to volume conduction	No nonlinearity; No conclusion about the strength of coupling

In the thesis, we explored the coupling between brain areas within particular frequency bands based on the up-to-date coherence algorithm, named isolated effective coherence (iCoh) [42], which is a multivariate approach to address the effective connectivity. Its advantages not only are insensitive to volume conduction but also can detect direct pathways linking brain regions. Firstly, the Source Information Flow Toolbox (SIFT) [68] in the EEGLAB was used to identify the optimal multivariate autoregressive model. Then, the magnitude of iCoh for channel $j \rightarrow$ channel i at the frequency of w is estimated from the following formula [42]

$$\boldsymbol{iCoh}_{j\rightarrow i}\,(w) = \frac{[\boldsymbol{S}_{\varepsilon}]_{\boldsymbol{ii}}^{-\mathbf{1}}|[\widehat{\boldsymbol{A}}(w)]_{\boldsymbol{ij}}|^{\mathbf{2}}}{[\boldsymbol{S}_{\varepsilon}]_{\boldsymbol{ii}}^{-\mathbf{1}}|[\widehat{\boldsymbol{A}}(w)]_{\boldsymbol{ij}}|^{\mathbf{2}}+[\boldsymbol{S}_{\varepsilon}]_{\boldsymbol{jj}}^{-\mathbf{1}}|[\widehat{\boldsymbol{A}}(w)]_{\boldsymbol{jj}}|^{\mathbf{2}}},$$

where $0 \leq \boldsymbol{iCoh}_{j\rightarrow i}\,(w) \leq 1$, the autoregressive coefficients $[\mathbf{A}(\mathrm{w})]_{kl} \equiv 0$**,** for all (k, l) such that $(k, l) \neq (i, j)$ and $k \neq l$ and the spectral density matrix $[\boldsymbol{S}_{\boldsymbol{\varepsilon}}]_{kl} \equiv 0$, for all (k, l) such that $k \neq l$.

3.3.3 Entropy measures

The time series of dynamic complexity have been investigated via several entropy measures, e.g., approximate entropy [46], sample entropy [27, 47] and fuzzy entropy [34]. Approximate entropy (ApEn) was presented as a measure of complexity in short and noisy recordings [46]. Sample entropy (SampEn) [47] was presented as having the advantage of being less dependent on the time series length. Multiscale sample entropy (MSE) [27] was presented as taking into account multiple time scales. Since MSE relies on the computation of the sample

entropy over a range of scales, coarse-grained time series that represent the system dynamics on different scales are analysed using the sample entropy algorithm. MSE has been used in different fields successfully, and is therefore a potential algorithm for quantifying the complexity of signals. Recently, to improve the reliability of complexity, the concept of fuzzy sets [69] was proposed to investigate the fuzzy entropy (FuzzyEn) measure [34, 70], which relies on fuzzy membership functions (smooth and continuous boundary) instead of the Heaviside function (hard and discontinuous boundaries). Since fuzzy entropy measures a fuzzy boundary, it corresponds to a stronger relative reliability and therefore provides a more accurate complexity assessment than sample entropy [70]. In previous theoretical analyses and experimental results [34, 70], fuzzy entropy allowed an improved evaluation of signal complexity and has been powerfully applied to short time series contaminated by noise.

However, the existence of superimposed trends in physiological signals generated by the human brain is so common that it is almost unavoidable [71]. With EEG signals, the high nonlinear and non-stationary brainwaves, especially superimposed trends in signals, could influence the estimation of entropy-based analysis by increasing the standard deviation of the data. The present entropy approaches cannot be applied in EEG signals. In order to eliminate trend oscillations in EEG signals, the inherent modes (called intrinsic mode functions or IMFs) extracted from the empirical mode decomposition (EMD) are considered an effective filter in this study for reducing superimposed trends in signals [72]. If the modified fuzzy entropy

algorithm works, it is possible to assess entropy values for monitoring the EEG complexity of different migraine phases.

1) Modified fuzzy entropy algorithm: Inherent Fuzzy Entropy

In this section, the algorithm of Inherent Fuzzy Entropy was represented as a flowchart (Fig. 3-2), and three components of Inherent Fuzzy Entropy algorithm were described in the following parts: A. EMD technology for the de-trending process; B. FuzzyEn algorithm for complexity evaluation; and C. Multiscale procedure.

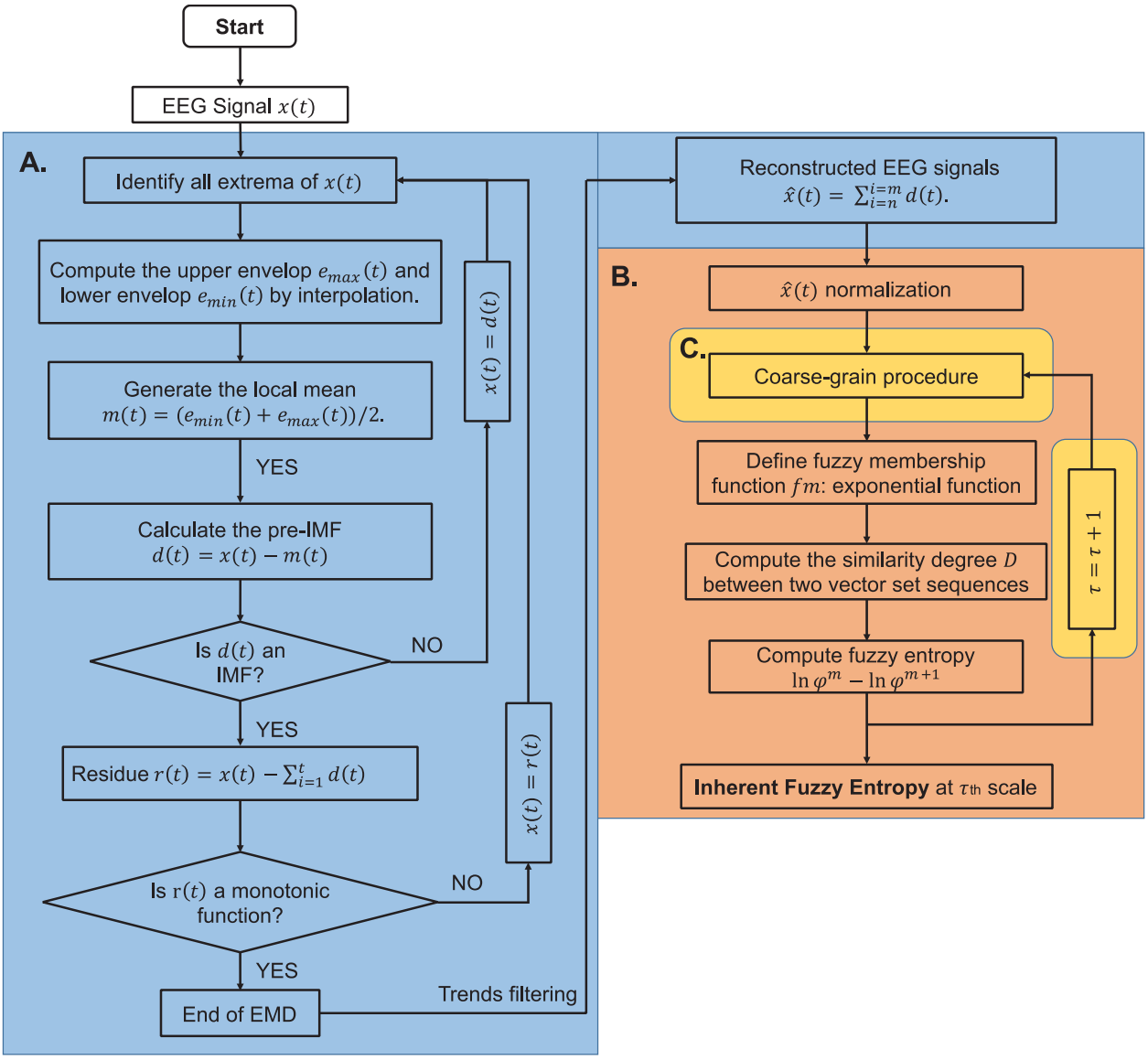

Figure 3-2. Flowchart of the Inherent Fuzzy Entropy algorithm: A. EMD; B. FuzzyEn; C. Multiscale procedure.

a. EMD technology for de-trending process

We apply the EMD technique to decompose the raw signal $x(t)$ into several IMFs, and re-construct the signal $\hat{x}(t)$. The procedures of EMD were showed as follows.

1) Find all extrema of signal $x(t)$: F_{minima} and F_{maxima}. Interpolate between F_{minima} and F_{maxima}, ending up with some envelope $e_{min}(t)$ and $e_{\max}(t)$.

2) Compute the mean: $m(t) = (e_{min}(t) + e_{max}(t))/2$ (1)

3) Extract the candidate of inherent functions: IMFs is $d(t) = x(t) - m(t)$ (2)

4) Is $d(t)$ an IMF? – $d(t)$ is an IMF that satisfies two conditions: first, in the whole data set, the number of extrema and the number of zero crossings must either equal or differ at most by one. Second, at any point, the mean value of the envelope defined by the local maxima and the envelope defined by the local minima is zero. If yes, save $d(t)$ and compute the residue

$$r(t) = x(t) - \sum_{i=1}^{t} d(t) \quad (3)$$

5) Do $t = t + 1$ and treat $r(t + 1)$ as input data. Otherwise, treat $d(t + 1)$ as input data. Iterate on the residual $m(t)$. Continue until the final residue r satisfies stopping criterion: when the residue, r, becomes a monotonic function from which no more IMF can be extracted.

6) The IMFs components surviving high trends were automatically removed by a trend filtering algorithm [73]. The remained IMFs were chosen for reconstructing signal $\hat{x}(t)$ by cumulative sums of the remained IMFs:

$$\hat{x}(t) = \sum_{i=n}^{i=m} d(t) \quad (4)$$

For the parameter in Equation (3) and (4), parameter i is the order number of IMFs components, and parameters m and n are the upper and lower boundary number of selected IMFs components, respectively.

Additionally, we also draw example figure for EMD processing in Fig. 3-3. Firstly, the raw EEG signal was decomposed to several IMFs (as shown in modes 1-12) and a residual

(as shown in mode 13) by the EMD algorithm. Secondly, to eliminate the superimposed trends in EEG signals, a trend filtering algorithm was applied to remove the IMFs surviving high trends automatically, and the remained IMFs were chosen (e.g., mode 4-8) for reconstructing the EEG signal. Finally, the EEG signal was reconstructed by cumulative sums of the remained IMFs (as shown in the reconstructed signal).

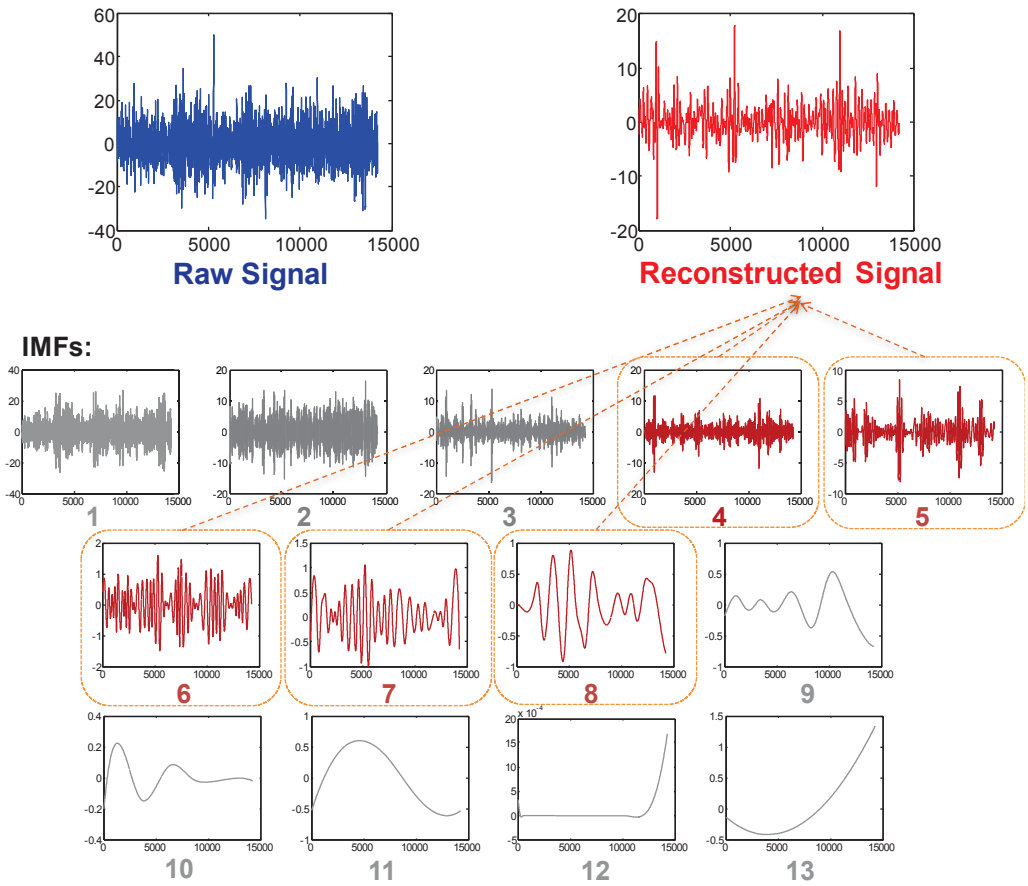

Figure 3-3. EMD processing and reconstruction of EEG signals.

b. Fuzzy entropy algorithm for complexity evaluation

1) Normalise the EEG signal:

$$y(t)^* = \frac{y(t) - mean(y(t))}{standard\ deviation} \tag{5}$$

2) The FuzzyEn considered the N sample time series $\{u(i): 1 \leq i \leq N\}$, given m, n,

and r, and a vector set sequences $\{X_i^m, i = 1, \ldots N - m + 1\}$ is calculated as follows:

$$X_i^m = \{u(i), u(i + 1), \ldots, u(i + m - 1)\} - u0(i) \tag{6}$$

Where $1 \leq i \leq N - m + 1$, and X_i^m presents m consecutive u values, commencing with the ith point and generalized by removing a baseline:

$$u0(i) = m^{-1} \sum_{j=0}^{m-1} u(i + j) \tag{7}$$

3) Given a vector X_i^m, define the similarity degree D_{ij}^m between X_i^m and X_j^m by a fuzzy membership function:

$$D_{ij}^m = fm\left(d_{ij}^m, n, r\right) \tag{8}$$

Where fuzzy membership function is an exponential function:

$$fm\left(d_{ij}^m, n, r\right) = exp\left(-\frac{\left(d_{ij}^m\right)^n}{r}\right) \tag{9}$$

and d_{ij}^m is the maximum absolute difference of the corresponding scalar components of X_i^m and X_j^m.

4) Construct the function φ^m as

$$\varphi^m(n, r) = (N - m)^{-1} \sum_{i=1}^{N-m} ((N - m - 1)^{-1} \sum_{j=1, j \neq i}^{N-m} D_{ij}^m) \tag{10}$$

Similarly, for $m + 1$, repeat the above steps:

$$\varphi^{m+1}(n,r) = (N - m)^{-1} \sum_{i=1}^{N-m}((N - m - 1)^{-1} \sum_{j=1,j\neq i}^{N-m} D_{ij}^{m+1}) \quad (11)$$

If the length of datasets N is finite, the parameter $FuzzyEn(m,n,r,N)$ of the sequence $\{u(i): 1 \leq i \leq N\}$ is defined as the negative natural logarithm of the deviation of φ^m from φ^{m+1} :

$$FuzzyEn(m,n,r,N) = \ln \varphi^m(n,r) - \ln \varphi^{m+1}(n,r) \quad (12)$$

For the parameter choices of FuzzyEn, the first parameter m, as in ApEn and SampEn, is the length of sequences to be compared. The other two parameters r and n determine the width and the gradient of the boundary of the fuzzy membership function, respectively.

c. Multiscale version

Multiscale version considered coarse-graining the signals into different time scales. For a given time series, multiple coarse-grained time series are constructed by averaging the data points within non-overlapping windows of increasing length, τ element of the coarse-grained time series, $y_j^{(\tau)}$ $y_j^{(\tau)}$ is calculated according to the Equation:

$$y_j^{(\tau)} = \frac{1}{\tau \sum_{i=(j-1)\tau+1}^{j\tau} x_i} \quad (13)$$

Where τ represents the scale factor and $1 \leq j \leq N/\tau$. The length of each coarse-grained time series is N/τ. For scale 1, the coarse-grained time series is simply the original time series. Choosing the appropriate scales (e.g., τ=10) before calculating FuzzyEn algorithm, multiscales Inherent FuzzyEn was performed in the Fig. 2-1C.

2) Experimental Analysis

a. EEG data collection

Twelve healthy young adults (5 men and 7 women, mean±std age: 31.5±2.3 years) participated in the resting-state experiment. It was requested that all the participants have no history of neurological, psychiatric, or addictive disorders according to self-reports. No participant had taken antipsychotic or other relevant psychoactive drugs in the two preceding weeks. This study was approved by the Institutional Review Board of the Veterans General Hospital, Taipei, Taiwan. All the participants were asked to read and sign an informed consent form before participating in the EEG experiment.

In the first 5 minutes, subjects were instructed to take several deep breathings to adapt to the environment. Then subjects were instructed to open their eyes for 1 minute and close their eyes for 1 minute three times (epochs) in total (as shown in Fig. 3-4), meanwhile EEG signals were recorded using Ag/AgCl electrodes by a 32-channel Quik-Cap (Compumedical NeuroScan). Thirty electrodes (Fp1, Fp2, F7, F3, Fz, F4, F8, FT7, FC3, FCz, FC4, FT8, T3, C3, Cz, C4, T4, TP7, CP3, CPz, CP4, TP8, T5, P3, Pz, P4, T6, O1, Oz and O2) were arranged according to a modified international 10-20 system, and two reference electrodes (A1 and A2) were placed on both mastoid bones. The skin under the reference electrodes were abraded using Nuprep (Weaver and Co., USA) and disinfected with a 70% isopropyl alcohol swab before calibration. The impedance of the electrodes was calibrated under 5 kΩ using NaCl-based

conductive gel (Quik-Gel, Neuromedical Supplies®). The EEG signals from the electro-cap were amplified using the Scan NuAmps Express system (Compumedics Ltd., VIC, Australia) and recorded at a sampling rate of 500 Hz with 16-bit quantization.

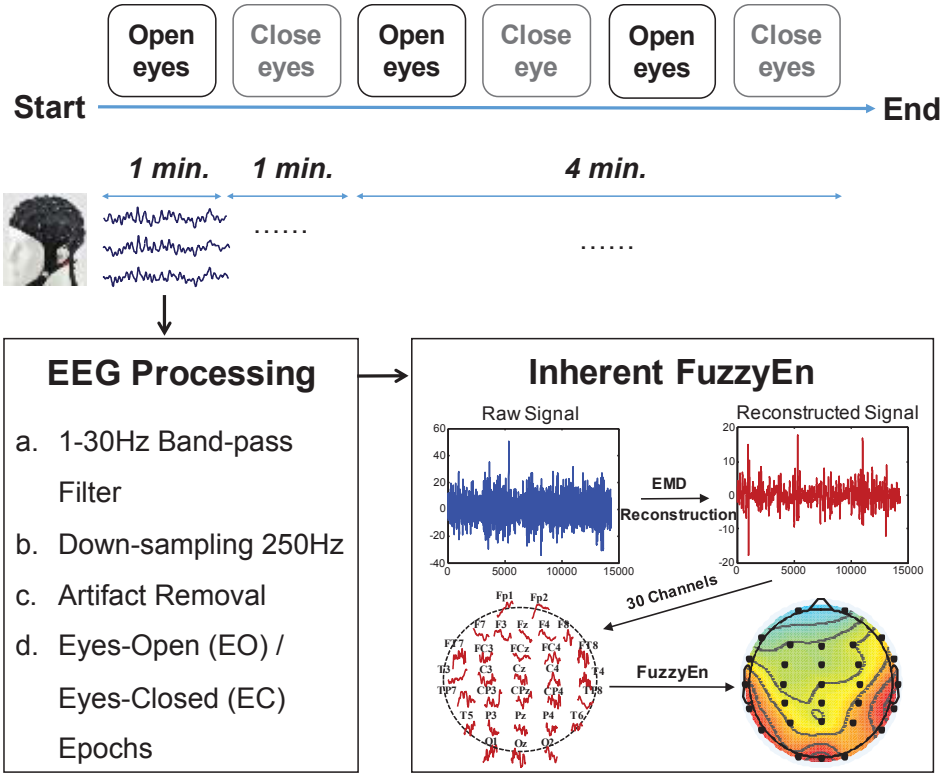

Figure 3-4. The analytical procedures: EEG recording, EEG processing and entropy evaluation.

b. EEG processing

The general scheme of the EEG analysis is illustrated in Fig. 2-4. The acquired EEG data were processed and analysed using EEGLAB (http://www.sccn.ucsd.edu/eeglab/, an open-source EEG toolbox for MATLAB) during the EEG processing and complexity calculation steps. For the part of EEG processing, the raw EEG signals were subjected to a 1-Hz high-pass

and 30-Hz low-pass infinite impulse response filter, and then down-sampled to 250 Hz from the sample recording rate of 500 Hz. For the artefact rejection, apparent eye contaminations in EEG signals were manually removed by visual inspection. Then, Independent Component Analysis (ICA) was applied to the EEG signals, and the components responsible for the eye movements and blinks were rejected. Finally, the EEG signals without these artifact components was reconstructed using the back-projection method. The EEG data were segmented into eyes-open (EO) and eyes-closed (EC) epochs for further complexity analysis. The EEG complexity of EO and EC conditions were calculated and compared by the entropy evaluation (ApEn, SampEn, FuzzyEn and Inherent FuzzyEn).

c. RMSD evaluation

EEG complexity was evaluated by comparing four types of entropy-based algorithms (Inherent FuzzyEn, FuzzyEn, SampEn and ApEn) using root mean square deviation (RMSD) in EO and EC conditions. The formula of RMSD was shown as follows:

$$RMSD = \sqrt{\frac{1}{n}\sum_{i=1}^{n}(y_i - \hat{y}_i))^2} \tag{14}$$

Where $\hat{y}$ is the mean value of entropy among 3 EO or EC epochs, and n = 3.

3) Results

a. EEG complexity

In this study, the EEG complexity of 12 participants between eyes-open (EO) and eyes-closed (EC) conditions were compared using ApEn, SamEn, FuzzyEn, and Inherent FuzzyEn algorithms (parameters $m = 2$, $r = 0.15$ and τ = 10). As shown in the Fig. 3-5, the EEG complexity of each epoch (EO1, EC1, EO2, EC2, EO3, and EC3) was the averaged entropy value from all participants.

By comparison of EEG complexity between EO and EC conditions, our results showed that the Inherent FuzzyEn employs the higher effect sizes than the other shallow models (ApEn, SamEn and FuzzyEn). Specifically, the Inherent FuzzyEn performed the significantly higher parietal and occipital and lower frontal EEG complexity in the EO condition (False Discovery Rate-*adjusted* $p < .05$), relative to that in the EC condition (Statistics: Wilcoxon signed-rank test). Moreover, fuzzy-based entropy models have more distinguished EEG complexity (EO vs. EC) than non-fuzzy entropy models. Furthermore, the Inherent FuzzyEn performed less variation than FuzzyEn, SampEn and ApEn in 3 EO epochs.

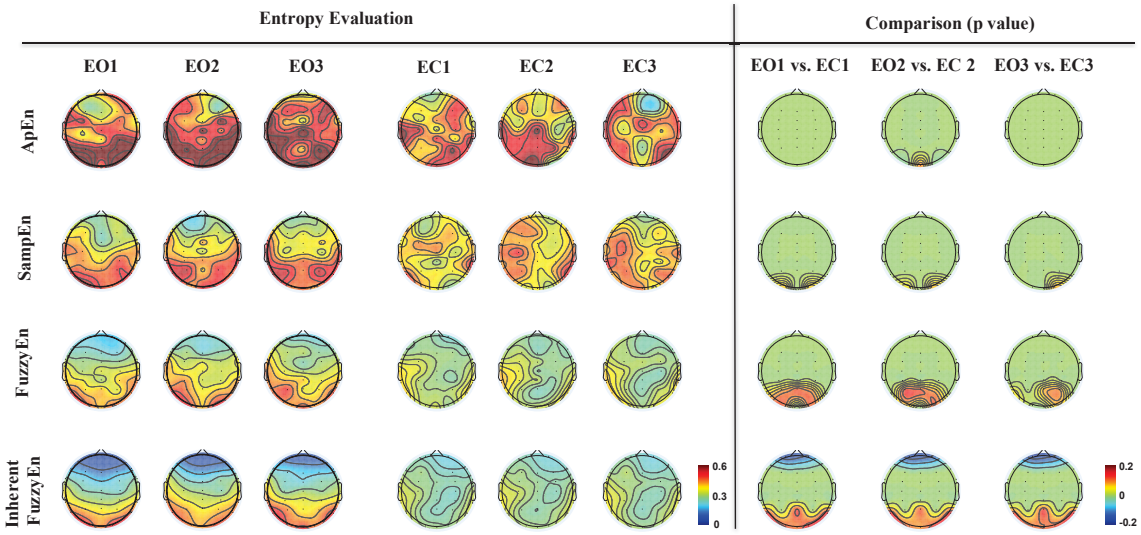

Figure 3-5. The EEG dynamic complexity by ApEn, SampEn, FuzzyEn and Inherent FuzzyEn evaluations.

b. RMSD evaluation

The feasibility of evaluating dynamic complexity in EO and EC conditions was examined by comparing ApEn, SampEn, FuzzyEn and Inherent FuzzyEn using RMSD. The performances of RMSD for ApEn, SampEn, FuzzyEn and Inherent FuzzyEn based on 1-30 channels (Fp1, Fp2, F7, F3, Fz, F4, F8, FT7, FC3, FCz, FC4, FT8, T3, C3, Cz, C4, T4, TP7, CP3, CPz, CP4, TP8, T5, P3, Pz, P4, T6, O1, Oz and O2) are described in Fig. 3-6. The results show that fuzzy-based entropy models have less RMSD than non-fuzzy entropy models in EO and EC conditions. Most importantly, the Inherent FuzzyEn algorithm has the lowest RMSD in all channels relative to previous entropy models in EO and EC conditions, which suggests our developed method offers a stable performance method for evaluating dynamic complexity.

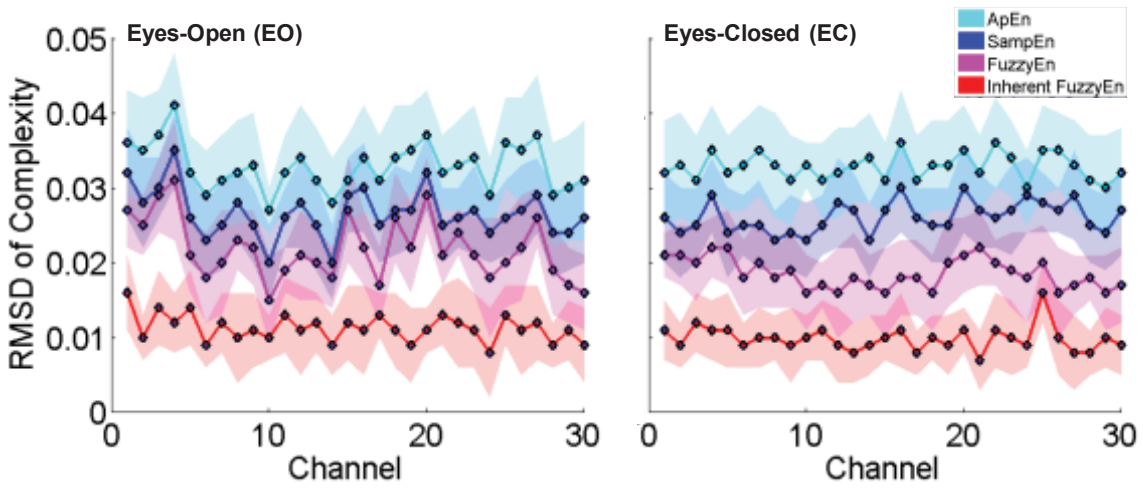

Figure 3-6. Complexity evaluation using RMSD in EO and EC conditions. The dash lines and envelope areas are the mean values and standard deviations, respectively.

4) Discussion

Regularity of EEG signals varies, it can thus be used as a characteristic feature of EEG signals for dynamics on the brain cortex activity. Entropy definitions can track qualitative changes in time series patterns and allow one to assess the temporal regularity of the time series. The best distinguishing result of the open and closed eyes by Inherent Fuzzy Entroy, compared with those by ApEn, SampEn and FuzzyEn, demonstrates that the new measure can characterise EEG signals more efficiently.

Taking advantage of the concept of fuzzy sets and EMD, Inherent FuzzyEn yields more satisfying results when characterising signals with different complexity. Both theoretical analysis (Appendix 3-1) and experimental tests (Figs. 3-3 and 3-4) show that FuzzyEn provides

an improved evaluation of complexity, and can thus serve as a convenient and powerful tool for short noisy experimental time series.

EEG complexity is fundamentally mercurial and varying during EEG study. In previous studies, researchers have generally ignored the superimposed trends in signals. To improve performance in realistic EEG applications, using an Inherent FuzzyEn algorithm can be made more effective by collecting EEG signals from healthy people, which endows fuzzy membership function with EMD function. In this study, we compared the EEG results (entropy values and RMSD) obtained using fuzzy structures (Inherent FuzzyEn and FuzzyEn) and non-fuzzy structures (SampEn and ApEn). Our findings showed that systems with fuzzy structures exhibit improved performance. Furthermore, the performance of the Inherent FuzzyEn algorithm was superior to FuzzyEn, SampEn and ApEn models.

3.4 Conclusion

In this Chapter, we reviewed state-of-the-art methodology in resting-state EEG research, including power, coherence and entropy analysis, as well as proposed a robust modified entropy algorithm to assess EEG complexity. Considering the number of the electrodes on the EEG cap, the EEG coherence must be analysed based on multiple signals, whereas EEG power and entropy can be extracted with the information of a single signal.

As migraine refers to a cyclic disorder with an inclusion of four phases (inter-ictal, pre-ictal, ictal, and post-ictal), the cyclic neurophysiological patterns of migraine can be discovered by revealed methodology in resting-state EEG research. If the dysfunction of brain cortical dynamics plays an important role in the pathophysiology of migraine, effective ways of evaluating the change of neurophysiologic signals are crucial to study the transition.

Chapter 4 EEG POWER, COHERENCE, AND ENTROPY CHANGES IN MIGRAINE

4.1 Experimental Materials

4.1.1 Subjects

Patients with migraine without aura, who were diagnosed by board-certified neurologists at the Headache Clinic, Taipei Veterans General Hospital (VGH) as having low-frequency migraine (1–5 days per month) were invited to join this study. Diagnoses of migraine without aura were based on the ICHD-2 criteria [74]. Age-matched HCs were enrolled from hospital colleagues, their relatives, or friends who did not have past or family histories of migraine, nor any headache attack during the past year.

Each patient kept a headache diary and completed a structured questionnaire on demographics, headache profile, medical history, and medication use. The headache profiles included the duration of migraine history (years), the severity of migraine, headache frequency (days per month), and Migraine Disability Assessment (MIDAS). In addition, the Beck Depression Inventory (BDI) and Hospital Anxiety Depression Scale (HADS) were administered to screen for psychological disturbances. On EEG study days, patients' migraine phases were designated as inter-ictal, pre-ictal, ictal, or post-ictal based on the patients' headache diaries (Figure 4-1A). Ictal phase was coded when patients had suffered a migraine attack on the day of EEG study. Pre-ictal and post-ictal phases were coded when patients were

within 36 hours before or after an ictal phase on the day of EEG study, respectively. Inter-ictal phase was coded for patients in a pain-free period between pre-ictal and post-ictal phases.

Subjects were excluded if they had systemic diseases, connective tissue disorders, neurological or psychiatric disorders, as well as other painful conditions according to their self-report. All subjects had normal vision after correction. To prevent the mis-classification of migraine phases or the distracted effect on EEG, patients were requested not to take analgesics within 2 days before EEG recording, nor take any psychotropic drugs within 4 weeks before the EEG study. None of our patients were on any migraine preventive agents. This study was approved by the Institutional Review Board at Taipei VGH (approved ID: 2011-06-009IC). Informed consent was obtained from all subjects before they joined the study.

4.1.2 Experimental design

Experiments were performed in a quiet, dimly light room in our hospital. During the first 2 minutes of the experiment, subjects were instructed to take several deep breaths while they adapted to the environment. Next, subjects were instructed to open their eyes for 30 seconds and close their eyes for 30 seconds and to repeat this sequence for a total of three times (Figure 4-1B). Meanwhile, EEG signals were recorded using Nicolet EEG system (Natus Medical, Incorporated, San Carlos, CA, USA) with Ag/AgCl electrodes. Eighteen EEG electrodes (Fp1, Fp2, F7, F3, Fz, F4, F8, T3, C3, Cz, C4, T4, T5, P3, P4, T6, O1, and O2) were placed according to the conventional 10-20 EEG system [75] and the guideline of American

Clinical Neurophysiology Society [76]. Fz was used as the reference channel. The skin under the reference electrodes were abraded and disinfected with a 70% isopropyl alcohol swab before calibration. The impedance of the electrodes was calibrated under 5 kΩ. The EEG signals were amplified and digitised at a sampling rate of 256 Hz with 16-bit quantization.

4.2 Data Analysis

The EEG data were analyzed with EEGLAB, an open-source MATLAB toolbox for electrophysiological signal processing and analysis [77]. The analytical procedures for EEG signal processing included a band-pass filter, artefact rejection, epoch extraction, time-frequency analysis, and coherence estimation (Figure 4-1C). During signal preprocessing, raw EEG signals were subjected to 1-Hz high-pass and 30-Hz low-pass finite impulse response (FIR) filters. For the artefact rejection, firstly, apparent eye contaminations in EEG signals were manually removed by visual inspection. Secondly, Independent Component Analysis (ICA) was applied to the EEG signals and the components responsible for the eye movements and blinks were rejected. Then, the EEG signals without these artefact components was reconstructed using the back-projection method [77]. Finally, the reconstructed EEG signals were inspected again using the "Automatic Channel Rejection (ACR)" function with Kurtosis measurement and Z-score threshold of 5 to remove noisy channels. Eyes-open and eyes-closed resting-state signals of three blocks were extracted and concatenated for further analyses.

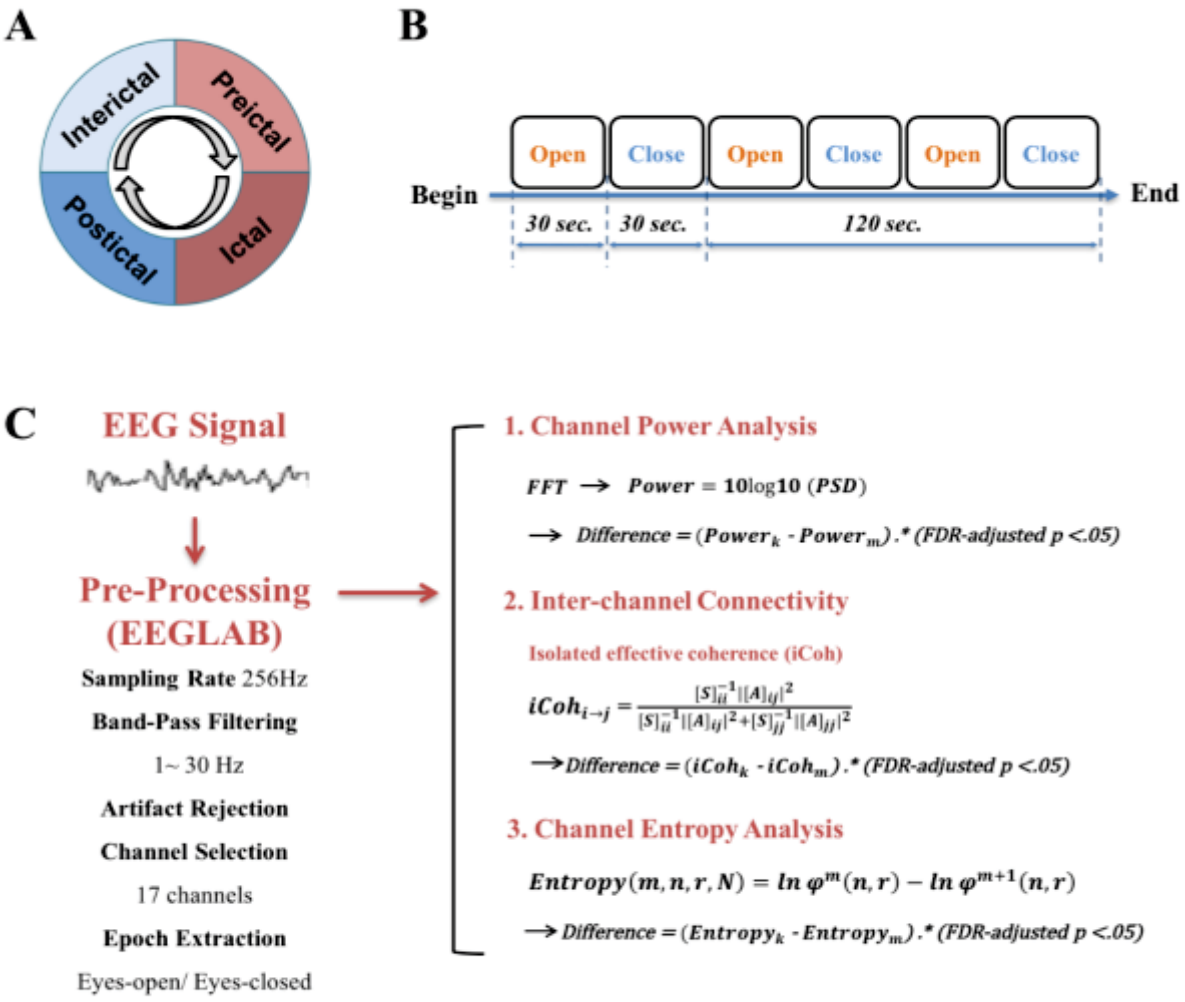

Figure 4-1. Analytical procedures. (A) Migraine cycle; (B) Resting-state EEG recording; (C) EEG signal processing.

4.2.1 EEG processing and measurements

1) EEG power analysis

Processed time-series data were transformed into the frequency domain by a 256-point fast Fourier transform with Welch's method. Specifically, 90-second spans of data were analyzed with a 256-point moving window with a 128-point overlap. Windowed data were

extended to 512 points by zero-padding to calculate power spectra, yielding an estimation of the power spectra with 60 frequency bins from 1 to 30 Hz (frequency resolution: 0.5 Hz). Power spectra of these windows were averaged and converted to a logarithmic scale. Mean delta (δ: 1–3.5 Hz), theta (θ: 4–7.5 Hz), alpha (α: 8–12.5 Hz), and beta (β: 13–30 Hz) band powers of 17 channels were visualised on a two-dimensional (2-D) topographic map.

2) EEG coherence analysis

For all groups (inter-ictal, pre-ictal, ictal, post-ictal, and HCs), we explored the coupling between brain areas within particular frequency bands based on the up-to-date coherence algorithm, named isolated effective coherence (iCoh) [42], which is a multivariate approach to address the effective connectivity. Its advantages not only are insensitive to volume conduction but also can detect direct pathways linking brain regions. Firstly, the Source Information Flow Toolbox (SIFT) [68] in the EEGLAB was used to identify the optimal multivariate autoregressive model. Then, the magnitude of iCoh for channel $j \rightarrow$ channel i at the frequency of w is estimated from the following formula [42]

$$\boldsymbol{iCoh}_{j\rightarrow i}\,(w) = \frac{[\boldsymbol{S}_{\varepsilon}]_{\boldsymbol{ii}}^{-\mathbf{1}}|[\widehat{\boldsymbol{A}}(w)]_{\boldsymbol{ij}}|^{\mathbf{2}}}{[\boldsymbol{S}_{\varepsilon}]_{\boldsymbol{ii}}^{-\mathbf{1}}|[\widehat{\boldsymbol{A}}(w)]_{\boldsymbol{ij}}|^{\mathbf{2}}+[\boldsymbol{S}_{\varepsilon}]_{\boldsymbol{jj}}^{-\mathbf{1}}|[\widehat{\boldsymbol{A}}(w)]_{\boldsymbol{jj}}|^{\mathbf{2}}},$$

where $0 \leq \boldsymbol{iCoh}_{j\rightarrow i}\,(w) \leq 1$, the autoregressive coefficients $[\mathbf{A}(\mathrm{w})]_{kl} \equiv 0$, for all (k, l) such that $(k, l) \neq (i, j)$ and $k \neq l$ and the spectral density matrix $[\boldsymbol{S}_{\boldsymbol{\varepsilon}}]_{kl} \equiv 0$, for all (k, l) such that $k \neq l$.

3) EEG entropy analysis

For all groups (inter-ictal, pre-ictal, ictal, post-ictal, and HCs), we explored the 17-channel EEG complexity based on the Inherent Fuzzy Entropy algorithm that we introduced in Chapter 2. We calculated EEG entropy at each epoch of eyes-open and eyes-closed conditions, respectively. The values of EEG entropy were averaged for the epochs at same condition. Of note, the varies of EEG entropy reflect to the brain dynamics of complexity.

4.2.2 Statistical analysis

Group differences in clinical profiles were analyzed by Student's t-test (migraine patients vs. HCs) or one-way ANOVA (four phases of migraine patients) for continuous variables and chi-square or Fisher's exact tests for categorical variables. Resting-state EEG band power, coherence and entropy values were compared across all five groups (HC and 4 migraine phase groups) by the Wilcoxon rank-sum test, followed by calculation of the false discovery rate (FDR) for multiple comparisons. The significance level was set to 0.05. Statistical analysis was performed in the SPSS software package (version 15.0) and MATLAB (2011a) Bioinformatics Toolbox.

4.3 Results

4.3.1 Demographic and Clinical Characteristics

A total of 61 patients with migraine without aura joined the study, of whom, 11 were excluded because of taking analgesic medications within 2 days before the EEG study, yielding a final sample of 50 patients for analysis. These 50 patients were classified into inter-ictal (n = 22), pre-ictal (n = 12), ictal (n = 8), and post-ictal (n = 8) phases. In addition, 20 HCs were also recruited. Demographic and clinical characteristics were similar between the migraine group and HC group and also similar across the four migraine phase groups (Table 4-1).

Table 4-1. Comparisons of demographics, headache profiles, and psychological characteristics.

Characteristic	Migraine patients (N = 50)	HCs (N = 20)	*P*	Migraine phase groups				*P*
				Inter-ictal (N = 22)	Pre-ictal (N = 12)	Ictal (N = 8)	Post-ictal (N = 8)	
Sex, F:M	35:15	11:9	0.24	16:6	6:6	7:1	6:2	0.49
Age, y	36.0 ± 9.9	36.9 ± 6.7	0.63	33.0 ± 9.0	39.0 ± 7.5	40.0 ± 11.5	38.0 ± 12.4	0.27
Migraine headache profile								
Disease duration, y	16.0 ± 9.3	N/A	N/A	15.0 ± 8.1	16.0 ± 7.8	20.0 ± 9.6	16.0 ± 13.8	0.72
Frequency, d/mo.	3.8 ± 1.3	N/A	N/A	3.8 ± 1.4	3.8 ± 1.3	3.6 ± 1.3	3.9 ± 1.0	0.81
Pain severity [a]	7.0 ± 1.9	N/A	N/A	8.0 ± 2.1	7.0 ± 1.8	8.0 ± 1.9	6.0 ± 1.7	0.42
MIDAS score[b]	16.3 ± 13.4	N/A	N/A	19.1 ± 16.6	17.8 ± 10.7	11.0 ± 11.8	15.7 ± 13.5	0.59
Psychometric scores								
BDI	8.7 ± 5.7	N/A	N/A	9.4 ± 6.1	7.7 ± 5.6	9.9 ± 5.3	7.9 ± 5.8	0.68
HADS-A	6.7 ± 3.7	N/A	N/A	7.6 ± 3.2	5.5 ± 3.4	6.6 ± 3.0	7.8 ± 5.7	0.41
HADS-D	4.6 ± 3.3	N/A	N/A	4.8 ± 3.4	3.6 ± 2.2	5.0 ± 2.8	4.2 ± 3.3	0.46

[a]0–10 scale. [b]0–270 range. Abbreviations: BDI, Beck Depression Inventory; F:M, ratio of females to males; HADS-A, Hospital Anxiety Depression Scale, Anxiety; HADS-D, Hospital Anxiety Depression Scale, Depression; HC, healthy controls; MIDAS, Migraine Disability Assessment Scale. Of note, group differences in clinical profiles were analysed by Student's t-test (migraine patients vs. HCs) or one-way ANOVA (four phases of migraine patients) for continuous variables and chi-square or Fisher's exact tests for categorical variables.

4.3.2 Comparisons of Resting-state EEG Dynamics between Migraine Patients and Healthy Controls

Dynamic changes in EEG power/coherence between migraine patients and HCs or between migraine phases were more robust in the eyes-open than in the eyes-closed condition (Appendix 4-1 - 4-4). Regarding of EEG entropy, significant differences were performed between inter-ictal patients and HCs or partial migraine phases in closed-eyes condition (Fig. 4-6), whereas there are no significant differences in eyes-open condition. Therefore, we used EEG data from the eyes-open condition in subsequent power and coherence analyses, and from the eyes-closed condition in subsequent entropy analyses.

1) EEG power

Significant differences in resting-state EEG power in the eyes-open condition in migraine patients from each phase versus HCs for the delta, theta alpha, and beta domains are shown in Figure 4-2. Inter-ictal patients had significantly lower delta, theta, alpha and beta EEG power in the fronto-central (F4, C3, Cz, C4) and parietal (P3, P4) regions, compared to HCs (FDR-adjusted $p < .05$, Figure 4-2A). EEG power values did not differ between pre-ictal patients and HCs in any of the four EEG frequency domains (Figure 4-2B). Ictal patients had lower delta, theta, alpha and beta (fronto-central and parietal regions) power than HCs (FDR-adjusted $p < .05$, Figure 4-2C). EEG power variability in post-ictal patients was similar to that in HCs (Figure 4-2D).

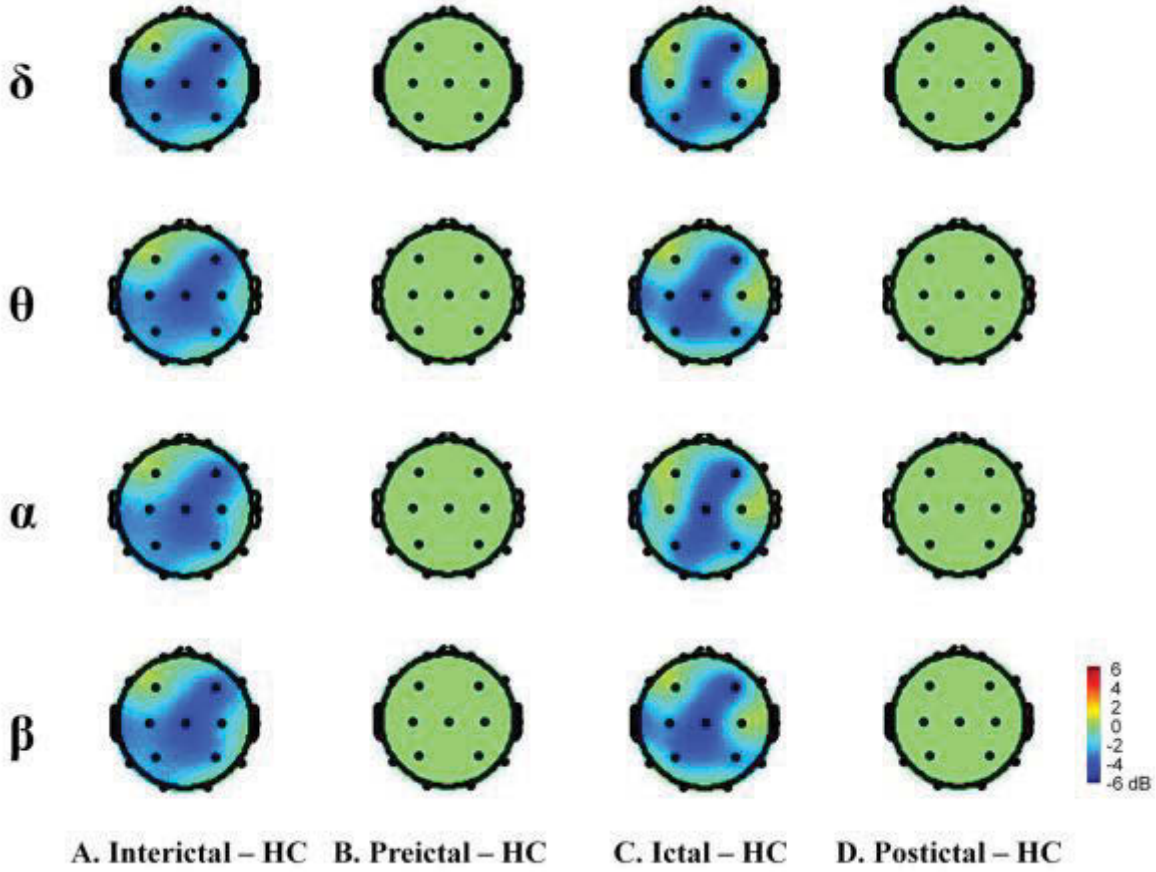

Figure 4-2. Topographical comparison of significant EEG power differences ($p < .05$) between migraine patients in different migraine phases and HCs during eyes-open recording. Colour intensity indicates the magnitude of the power difference (red for increased power, blue for decreased power) in each channel.

2) EEG coherence

Comparisons of resting-state EEG coherence between migraine patients in each phase of the migraine cycle versus HCs are shown in Figure 4-3. Delta, theta, alpha, and beta EEG coherence networks were lower in inter-ictal patients than in HCs (FDR-adjusted $p < .05$; Figure 4-3A), with the exception of fronto-occipital network. Specifically, inter-ictal patients had decreased delta EEG coherence in fronto-central network, theta and alpha EEG coherence in fronto-central and posterior networks, and centro-parietal reductions in beta EEG coherence. Of note, the fronto-occipital network showed enhanced EEG coherence in theta, alpha, and beta bands (FDR-adjusted $p < .05$; Figure 4-3A). The EEG coherence networks of pre-ictal patients, generally, did not differ from those of HCs, except for a slight increase in posterior beta EEG coherence (Figure 4-3B). The cortical connection intensities of EEG coherence networks for theta and alpha frequency bands in ictal patients were lower than those in HCs (FDR-adjusted $p < .05$; Figure 4-3C). Coherence in post-ictal patients was similar to that in HCs, with the exception of a small downtrend in posterior alpha EEG coherence. (Figure 4-3D).

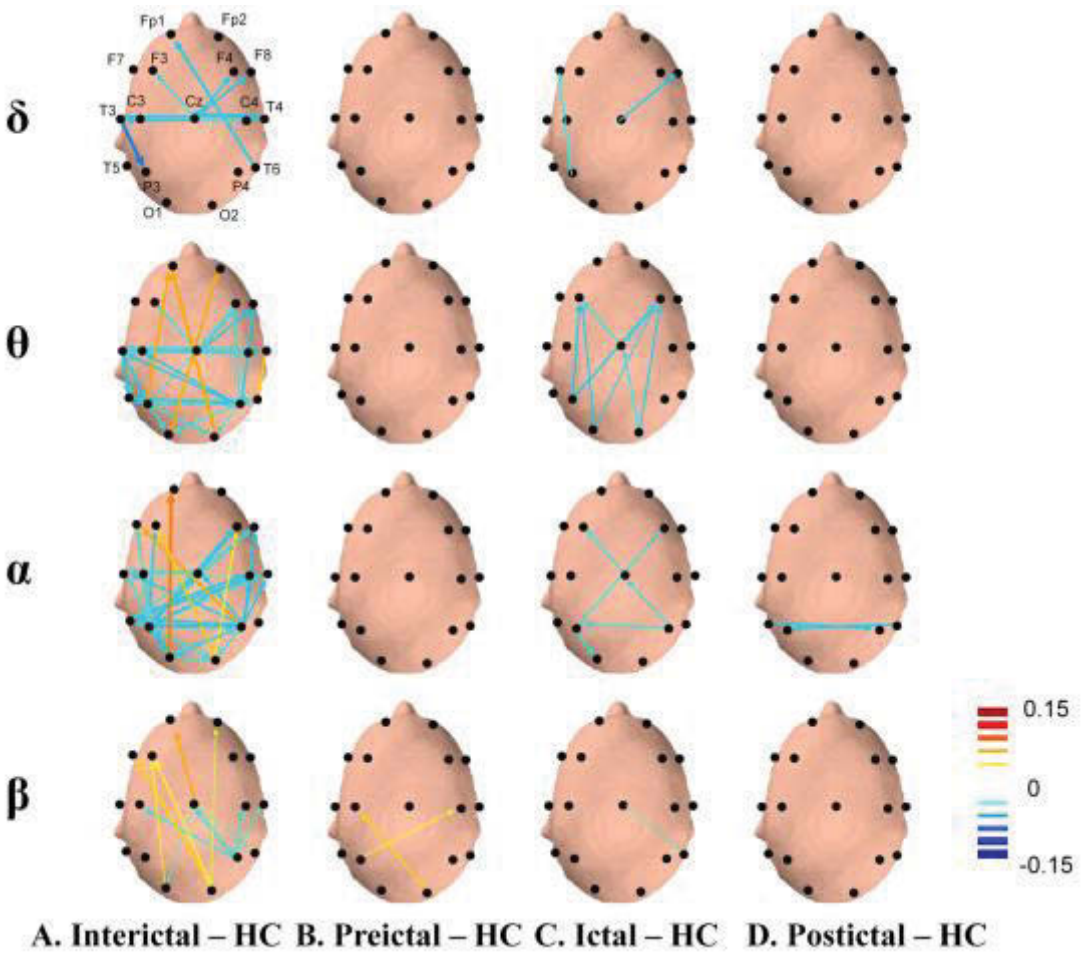

Figure 4-3. Topographical comparisons of significant EEG coherence differences ($p < .05$) between patients in different migraine phases and HCs during eyes-open recording. Line sizes and colours reflect the magnitude of the difference in coherence intensity between electrode pairs, with red indicating positive differences (more coherent) and blue indicating negative differences (more independent). The directions of arrows represent the direct paths of inter-channel coupling.

3) EEG entropy

Comparisons of resting-state EEG complexity between patients in different migraine phases versus HCs, as well as between migraine patients in each phase of the migraine cycle are shown in Figure 4-4. In particular, EEG entropy were lower in inter-ictal patients than in HCs at partial frontal and central areas (FDR-adjusted $p < .05$), whereas no significant differences of EEG entropy were shown between HCs and pre-ictal patients, ictal patients or post-ictal patients.

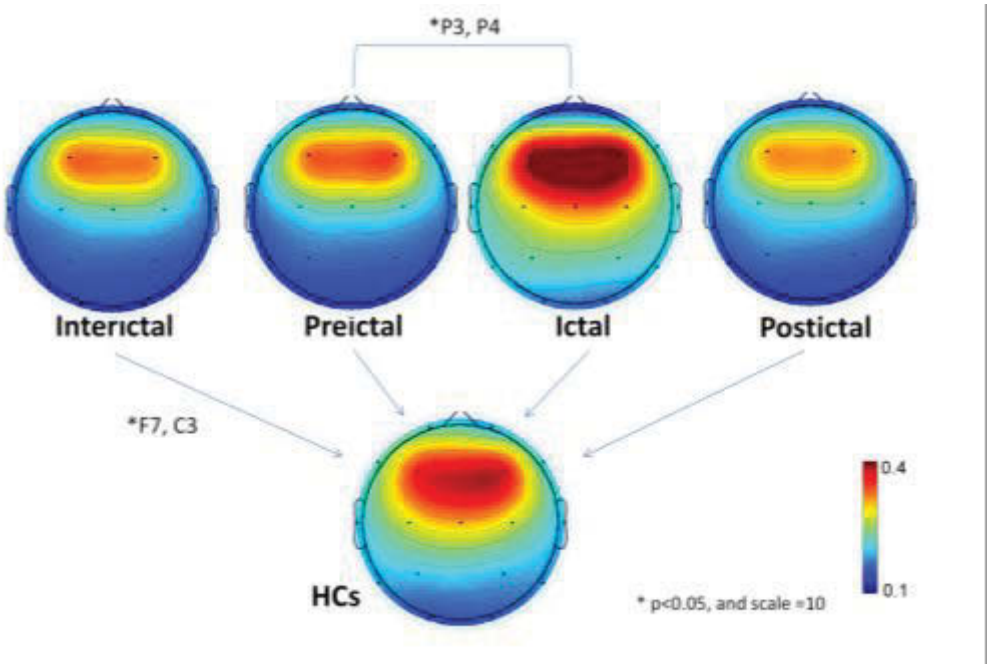

Figure 4-4. Topographical comparisons of significant EEG complexity differences (FDR-adjusted $p < .05$) between patients in different migraine phases and HCs, as well as between migraine patients in each of the four phases of the migraine cycle during eyes-closed recording.

4.3.3 Comparisons of Resting-state EEG Dynamics across Migraine Phases

1) EEG power

Significant differences in resting-state EEG power between the four migraine-phase groups are shown in Figure 4-5. EEG power intensity of pre-ictal patients in the fronto-central and parietal regions of delta theta, alpha and beta bands were higher than the corresponding values in inter-ictal patients (FDR-adjusted $p < .05$, Figure 4-5A). Compared to pre-ictal patients, ictal patients had lower fronto-central and parieto-occipital delta, theta, alpha, and beta EEG power (FDR-adjusted $p < .05$, Figure 4-5B). Centro-parietal delta, theta, alpha, and beta EEG power intensity were higher in post-ictal patients than in ictal patients (FDR-adjusted $p < .05$, Figure 4-5C). Right centro-parietal delta, theta, alpha, and beta EEG power intensity were lower in inter-ictal patients than in post-ictal patients (FDR-adjusted $p < .05$, Figure 4-5D).

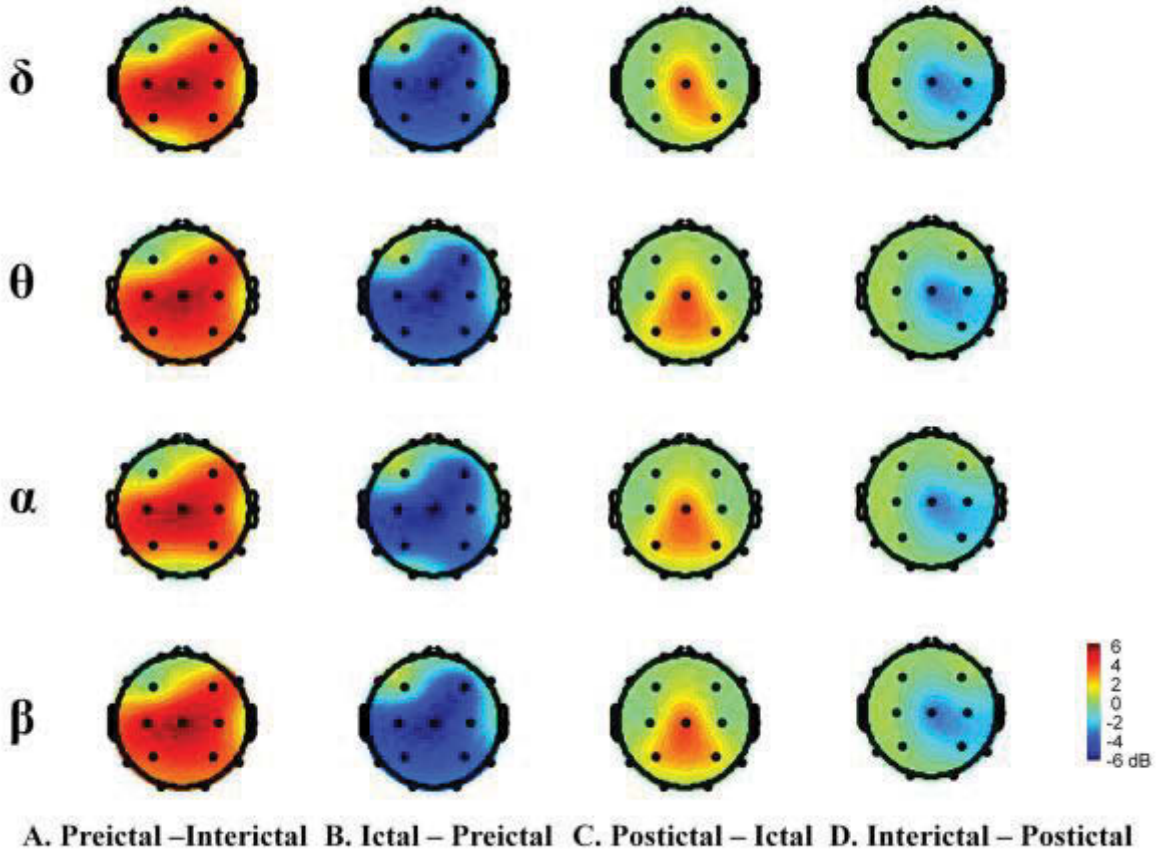

Figure 4-5. Topographical comparisons of significant EEG power differences ($p < .05$) between patients in each of the four migraine phases during eyes-open recording. Colour intensity indicates the magnitude of the power difference (red for increased power, blue for decreased power) in each channel.

2) EEG coherence

As demonstrated in Figure 4-6, significant differences in resting-state EEG coherence were observed between all pairs of consecutive migraine phases. Large significant differences in EEG coherence networks were observed in the delta, theta, and alpha bands in the frontal, central, temporal, parietal, and occipital regions. Specifically, compared to inter-ictal patients, pre-ictal patients had higher EEG coherence in the delta, theta, alpha, and beta bands (FDR-adjusted $p < .05$; Figure 4-6A) except for a reduction of EEG coherence in fronto-occipital network in delta, theta, alpha and beta bands (FDR-adjusted $p < .05$; Figure 4-6A). Meanwhile, ictal patients had significantly lower EEG coherence networks in the delta, theta, and beta bands than did pre-ictal patients (FDR-adjusted $p < .05$; Figure 4-6B). Moreover, as in Figure 4-6C, compared to ictal patients, post-ictal patients had greater EEG coherence, particularly in the delta and theta centro-occipital network (FDR-adjusted $p < .05$). Finally, compared to post-ictal patients, inter-ictal patients had markedly lower EEG coherence networks in the alpha band (FDR-adjusted $p < .05$; Figure 4-6D).

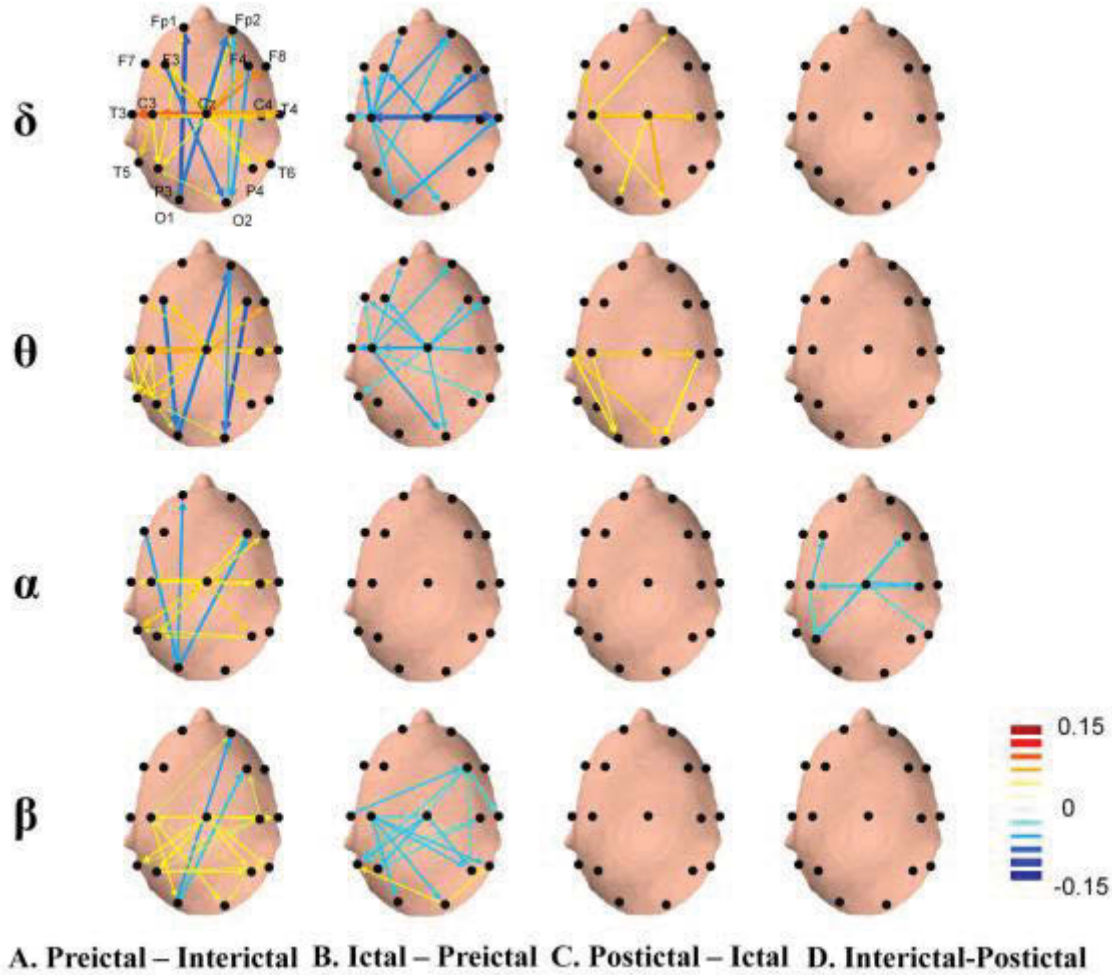

Figure 4-6. Topographical comparisons of significant EEG coherence differences ($p < .05$) between migraine patients in each of the four phases of the migraine cycle during eyes-open recording. Line sizes and colours reflect the magnitude of the difference in coherence intensity between electrode pairs, with red indicating positive differences (more coherent) and blue indicating negative differences (more independent). The directions of arrows represent the direct paths of inter-channel coupling.

3) EEG entropy

As shown in Fig. 4-3, our results found the increased EEG entropy from pre-ictal patients to ictal patients at the parietal area (FDR-adjusted $p < .05$), nor distinction between other phases in the migraine cycle.

4.4 Discussion

In the present study, using resting-state EEG, we showed that migraine patients in the inter-ictal and ictal phases, but not in the pre- and post-ictal phases, exhibited lower EEG power and coherence than HCs. Comparing the phase groups in series pairs (inter-ictal, pre-ictal, ictal, post-ictal), we observed increases in EEG power and coherence from the inter-ictal to the pre-ictal phase, decreases from the pre-ictal to the ictal phase, and finally increases from the ictal to the post-ictal phase. The fronto-occipital network in inter-ictal patients showed enhanced EEG coherence as compared to HC or pre-ictal patients. For the assessment of brain complexity, there is no significant EEG entropy difference between pre-ictal patients and inter-ictal patients or HCs. But our results showed the decreased EEG entropy in inter-ictal patients relative to HCs, suggesting the lower level of brain complexity in migraine. Of note, our results of EEG power and coherence showed higher effect sizes in the eyes-open EEG than eyes-closed EEG. The exact mechanisms are not clear. We do not know whether there is a link to the facts that visual cortical hyperexcitibility is more common in patients with migraine and visual areas in

eyes-open condition show greater activation than in eyes-closed condition [79].

4.4.1 Abnormal resting-state EEG activity in migraine

Migraine attacks have been hypothesised to start at the cortical level [19-21]. Previously, the synchronisation levels of cortical activity during visual stimulation in migraine patients have been shown to differ from those in HCs [22, 23]. Our findings provide new evidence of cortical abnormalities during a resting state as detected by EEG power spectra and coherence analyses. Furthermore, our findings complement prior resting-state EEG studies demonstrating cortical activity differences between adjacent migraine phases [24, 25].

Extending prior work showing abnormal cortical activity in migraine patients, particularly in the inter-ictal phase [20], we found that the EEG power and coherence, except for the effective connectivity in fronto-occipital network, were lower in the inter-ictal patients than in HCs. That is, migraine patients in the inter-ictal phase exhibited hypo-coupling in the frontal and centro-posterior networks, and hyper-coupling in the fronto-occipital network. Unlike our study results, previous studies showed similar EEG power between inter-ictal patients and HCs [25, 80]. Nevertheless, during the tasks for evoked potentials, inter-ictal patients have been reported to exhibit reduced EEG power [17] and synchronisation [22] in relation to HCs. Compared to HCs, migraine patients showed significantly reduced EEG power and coherence during migraine attacks, which normalised after migraine attacks. These power

results are in line with the results of two prior studies [81, 82]. Moreover, the decreased EEG coherence in our ictal patients suggests that hypo-coupling may occur during migraine attacks.

Our resting-state EEG results also provide information about the cortical state in the pre-ictal phase. We found significantly higher EEG power and coherence in pre-ictal versus inter-ictal phases. This increased EEG power suggests a relatively excessive cortical power intensity in the pre-ictal phase, which is generally consistent with a higher anterior delta EEG power relative to the inter-ictal phase [24]. Our elevated EEG resting-state coherence in pre-ictal phase points to hyper-coupling of regional brain connectivity, especially in the fronto- and centro-posterior networks. Intriguingly, prior studies have described a pre-ictal "normalisation" (towards HCs) of cortical responses to visual and auditory evoked potentials [38, 52, 53]. The exact underlying mechanisms accounting for our findings are not known. In fact, Sakai et al. [83] demonstrated an increase or normalisation of cerebral serotonin synthesis from the inter-ictal stage to migraine attacks. Nevertheless, one recent study [84] reported activation of the hypothalamus and brainstem during the prodromal phase (i.e. pre-ictal state) of migraine patients. Because our study did not employ source localisation methods, the brain regions responsible for our observations in EEG power and coherence require further investigations.

4.4.2 Strength and weakness of EEG coherence

In contrast to the power spectral or entropy measures, EEG coherence is a measure of synchronisation or coupling between two signals; in other words, it is a constant ratio of amplitude/ phase difference or direct coupling degree between two channels. However, the essential element for coherence analysis is multi-channel EEG signals. It cannot assess brain dynamics based on one channel EEG signal. In this Chapter, we used 17-channel EEG signals to investigate coherence varies. The coherence result is good, but it is not convenient for practical applications. By measuring with single-channel based analysis, we did not distinguish EEG entropy from inter-ictal patients to pre-ictal patients in this Chapter, which might be caused by the cross-sectional design.

4.4.3 Limitations

This study's major strengths were a sizable number of patients in different migraine phases and headache diary recordings for classifications of migraine phases in each patient. However, this study also had limitations. First, it is known that EEG power, concordance and coherence differences were reported in patients with psychiatric disorders, such as unipolar or bipolar disorders, as well as attention deficit hyperactivity disorder [85, 86]. We could not completely exclude the possibility that some of our participants might have such disorders since not all participants had psychiatric consultations. Second, because we recruited low-frequency

episodic migraine patients only, one should be cautious about generalising the findings to other migraine patient groups, such as high-frequency or chronic migraine patients. Third, because we employed a cross-sectional design, it is unknown whether the present results could be repeated in an examination of the same individuals with a longitudinal study design. Fourth, the number of participants and the sex ratio in each group was not fully matched. The imbalance can be explained by the low frequency of migraine attacks in our participants. The sex imbalance in different migraine cycles might be due to the small number in some cycles. Moreover, the vulnerability of coherence measures to volume conduction represents a potential confounder in our study. However, such an influence would be reduced in our study because we calculated differences only between pairs of migraine phases. Last, our study employ EEG, which records signals that are principally of cortical origin. Thus further investigations combining functional MRI with EEG should be pursued to examine the involvement of cortical/subcortical dysfunction in different migraine phases.

4.5 Conclusion

The present study revealed dynamic changes in resting-state EEG power, effective connectivity and complexity using band power, iCoh and entropy analysis, respectively, across different migraine phases in patients with low-frequency migraine. EEG effective connectivity in pre-ictal patients showed an augmented coupling in the fronto-central and centro-posterior networks and a reduced coupling in the fronto-occipital network. Such brain network dynamics could have implications for understanding complex neurophysiology of migraine before a headache attack.

Chapter 5 EEG-BASED MIGRAINE ATTACKS PREDICTION

5.1 Experimental Materials

5.1.1 Participants

Outpatients with MO were recruited from the Headache Clinic of Taipei Veterans General Hospital, and were requested to keep a headache diary to determine migraine phases on each day. All the enrolled patients fulfilled the diagnostic criteria of the International Classification of Headache Disorders 2nd edition (ICHD-II) [74], and had a migraine frequency ranging from 1 to 6 days per month. Age- and sex-matched healthy controls (HCs) were recruited from hospital colleagues and their relatives or friends. The individuals who served as HCs did not have a past medical history or family history of migraine. But low-frequency tention type headache (< 1/m) was allowed. Each patient was required to complete a structured questionnaire on demographics, headache profile, medical history, and medication use at the first examination. The headache profile included the duration of migraine history (years), onset age of migraine, headache frequency (days per month), and Migraine Disability Assessment (MIDAS). In addition, the Beck Depression Inventory (BDI), and Hospital Anxiety Depression Scale - Anxiety (HADS-A) and Depression (HADS-D) were administered to screen for psychological disturbances.

The days on EEG examination were classified into one of four migraine phases (inter-ictal, pre-ictal, ictal, or post-ictal) based on headache diaries. As shown in Fig. 5-1A, the ictal

phase was coded when the patient was suffering from a migraine attack on the day of EEG study. As per the criteria [87, 88], the pre-ictal and the post-ictal phases were coded on the day of EEG study when the patient was within 72 hours before and after an ictal phase, respectively. The inter-ictal phase was coded if the patient did not have any migraine attack within 72 hours before and after EEG examination. Only those EEG data collected during inter-ictal and pre-ictal phases were selected for analysis in this study.

All the participants had normal vision and no systemic diseases, connective tissue disorders, neurological or psychiatric disorders, or other painful conditions according to their self-reports. None of them received preventive treatment, and they were requested not to take any analgesics within 2 days before the EEG recording. The Institutional Review Board of the Taipei Veterans General Hospital approved this study. Informed consent was obtained from all participants before participating in this study.

5.1.2 Experimental paradigm

This experiment was performed in a static and lightless room at Taipei Veteran General Hospital. The fluorescent lamps were turned off throughout the EEG recording to avoid light source interference. As shown in Fig. 5-1B, each patient and health control participated in an identical resting-state EEG examination five times (exam 1-5) during 3-7 months, and each examination was separated by an interval of 2-8 weeks. This protocol aimed to inspect EEG

data recorded from patients who were experiencing different migraine phases, particularly inter-ictal and pre-ictal phases. The EEGs of ictal and post-ictal phases were not reported in this article. Each examination consisted of five epochs, namely, three 1-min epochs with the patient's eyes closed and two 1-min epochs with the patient's eyes open (Fig. 5-1C).

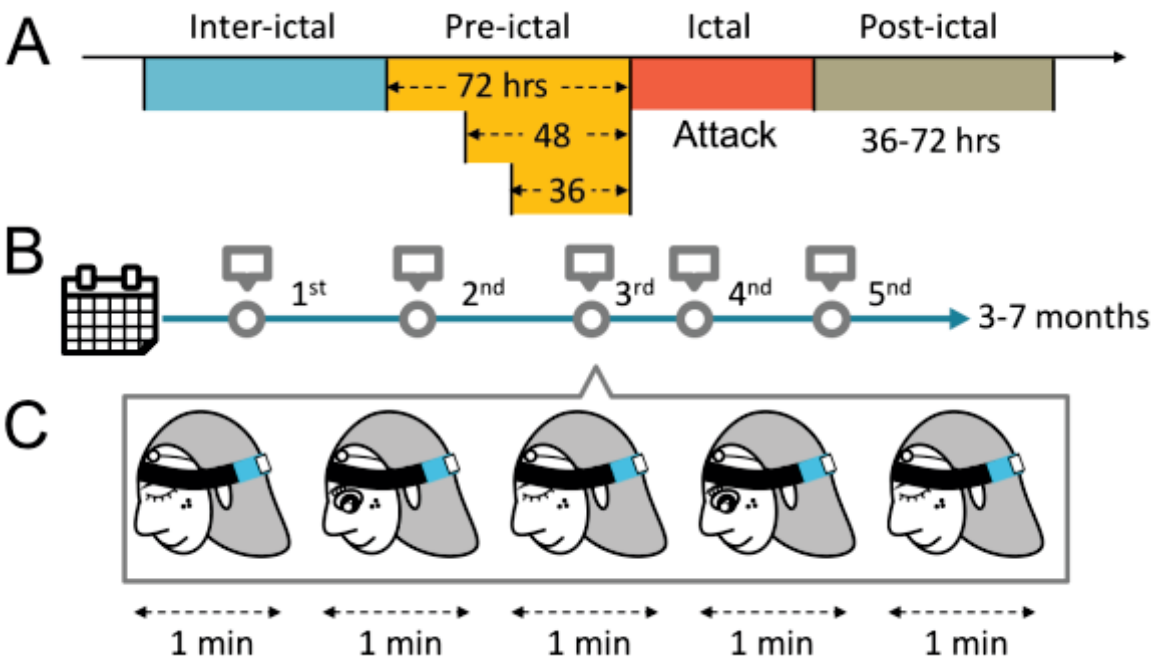

Figure 5-1. Experiment procedure. (A) Definition of migraine phases. (B) Five times of resting-state EEG test were conducted within 3-7 months. Each test recorded from a patient was classified as a migraine phase according to the migraine diary which was kept by him or her. The interval between two consecutive tests was 2-8 weeks. (C) Each resting-state EEG test consisted of three blocks of eyes-closed and two blocks of eyes-open. The eyes-closed and eyes-open blocks were performed alternatively, where each block of the recording lasted for one minute.

5.2 Data Analysis

As shown in Fig. 5-2A, EEG signals were recorded using Mindo-4S (Hsinchu, Taiwan) [89] which is a wireless and wearable EEG device featuring four dry electrodes and miniature amplifier attached to a lightweight bandage. These dry electrodes are more convenient than and preferred over conventional wet electrodes for measuring EEG signals because they avoid the use of conductive gel and skin preparation, meanwhile, reach signal quality comparable to wet electrodes. The EEG signals were recorded at Fpz, O1, Oz, and O2 sites at a sampling of 500 Hz, where the electrodes were placed according to the extended International 10-20 system and two extra channels, A1 and A2, were used as the reference channels.

An experienced EEG specialist monitored the experiment to ensure that the location of the wearable EEG device did not shift throughout the recording. The artifacts, such as eye movements, blinks, muscle activities, or other artifacts, were visually identified and excluded. All EEG data were analyzed using EEGLAB [62] which is an open source Matlab toolbox supporting electrophysiological signal processing, artifact signal rejection, time/frequency analysis, and visualization. The analytical procedure for EEG signal pre-processing is demonstrated in Fig. 5-2B. The eye-closed epochs of resting state EEG were used for data analysis. The raw EEG signals were down-sampled to 250 Hz then filtered through 1-Hz high-pass and 30-Hz low-pass finite impulse response filters. Finally, the filtered EEG signals were

inspected again using Automatic Continuous Rejection (EEGLAB's plugin function) to remove noisy signals.

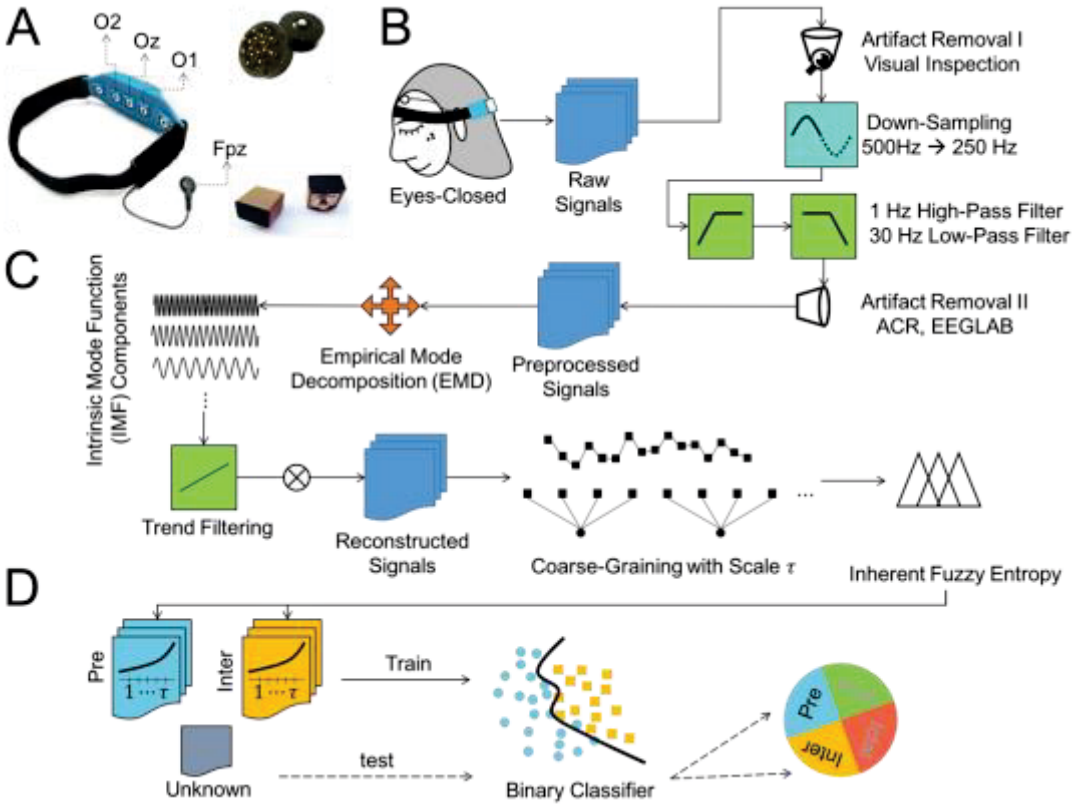

Figure 5-2. Data preprocessing, processing, and analysis. (A) Wearable and wireless EEG device (Mindo-4S) [89]. The EEG signals of the prefrontal (Fpz) and occipital regions (O1, Oz, and O2) were recorded using foam-based and spring-loaded sensors, respectively. (B) EEG data pre-processing including artifact removals, down-sampling, and filtering; (C) EEG complexity estimation using EMD, tread filtering, data reconstruction, coarse-graining, and inherent fuzzy entropy; (D) Binary classification.

5.2.1 EEG processing and measurements

In the power analysis, processed time-series data were transformed into the frequency domain by a 256-point fast Fourier transform with Welch's method. Specifically, 1-min spans of data were analysed with a 256-point moving window with a 128-point overlap. Windowed data were extended to 512 points by zero-padding to calculate power spectra, yielding an estimation of the power spectra with 60 frequency bins from 1 to 30 Hz (frequency resolution: 0.5 Hz). Power spectra of these windows were averaged and converted to a logarithmic scale. Mean delta (δ: 1–3.5 Hz), theta (θ: 4–7.5 Hz), alpha (α: 8–12.5 Hz), and beta (β: 13–30 Hz) band powers of 4 channels were visualised on a two-dimensional (2-D) topographic map.

For EEG signals, the sustainable trends from high non-linear and non-stationary signals could influence the estimation of entropy analysis [90]. To capture the EEG complexity under the circumstances of non-stationarity and non-linearity [90], this study applied multi-scale inherent fuzzy entropy analysis, which employs empirical mode decomposition (EMD) and fuzzy membership function to improve the estimation (Fig. 5-2C). Given a time series EEG signal, the coarse-graining process was applied to non-overlapping segmented EEG data of length τ following EMD [72] to obtain intrinsic mode function (IMF) components at scale τ. The signals were reconstructed using IMF components of interest selected automatically by trend filtering algorithm [73]. Then, fuzzy entropy of each coarse-grained time series was calculated for different temporal scales from 1 to 20. Of note, the entropy estimates of each

patient were averaged over the same migraine phase, and the entropy estimates of each HC were averaged over the examinations.

5.2.2 Individualised prediction models

The concept of training and testing predictors (classification models) was shown in Fig. 5-2D. In this study, we reviewed EEG-based classification algorithms [91] that involved shallow models, multilayer perceptron (MLP), nonlinear Bayesian classifier and support vector machine (SVM) to recognise inter-ictal and pre-ictal phases. The shallow models included the linear discriminant analysis (LDA) that use hyperplanes to separate the data representing the different classes and the k-nearest neighbours (k-NN) algorithm that assign to an unseen point the dominant class among its k nearest neighbours within the training set [92]. An MLP is composed of several layers of neurones: an input layer, possibly one or several hidden layers, and an output layer. Each neurone's input is connected with the output of the previous layer's neurones whereas the neurones of the output layer determine the class of the input feature vector [93]. The Bayes quadratic was used to Bayesian classification that aims at assigning to a feature vector the class it belongs to with the highest probability [92]. The SVM with linear and radial basis function (RBF) kernels also joined in this study, which also uses a discriminant hyperplane to identify classes, but the selected hyperplane is the one that maximises the margins [94]. The classification algorithms can be trained in PRTools (prtools.org/) or LIBSVM toolbox

(www.csie.ntu.edu.tw/~cjlin/libsvm/) in Matlab software. Additionally, we considered a three-fold cross validation (66.7% training set and 33.3% testing set) to train and test the predictors. The assessment criterions that covered accuracy, recall, precision, and F-measure, were used for evaluating the performance of the proposed predictors. In the following, we provided a brief introduction for selected predictors.

1) Shallow models:

Linear Discriminant Analysis

Linear Discriminant Analysis (LDA) [95-97] is a generalisation of Fisher's linear discriminant, which is a method used in statistics, pattern recognition and machine learning to find a linear combination of features that characterises or separates two or more classes of objects or events. As shown in Figure 5-3, the original data was projected to a new space by the projection formula: $y = w^T x$, which minimises the within-class scatter and maximises the scatter between classes

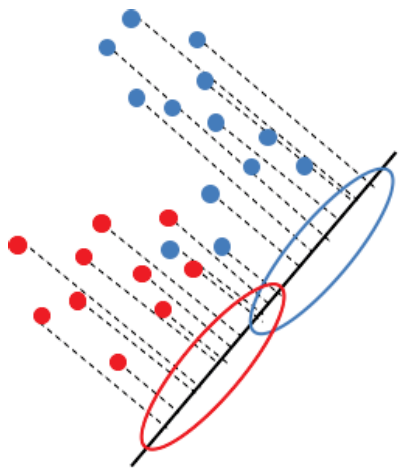

Figure 5-3 LDA projection.

LDA assumes a normal distribution of the data, with equal covariance matrix for both classes. Firstly, the sample mean of data was calculated for each class i :

$$y_i = \frac{1}{n_i}\sum_{x \in D_i} x \tag{1}$$

D_i is the set of data points x for class i , and the projection of y_i is $\overline{y_i} = w^T y_i$.

Then, the scatter matrix for the i-th class, E_i, was computed as

$$E_i = \sum_{x \in D_i}(x - y_i)(x - y_i)^T \tag{2}$$

As considering a two-class problem, i is either 1 or 2, the within-class scatter matrix is defined as:

$$E_W = E_1 + E_2 \tag{3}$$

Next, the scatter of each class i was marked as:

$$\overline{e_i}^2 = \sum_{x \in D_i}(w^T x - w^T u_i)^2 \tag{4}$$

$$= \sum_{x \in D_i} w^T (x - u_i)(x - u_i)^T w \tag{5}$$

$$= w^T E_i w \tag{6}$$

In the following, the sum of scatters of the projected points was represented as:

$$\bar{e_1}^2 + \bar{e_2}^2 = w^T E_W w \tag{7}$$

Similarly, the separations of projected means were represented as:

$$(\overline{y_1} - \overline{y_2})^2 = (w^T y_1 - w^T y_2)^2 \tag{8}$$

$$= w^T (y_1 - y_2)(y_1 - y_2)^T w \tag{9}$$

$$= w^T E_B w \tag{10}$$

where

$$E_B = (y_1 - y_2)(y_1 - y_2)^T \tag{11}$$

Note that E_B is the between-class scatter, and both E_W and E_B are symmetric. In term of E_W and E_B, the criterion function *R(w)* was represented as:

$$R(w) = \frac{w^T E_B w}{w^T E_W w} \tag{12}$$

Considering a two-class problem, the sum of scatters of the projected points was represented as:

$$w E_W w = E_1 + E_2 \tag{13}$$

$$= \sum_{i=1}^{4} \sum_{x \in D_i} (x - y_i)(x - y_i)^T \tag{14}$$

The separations of projected means were represented as:

$$w^T E_B w = \sum_{i=1}^{2} n_i (y_i - M)(y_i - M)^T \tag{15}$$

Where n_i is the number of training samples of *i*-th class, and *M* is total mean vector.

LDA algorithm is to find the *w* that maximises the criterion function *J(w)* and the optimal *w* to design a linear classification algorithm.

K-nearest Neighbor Algorithm

As shown in Fig. 5-4, k-nearest neighbour algorithm (k-NN) [98] is a non-parametric method used for classification and regression. The aim of this technique is to assign to an unseen point the dominant class among its k nearest neighbours within the training set.

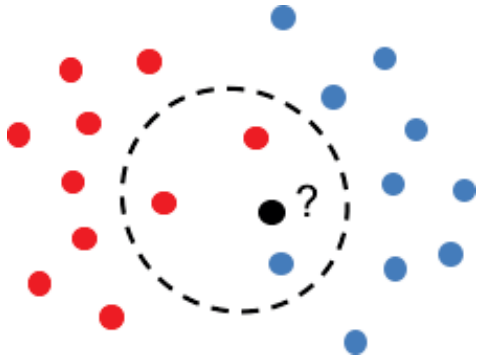

Fig. 5-4 K-nearest neighbour algorithm

In binary (two class) classification problems, k-NN algorithm can figure a boundary by majority vote of its k neighbours. The parameter k in k-NN algorithm is a positive integer which represents the number of nearest neighbour involved in the classification vote. The best choice of *k* depends upon the data. If $k = 1$, then the object is assigned to the class of its nearest neighbour. Larger values of *k* reduce the effect of noise on the classification, but make boundaries between classes less distinct. Generally, *k* is much small than *N*, the sample size. For each x, the distance between *a* and *b*, $|a - b|$, was been defined as follows:

$$d_1(x) \leq d_2(x) \leq \cdots \leq d_N(x) \tag{16}$$

Where $d_1(x)$ is the distance to the nearest sample data, $d_2(x)$ is the distance to the next nearest sample data, and so on.

If x^n are the data points, then define

$$d_N(x) = \min_n |x - x^n| \tag{17}$$

If i is the index of the nearest sample, then define

$$\mathrm{i} = \arg\min_n |x - x^n| \tag{18}$$

The k-nearest neighbour density estimate is

$$\hat{p}(x) = \frac{k}{2Nd_k(x)} \tag{19}$$

Additionally, a kernel function was applied to obtain smoother outcome:

$$\hat{p}(x) = \frac{1}{Nd_k(x)} \sum_{n=1}^{N} \left(\frac{x - x^n}{d_k(x)}\right) \tag{20}$$

The class-conditional densities

$$\hat{p}(x|C_i) = \frac{1}{N_i d_{\text{-}k}(x)} \sum_{n=1}^{N} \left(\frac{x - x^n}{d_k(x)}\right) r_i^n \tag{21}$$

Where r_i^n is 1 if $\mathrm{x}^n \in C_i$ and 0 otherwise. N_i is the number of sample data of C_i:

$$N_i = \sum_n r_i^n \tag{22}$$

Moreover, the prior density is

$$\widehat{\mathrm{P}}(C_i) = \frac{N_i}{N} \tag{23}$$

Finally, the discriminant function was represented as:

$$g_i(x) = \hat{\mathrm{p}}(x|C_i)\widehat{\mathrm{P}}(C_i) \tag{24}$$

$$= \frac{1}{N_i d_{-k}(x)} \sum_{n=1}^{N} \left(\frac{x - x^n}{d_k(x)}\right) r_i^n \qquad (25)$$

2) Multilayer Perception

An Multilayer Perception (MLP) is composed of several layers of neurones: an input layer, possibly one or several hidden layers, and an output layer. Each neurone's input is connected with the output of the previous layer's neurones whereas the neurones of the output layer determine the class of the input feature vector. An MLP with a single hidden layer can be represented graphically as the following Figure 5-5:

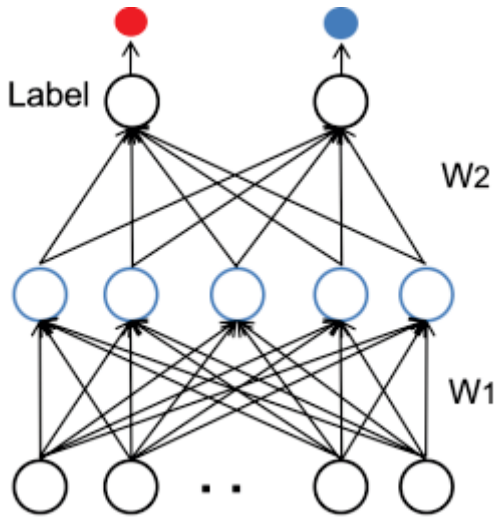

Figure 5-5 A multilayer perception

Formally, a one-hidden-layer MLP is a function $f: Q^D \rightarrow Q^L$, where D is the size of input vector x and L is the size of the output vector $f(x)$, such that, in matrix notation: $f(x) =$

$$F(b^{(2)} + W^{(2)}(s(b^{(1)} + W^{(1)}x))) \qquad (26)$$

Where bias vectors are $b^{(1)}b^{(2)}$, and weight matrices are $W^{(1)}$, $W^{(2)}$ and activation functions are F and s.

The vector $h(x) = \varpi(x) = s(b^{(1)} + W^{(1)}x)$ (27)

It constitutes the hidden layer. $W^{(1)} \in R^{DxDh}$ is the weight matrix connecting the input vector to the hidden layer. Each column $W_i^{(1)}$ represents the weights from the input units to the i-th hidden unit.

Typical choices for s include $tanh$, or the logistic $sigmoid$ function, which was represented as:

$$tanh(a) = (e^a - e^{-a})/(e^a + e^{-a}) \quad (28)$$

$$sigmoid(a) = 1/1(1 + e^{-a}) \quad (29)$$

The $tanh$ function was in this section, because it typically yields to faster training (and sometimes also to better local minima). Both the $tanh$ and $sigmoid$ are scalar-to-scalar functions but their natural extension to vectors and tensors consists in applying them element-wise (e.g. separately on each element of the vector, yielding a same-size vector).

The output vector is then obtained as:

$$f(x) = F(b^{(2)} + W^{(2)}(h(x)) \quad (30)$$

To train an MLP, we learn all parameters of the model, and here we use Stochastic Gradient Descent with mini-batches. The set of parameters to learn is the set $\Phi = \{W^{(2)}, b^{(2)}, W^{(1)}, b^{(1)}\}$. Obtaining the gradients $\Delta L/\Delta\Phi$ can be achieved through the

backpropagation algorithm.

3) Bayesian Classification

Bayesian classification [99] aims at assigning to a feature vector the class it belongs to with the highest probability. The Bayes rule is used to compute the so-called a posteriori probability that a feature vector has of belonging to a given class. Abstractly, naive Bayes is a conditional probability model: given a problem instance to be classified, represented by a vector:

$$x = (x_1, \dots, x_n) \tag{31}$$

It represents some *n* features (independent variables), and assigns to this instance probabilities:

$$p(C_k | x_1, \dots, x_n) \tag{32}$$

for each of k possible outcomes or classes C_k.

The problem with the above formulation is that if the number of features *n* is large or if a feature can take on a large number of values, then basing such a model on probability tables is infeasible. Therefore, we reformulate the model to make it more tractable. Using Bayes' theorem, the conditional probability can be decomposed as:

$$p(C_k | x) = \frac{p(C_k) p(x | C_k)}{p(x)} \tag{33}$$

4) Support Vector Machine

A Support Vector Machine (SVM) also uses a discriminant hyper-plane to identify classes [100]. However, concerning SVM, the selected hyper-plane is the one that maximises the margins, i.e., the distance from the nearest training points. Maximising the margins is known to increase the generalisation capabilities. Thus, the goal of SVM method is to find a hyper-plane by which can separate the data into two parts.

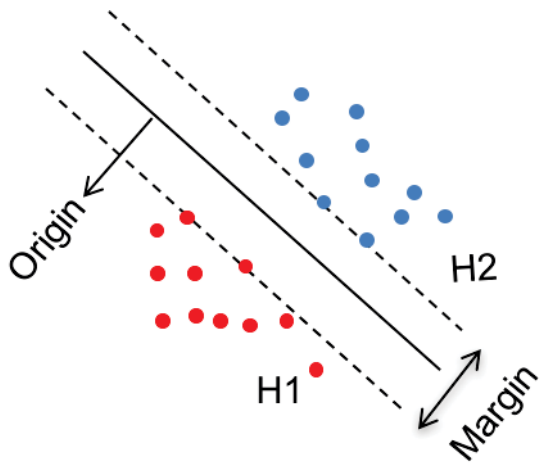

Figure 5-6 Hyper-plane and two classes of data.

For example, figure 5-6 shows a two group data set (H_1 and H_2) with i elements. x_i means each point in data set H_1 and H_2, $i = 1, \ldots, k$. Elements and their labels in data set are defined as:

$$y_i = \begin{cases} 1, if\ x_i\ in\ class\ 1 \\ -1, if\ x_i\ in\ class\ 2 \end{cases} \quad (1)$$

The black solid line in figure 4-6 is a hyper-plane which separates two group data set. The definition of hyper-plane is as following:

$$w^T x + b = 0 \quad (2)$$

Apply the data set into the Equation, then

$$(w^T x_i) + b > 0 \quad if\ y_i = 1 \tag{36}$$

$$(w^T x_i) + b < 0 \quad if\ y_i = -1 \tag{37}$$

It is noteworthy to estimlate the margins of the two groups of data. The larger margin represents the larger distance of the two groups, and support vector machine algorithm try to find the maximum margin of the two groups of data.

Additionaly, the parameters *w* and *b* were be chosen in the maximal margin, which is to find the maximal distance between $w^T x + b = \pm 1$. The distance between $w^T x + b = 1$ and -1 can be written as:

$$\frac{2}{\|w\|} = \frac{2}{\sqrt{w^T w}} \tag{38}$$

And the maximum distance can be written as:

$$max \frac{2}{\|w\|} \equiv min \frac{w^T w}{2} \tag{39}$$

The objective function is

$$min \frac{\|w\|^2}{2} \ \ subject\ to\ y_i(w^T x_i - b) - 1 \geq 0 \ \ \forall i \tag{40}$$

Of note, the Lagrange multiplier method is applied here to transform it into a quadratic equation in one variable:

$$L(w, b, \alpha) = \frac{\|w\|^2}{2} - \sum_{i=1}^{N} \alpha_i [y_i(w^T x_i - b) - 1] \tag{41}$$

The extreme value point match the conditions if:

$$y_i(w^T x_i - b) - 1 = 0, \alpha_i \geq 0 \tag{42}$$

$$y_i(w^T x_i - b) - 1 > 0, \alpha_i = 0 \quad (43)$$

These points locate on support hyper-plane and they are regarded as the "support vector". The α_i of support vectors are greater than zero.

5.2.3 Statistical analysis

The demographic and clinical characteristics between two groups (patients vs. HCs), i.e. categorical variable (gender) and continuous variables (age, BDI, HADS-A, and HADS-D) were compared by using chi-square test and independent *t*-test, respectively. The paired and unpaired *t*-test was performed on each entropy scale to compare respectively the EEG complexity between two phases and between two groups, respectively. The false discovery rate (FDR) correction was used to control for multiple comparisons. The intra-class correlation was estimated to quantify a test-retest reliability. To compare the performance between classification algorithms, one-way ANOVA was used, followed by Turkey's post hoc test to test all pairwise comparisons. The significance level of all tests was set at 0.05.

5.3 Results

5.3.1 Demographic and clinical characteristics

A total of 47 MO patients were recruited in the study. On the basis of headache diary, each EEG examination day was classified as a migraine phase. Seven of patients were excluded due to the lack of EEG examination before migraine attacks within 72 hours. The remaining 40

patients consisted of 10 males and 30 females aged 38.1±8.2 years, where eight patients had at least two examinations during the pre-ictal phase. In terms of the HC group, 40 volunteers consisting of 8 males and 32 females aged 36.1±9.8 years were recruited.

The number of EEG examinations which subjects participated in is summarized in Table 5-1. In total, 198 out of 235 (84.3%) and 151 out of 200 (75.5%) EEG examinations were successfully conducted on patients and HCs, respectively. Most of patients and HCs completed scheduled examinations, but some EEG examinations had not been collected due to subjects' absence. Additionally, the demographics, headache profile, and psychological characteristics of HCs and patients are summarized in Table 5-2. The gender, age, and HADS-A compositions of patients resembled those of HCs, but two psychometric scores, BDI and HADS-D, were significantly higher in migraine patients relative to HCs ($p<0.05$).

Table 5-1 Statistics of EEG Examinations

Number of EEG Examinations	Number of Patients (Proportion)	Number of HCs (Proportion)
5 times	24 (51.0%)	12 (30.0%)
4 times	11 (23.4%)	13 (32.5%)
3 times	10 (21.3%)	9 (22.5%)
2 times	2 (4.3%)	6 (15.0%)

Table 5-2 Demographics, Headache Profile and Psychological Characteristics

Characteristics	HCs (N=40)	Patients (N=40)	*P*
Demographics			
Gender, F:M	32:8	30:10	0.813
Age, y	36.1 ± 9.8	38.1 ± 8.2	0.327
Headache Profile			
Disease duration, y	n/a	18.3 ± 7.8	n/a
Frequency, d/mo	n/a	4.7 ± 2.3	n/a
Onset Age	n/a	19.6 ± 8.9	n/a
MIDAS score[a]	n/a	13.4 ± 12.3	n/a
Psychometric Scores			
BDI	5.5 ± 5.9	9.5 ± 6.3	**0.005**
HADS-A	5.3 ± 3.9	6.8 ± 4.0	0.113
HADS-D	3.2 ± 2.9	4.9 ± 3.6	**0.032**

[a]0–270 range;

Abbreviations: HCs, healthy controls; F:M, ratio of females to males; MIDAS, Migraine Disability Assessment Scale; BDI, Beck Depression Inventory; HADS-A, Hospital Anxiety Depression Scale, Anxiety; HADS-D, Hospital Anxiety Depression Scale, Depression;

Of note, group differences in clinical profiles were analyzed by independent *t*-test for continuous variables and the chi-square test for categorical variables.

5.3.2 Comparisons of EEG dynamics between healthy controls and inter-ictal or pre-ictal patients

Compared with HCs, the EEG power showed no significant change for the inter-ictal or pre-ictal patients. For the estimation of EEG entropy, compared with HCs, the entropy of the inter-ictal phase was significantly lower in all time scales (FDR-adjusted $p<0.01$) (Fig. 5-7A). Nevertheless, the entropy of the pre-ictal phase was similar to that of HCs in each time scale (Fig. 5-7B). At the occipital channels, there was no significant difference in entropy between HCs and patients who were experiencing inter-ictal or pre-ictal phases.

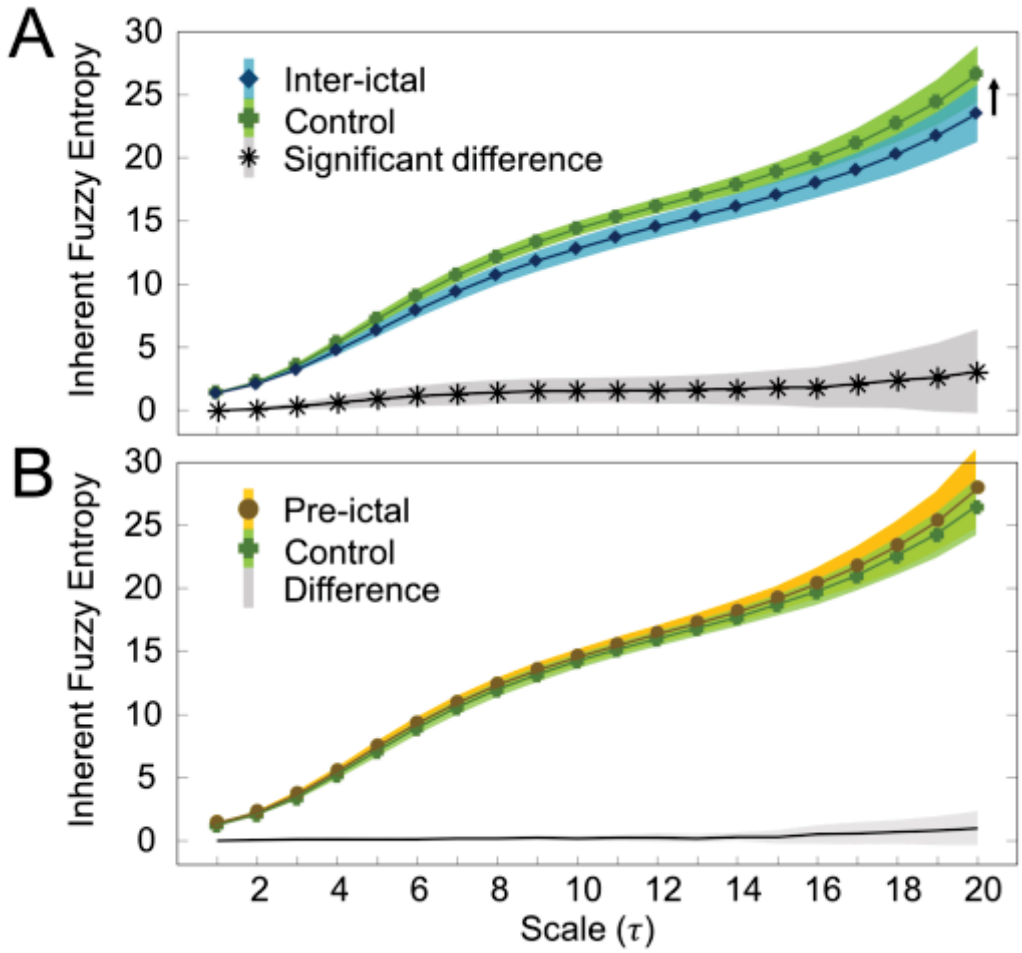

Figure 5-7. EEG entropy of the Fpz channel of inter-ictal and pre-ictal phases vs. HCs. (A) Comparison of EEG entropy between the inter-ictal phase and HCs over the time scales (τ) from 1 to 20. The blue and green traces represent the mean ± the standard deviation of the EEG entropy of the inter-ictal phase and the HCs, respectively. The black trace represents the mean ± the standard deviation of the difference of EEG entropy between two groups. The black asterisk denotes a significantly decreased EEG entropy observed in the inter-ictal phase compared to the HCs (FDR-adjusted p-value<0.01). (B) Comparison of EEG entropy between the pre-ictal phase and HCs over the time scales (τ) from 1 to 20. The yellow and green traces represent the mean ± the standard deviation of the EEG entropy of the pre-ictal phase and the HCs, respectively. There is no significant difference of EEG entropy between two groups.

5.3.3 Comparisons of EEG dynamics between inter-ictal and pre-ictal phases

In the paired comparison (inter-ictal vs. pre-ictal) with 72-hours criterion, there was no differ EEG power between inter-ictal and pre-ictal phases. For the estimation of EEG entropy, the entropy at the Fpz site, measured by inherent fuzzy entropy, over different time scales from 1 to 20 in patients experiencing the inter-ictal as well as the pre-ictal phase is shown in Fig. 5-8. Both phases showed a monotonic increase in entropy with an increasing scale. The difference in entropy between two phases also became large with an increasing scale. The paired *t*-tests revealed a significant increment of EEG entropy in the pre-ictal phase, compared to the inter-ictal phase (FDR-adjusted $p<0.01$) (Fig. 5-8A). The results of the entropy analysis at the O1, Oz, and O2 sites did not show significant difference between two migraine phases.

Given the scale at $\tau = 20$, the increasing trend of the entropy occurred in 29 out of 40 total patients (72.5%) when entering the pre-ictal phase from the inter-ictal phase (Fig. 5-8B). On the contrary, the entropy observed in 11 patients declined. Eight patients with two pre-ictal examinations were selected to analyze the test-retest reliability (Fig. 5-8C). The result showed that intra-class correlation coefficient (ICC) was $r1=0.73$ ($p=0.01$).

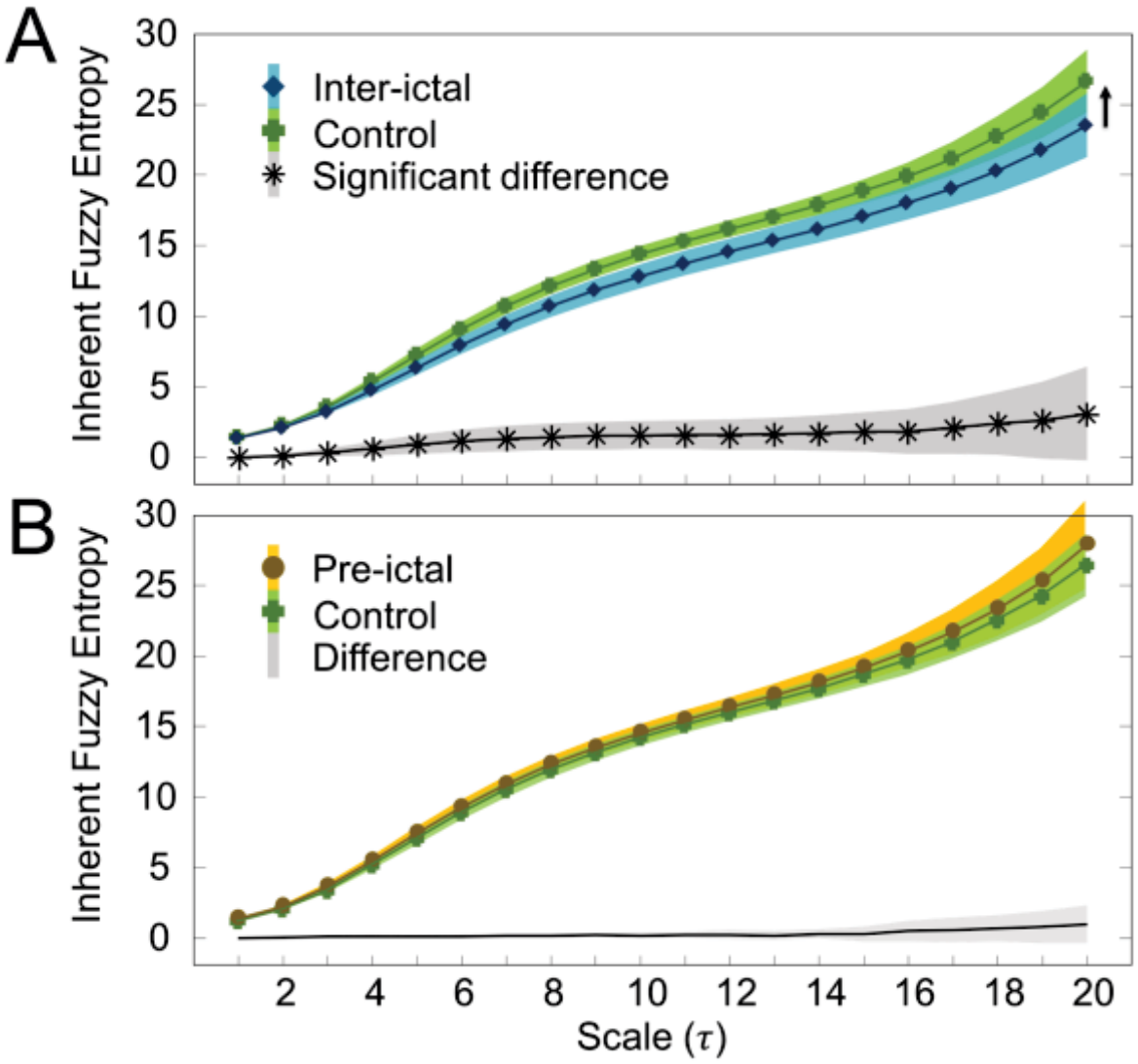

Figure 5-8. EEG entropy of the Fpz channel of inter-ictal and pre-ictal phases. (A) Comparison of EEG entropy between inter-ictal and pre-ictal phases over the time scales (τ) from 1 to 20. The blue and yellow traces represent the mean ± the standard deviation of the EEG entropy of the inter-ictal and pre-ictal phases, respectively. The black trace represents the mean ± the standard deviation of the difference of EEG entropy between two phases. The black asterisk denotes a significantly increased EEG entropy observed in the pre-ictal phase compared to the inter-ictal phase (FDR-adjusted p-value<0.01). (B) Individual changes of the EEG entropy at τ=20 from inter-ictal to pre-ictal phases. The green and red lines represent the increased and decreased

entropy, respectively, when changing from the inter-ictal phase to the pre-ictal phase. (C) Test-retest reliability analysis. The scatter plot reveals the relationship between the 1st pre-ictal and the 2nd pre-ictal phases, where each square represents the entropy of the 1st pre-ictal phase (X-axis) and the 2nd pre-ictal phase (Y-axis) relative to the entropy of the inter-ictal phase.

5.3.4 Performance of the EEG prediction model

As shown in Table 5-3, the performance of the predictors (binary classification) using six selected algorithms (LDA, *k*NN, MLP, Bayesian, SVM-linear and SVM-RBF) in recognizing migraine phases were assessed by four performance matrices, including Accuracy, Recall, Precision, and F-measure. The results showed that SVM-RBF predictor in terms of Accuracy (0.76±0.04) and Recall (0.75±0.05) significantly outperformed other predictors ($p<0.05$). In terms of Precision and F-measure, *k*NN (0.72±0.06 and 0.70±0.06), SVM-linear (0.73±0.05 and 0.70±0.05), and SVM-RBF (0.75±0.05 and 0.74±0.06) had comparable results which were significantly better than the results obtained by LDA, MLP, and Bayesian ($p<0.05$).

Table 5-3 Performance of various predictors

Performance		*Accuracy*	*Recall*	*Precision*	*F-measure*
LDA		0.63±0.06*	0.58±0.06*	0.60±0.06*	0.61±0.07*
***k*NN**		0.71±0.05*	0.68±0.05*	0.72±0.06	0.70±0.06
MLP		0.67±0.06*	0.61±0.06*	0.65±0.06*	0.63±0.06*
Bayesian		0.65±0.05*	0.62±0.05*	0.64±0.06*	0.63±0.06*
SVM Model	**Linear kernel**	0.71±0.04*	0.67±0.05*	0.73±0.05	0.70±0.05
	RBF kernel	**0.76±0.04**	**0.75±0.05**	**0.75±0.05**	**0.74±0.06**

Parameters: LDA: default settings; KNN: k=3; MLP: structure with one hidden layer, and number of units = 5; Bayesian: default settings; SVM with linear kernel: c=0; SVM with RBF kernel: c=10, g=10.

*: After utilizing one-way ANOVA, the Turkey's post hoc test was performed for pair comparison: p <0.05.

5.4 Discussion

Despite progress in migraine research in recent years, extracting a reliable clinical feature that can be used to differentiate migraine phases is still challenging, resulting in a clinical prediction with difficulty to warn patients of imminent headache attack. To the best of our knowledge, this is a pioneering discovery investigating the brain complexity in migraine patients by applying a multi-scale inherent fuzzy entropy algorithm to the resting-state EEG of inter-ictal and pre-ictal phases. The main finding of this study revealed the significantly increased EEG entropy of the Fpz site in migraine patients when entering the pre-ictal phase from the inter-ictal phase. This augmented EEG entropy observed in the pre-ictal phase reached the level comparable with the entropy observed in HCs. Additionally, using EEG entropy of the Fpz site to build a predictor (binary classification) reached a promising accuracy in classify migraine phases.

5.4.1 Prefrontal EEG Complexity in Migraine Patients

This study revealed that the resting-state EEG complexity over prefrontal region, measured using entropy, was altered in patients with MO even during their inter-ictal phase. This cyclic alteration in EEG complexity was identified in the Fpz electrode. Since decreased complexity may represent reduced robustness of the system, our finding may thus reflect a structural or functional abnormality of the underlying cortex, as previous studies on patient with MO have demonstrated both structural (39), and functional (22) abnormality in the

frontal/prefrontal regions. Nevertheless, given that our study also demonstrated a dynamic change of EEG complexity during headache phase transition, such alteration in complexity could likely be generated by functional abnormality. A recent study demonstrating normalization of EEG complexity after treatment in schizophrenic patients also supports this point (14).

Cortical function can be evaluated by different methodologies, such as activation pattern in task-specific fMRI paradigm, and also the analysis of functional connectivity network (FCN) in resting fMRI setting. As shown in previous studies, prefrontal dysfunction in patients with MO could be observed as less activation in response to painful stimuli (23), or even an opposite response pattern in the prefrontal cortex during repeated painful stimulation over the trigeminal nerve area (40). Both studies suggest the pain inhibition control, which is an important function of prefrontal cortex, is impaired in patients with migraine. Additionally, FCN analysis also demonstrated an impaired frontal functional network in patients with MO during their inter-ictal phase (22). All these findings, together with the present results, suggest that the prefrontal cortex may serve as a pivot to regulate pain coping and may be involved in the phase transition in migraine patients.

Nevertheless, we did not observe the difference in complexity between HC and inter-ictal migraine patients over the occipital region. The strong alpha activity during eyes-closed periods may have interfered with the complexity measurement, leading to such results. Prior

studies have shown that a visual stimulus task (25, 28) might be preferable for deciphering how the occipital region handles visual functions in migraine patients during different phases.

5.4.2 EEG Complexity Normalization in Pre-Ictal Phase

The other interesting finding of our study is that although patients with MO presented with a decreased prefrontal complexity during their inter-ictal phase, the complexity increased during their pre-ictal phase, and up to the level comparable to that of HCs. EEG complexity capturing migraine phase transition provided an opportunity for us to develop a classifier to recognize the patient's phase in which the patient was situated. Although not being completely understood, the mechanism behind this "pre-ictal normalization" of various electrophysiological properties, e.g. resting-state EEG power and coherence, visual and auditory evoked response (5, 11-13), may be related to the increased serotonin synthesis (41), or the reorganization of inhibitory/excitatory control of brain homeostasis (42) during the pre-ictal phase. There were only few studies addressing the issue of pre-ictal functional change in patients with migraine, mainly owing to the difficulty in recruiting patients during this period. A recent PET study observing the activation pattern during the pre-monitory phase by nitroglycerin induction may provide some clues (24). In that study, an increased frontal activity was found in the pre-monitory phase, compared to that in the inter-ictal phase. The result supports our finding, as an increased complexity may represent an enhanced system function.

Taken together, brain activity normalization may be a signature that may be used to predict at least in some MO patients the forthcoming migraine attacks.

5.4.3 EEG-based Migraine Phase Classification

With the rapid development of bio-sensing technology [107-109], a wireless and wearable EEG device featuring dry electrodes and miniature circuits benefit immeasurably the neurophysiological signal recording. The present study used one of the EEG recording systems with dry electrodes, Mindo-4S (Hsinchu, Taiwan) [89], to capture brainwave activity in a convenient and comfortable way from patients and also used one of the effective complexity measurements, multi-scale inherent fuzzy entropy, to evaluate cyclic patterns of the migraine phases. As the study population are all migraine patients who have no aura symptom in the pre-ictal phase, the characteristics in terms of the easily-assessed brain region, the wearable EEG solution, and the low computational complexity algorithm make the prefrontal EEG complexity a feasible signature of an imminent migraine attack in clinical usage.

5.4.4 Results of 48-hour and 36-hour Criteria

If 48- and 36-hour criteria were applied to the definition of the pre-ictal phase, the selected sample would be 30 patients (6 males and 24 females aged 38.8±7.9 years) and 25 patients (6 male and 19 females aged 38.0±7.2 years), respectively. The demographics,

headache profiles, and psychological characteristics of patients being classified by 48- and 36-hour criteria are summarized in Appendix Table 4-1. The conclusion was the same as Table 4-2 that the gender, age, and HADS-A of patients were not significantly different with HCs. Patients exhibited significantly higher BDI and HADS-D compared to HCs ($p<0.05$). All demographics, headache profile, and psychological characteristics showed no significant difference among patient groups of different criteria.

Similar EEG results were obtained with different definitions of the pre-ictal phase. A total of 21 out of 30 patients (48-hour criterion) (70%) and 17 out of 25 patients (36-hour criterion) (68%) had a higher entropy during the pre-ictal phase compared to the inter-ictal phase. The entropy of the inter-ictal phase was significantly lower in all time scales relative to HCs (FDR-adjusted $p<0.01$), and no significant difference was found in the entropy of the pre-ictal phase and the HCs in each time scale. The test-retest reliability analysis could not be performed due to small case number with two or more pre-ictal EEG examinations based on the 36-hour or 48-hour criteria.

5.4.5 Limitations

This study has limitations. First, the number of data which were used to perform the test-retest reliability analysis was small. Although 47 migraine patients were recruited, only eight of them had at least two pre-ictal EEG recordings. If possible, the result needs to be

confirmed with a larger patient number. Second, the placement of the EEG electrodes (Fpz, O1, Oz, and O2 sites) was limited due to the design of the headband. Although the considerable literature has fully justified the reason of selecting these migraine-related brain regions, mining the whole brain activity especially for the coupling between distinct brain areas in migraine patients is preferable to fill in the knowledge gap. Third, the current study focused on deciphering the EEG patterns which can be used to warn the patients of imminent migraine attack. The migraine phases of interest are only the inter-ictal and pre-ictal states. A mega longitudinal experiment covering inter-ictal, pre-ictal, ictal, and post-ictal phases is recommended to be capable of comprehensively obtaining full spectrum of the phase transition.

5.5 Conclusion

This study had longitudinally collected resting-state EEG data from migraine without aura patients to investigate the complexity of brain activity. Our results highlighted the feasibility of the entropy measurement used in EEG analysis involving the comparison of the brain complexity between migraine phases. The reliability test revealed that the prefrontal EEG

complexity of the migraine patients increased to the level comparable with heathy participants within hours before a forthcoming headache attack. The binary classification built by using prefrontal EEG complexity patterns could achieve a sound classification accuracy in classifying inter-ictal and pre-ictal phases. The findings conclude that brain signature of the migraine patients discovered by entropy measurement not only explore insights into complex brain complexity, but also provide the clinical usage for migraine prediction.

Chapter 6 SUMMARY AND FUTURE WORKS

6.1 Summary

Migraine is a common episodic neurological disorder with complex pathophysiology characterised by recurrent headaches during a given period, such as one month. Only a small group of migraine patients (13-31%) experience transient neurological symptoms, most frequently visual aura, prior to headache onset, with the majority of patients experiencing no premonitory symptoms. This study explored neurophysiological evidence of the resting-state electroencephalogram (EEG) power, coherence and entropy to support the cortical signals relating to different migraine phases, and then used this to develop an EEG-based system for predicting migraine attacks.

Most of the data described in the thesis suggest brain cortical activity relates to different migraine phases and highlights differences between migraine patients and healthy controls. First, we investigated EEG devices, pre-processing and artefact removal methods, and feature extraction technologies, including power, coherence and entropy analysis. Then, we examined the EEG dynamics of a migraine cycle in resting-state condition. The results indicated that EEG power spectral and coherence were significantly increased in the pre-ictal group, relative to EEG data obtained from the inter-ictal group. Inter-ictal patients had decreased EEG power and connectivity relative to healthy controls, which were “normalised” in the pre-ictal patients. These findings suggested that pre-ictal patients augmented coupling in the fronto-central and centro-posterior networks and reduced coupling in the fronto-occipital network.

On the basis of longitudinal design, we estimated personalised brain dynamics before migraine attacks using a wearable EEG device. The results showed the EEG entropy of individual patients in the pre-ictal phase, resembling normal control subjects, was significantly higher than that in their inter-ictal phase in prefrontal area. That is, the entropy measures identified enhancement or "normalisation" of frontal EEG complexity in pre-ictal phase. Based on this discovery of inter- and pre-ictal EEG entropy in individuals, we proposed a support vector machine (SVM) based system with 76% accuracy to predict migraine attacks. The prediction system characterises the EEG entropy of a single (prefrontal) area and favours the application of brain-computer interface in migraine.

6.2 Future Works

This study represents the first large-scale collection of pre-attack migraine data used to explore the EEG power, coherence and entropy in brain cortical dynamics. However, the computing times of coherence and entropy and training times of predictors are important considerations when applying it to practical or on-line applications. Given this limitation, we aim to improve the algorithms and predictors with the characteristics of accelerated speed. In addition, the classification of a migraine cycle is restricted to four phases, i.e., inter-ictal, pre-ictal, ictal, and post-ictal. Future longitudinal studies and examining long-term EEG entropy are necessary to extend the current findings.

References

[1] L. Stovner, K. Hagen, R. Jensen, Z. Katsarava, R. Lipton, A. Scher*, et al.*, "The global burden of headache: a documentation of headache prevalence and disability worldwide," *Cephalalgia,* vol. 27, pp. 193-210, 2007.

[2] R. J. Stark, L. Valenti, and G. C. Miller, "Management of migraine in Australian general practice," *Medical Journal of Australia,* vol. 187, p. 142, 2007.

[3] S. J. Wang, J. L. Fuh, Y. H. Young, S. R. Lu, and B. C. Shia, "Prevalence of migraine in Taipei, Taiwan: a population-based survey," *Cephalalgia,* vol. 20, pp. 566-572, 2000.

[4] P. J. Goadsby, R. B. Lipton, and M. D. Ferrari, "Migraine--current understanding and treatment," *N Engl J Med,* vol. 346, pp. 257-70, Jan 24 2002.

[5] M. E. Bigal, J. N. Liberman, and R. B. Lipton, "Obesity and migraine: a population study," *Neurology,* vol. 66, pp. 545-50, Feb 28 2006.

[6] R. K. Cady, F. Sheftell, R. B. Lipton, S. O'Quinn, M. Jones, D. G. Putnam*, et al.*, "Effect of early intervention with sumatriptan on migraine pain: retrospective analyses of data from three clinical trials," *Clin Ther,* vol. 22, pp. 1035-48, Sep 2000.

[7] L. P. Queiroz, A. M. Rapoport, R. E. Weeks, F. D. Sheftell, S. E. Siegel, and S. M. Baskin, "Characteristics of migraine visual aura," *Headache,* vol. 37, pp. 137-41, Mar 1997.

[8] C. D. Chong, N. Gaw, Y. Fu, J. Li, T. Wu, and T. J. Schwedt, "Migraine classification using magnetic resonance imaging resting-state functional connectivity data," *Cephalalgia,* p. 0333102416652091, 2016.

[9] J. Olesen, R. Burstein, M. Ashina, and P. Tfelt-Hansen, "Origin of pain in migraine: evidence for peripheral sensitisation," *The Lancet Neurology,* vol. 8, pp. 679-690, 2009.

[10] D. Levy, "Migraine pain and nociceptor activation—where do we stand?," *Headache: The Journal of Head and Face Pain,* vol. 50, pp. 909-916, 2010.

[11] T. A. Smitherman, R. Burch, H. Sheikh, and E. Loder, "The prevalence, impact, and treatment of migraine and severe headaches in the United States: a review of statistics from national surveillance studies," *Headache: The Journal of Head and Face Pain,* vol. 53, pp. 427-436, 2013.

[12] D. Mantini, M. G. Perrucci, C. Del Gratta, G. L. Romani, and M. Corbetta, "Electrophysiological signatures of resting state networks in the human brain," *Proceedings of the National Academy of Sciences,* vol. 104, pp. 13170-13175, 2007.

[13] B. A. Taheri, R. T. Knight, and R. L. Smith, "A dry electrode for EEG recording," *Electroencephalography and clinical neurophysiology,* vol. 90, pp. 376-383, 1994.

[14] E. Niedermeyer and F. L. da Silva, *Electroencephalography: basic principles, clinical applications, and related fields*: Lippincott Williams & Wilkins, 2005.

[15] B. A. Diaz, S. Van Der Sluis, S. Moens, J. S. Benjamins, F. Migliorati, D. Stoffers*, et al.*, "The Amsterdam Resting-State Questionnaire reveals multiple phenotypes of resting-state cognition," *Frontiers in human neuroscience,* vol. 7, p. 446, 2013.

[16] S. Aurora and F. Wilkinson, "The brain is hyperexcitable in migraine," *Cephalalgia,* vol. 27, pp. 1442-1453, 2007.

[17] G. Coppola, F. Pierelli, and J. Schoenen, "Habituation and migraine," *Neurobiol Learn Mem,* vol. 92, pp. 249-59, Sep 2009.

[18] A. Humeau-Heurtier, "The multiscale entropy algorithm and its variants: A Review," *Entropy,* vol. 17, pp. 3110-3123, 2015.

[19] T. Sand, N. Zhitniy, L. R. White, and L. J. Stovner, "Visual evoked potential latency, amplitude and habituation in migraine: a longitudinal study," *Clin Neurophysiol,* vol. 119, pp. 1020-7, May 2008.

[20] G. Cosentino, B. Fierro, and F. Brighina, "From different neurophysiological methods to conflicting pathophysiological views in migraine: a critical review of literature," *Clin Neurophysiol,* vol. 125, pp. 1721-30, Sep 2014.

[21] M. de Tommaso, A. Ambrosini, F. Brighina, G. Coppola, A. Perrotta, F. Pierelli*, et al.*, "Altered processing of sensory stimuli in patients with migraine," *Nat Rev Neurol,* vol. 10, pp. 144-55, Mar 2014.

[22] M. de Tommaso, S. Stramaglia, D. Marinazzo, G. Trotta, and M. Pellicoro, "Functional and effective connectivity in EEG alpha and beta bands during intermittent flash stimulation in migraine with and without aura," *Cephalalgia,* vol. 33, pp. 938-47, Aug 2013.

[23] M. de Tommaso, G. Trotta, E. Vecchio, K. Ricci, F. Van de Steen, A. Montemurno*, et al.*, "Functional Connectivity of EEG Signals Under Laser Stimulation in Migraine," *Front Hum Neurosci,* vol. 9, p. 640, 2015.

[24] M. Bjork and T. Sand, "Quantitative EEG power and asymmetry increase 36 h before a migraine attack," *Cephalalgia,* vol. 28, pp. 960-8, Sep 2008.

[25] M. H. Bjork, L. J. Stovner, M. Engstrom, M. Stjern, K. Hagen, and T. Sand, "Interictal quantitative EEG in migraine: a blinded controlled study," *J Headache Pain,* vol. 10, pp. 331-9, Oct 2009.

[26] T. Takahashi, R. Y. Cho, T. Mizuno, M. Kikuchi, T. Murata, K. Takahashi*, et al.*, "Antipsychotics reverse abnormal EEG complexity in drug-naive schizophrenia: a multiscale entropy analysis," *Neuroimage,* vol. 51, pp. 173-182, 2010.

[27] M. Costa, A. L. Goldberger, and C.-K. Peng, "Multiscale entropy analysis of complex physiologic time series," *Physical review letters,* vol. 89, p. 068102, 2002.

[28] T. Mizuno, T. Takahashi, R. Y. Cho, M. Kikuchi, T. Murata, K. Takahashi*, et al.*, "Assessment of EEG dynamical complexity in Alzheimer's disease using multiscale entropy," *Clinical Neurophysiology,* vol. 121, pp. 1438-1446, 2010.

[29] J. Olesen, M. G. Bousser, H. C. Diener, D. Dodick, M. First, P. Goadsby*, et al.*, "New appendix criteria open for a broader concept of chronic migraine," *Cephalalgia,* vol. 26, pp. 742-746, 2006.

[30] M. Piane, P. Lulli, I. Farinelli, S. Simeoni, S. De Filippis, F. R. Patacchioli*, et al.*, "Genetics of migraine and pharmacogenomics: some considerations," *The journal of headache and pain,* vol. 8, pp. 334-339, 2007.

[31] S. Tutunchi and S. Akhavan, "Evaluation of NOS3 Gene rs1800779 Polymorphism in Iranian Patients affected by Migraine and Normal individuals," *Advances in Bioresearch,* vol. 7, 2016.

[32] C. Armstrong and A. A. o. Neurology, "AAN/AHS update recommendations for migraine prevention in adults," *American family physician,* vol. 87, p. 584, 2013.

[33] J. Schoenen, "Neurophysiological features of the migrainous brain," *Neurol Sci,* vol. 27 Suppl 2, pp. S77-81, May 2006.

[34] W. Chen, Z. Wang, H. Xie, and W. Yu, "Characterization of surface EMG signal based on fuzzy entropy," *Neural Systems and Rehabilitation Engineering, IEEE Transactions on,* vol. 15, pp. 266-272, 2007.

[35] A. C. Yang, S.-J. Wang, K.-L. Lai, C.-F. Tsai, C.-H. Yang, J.-P. Hwang*, et al.*, "Cognitive and neuropsychiatric correlates of EEG dynamic complexity in patients with Alzheimer's disease," *Progress in Neuro-Psychopharmacology and Biological Psychiatry,* vol. 47, pp. 52-61, 2013.

[36] G. Coppola, F. Pierelli, and J. Schoenen, "Is the cerebral cortex hyperexcitable or hyperresponsive in migraine?," *Cephalalgia,* vol. 27, pp. 1427-39, Dec 2007.

[37] E. M. Khedr, M. A. Ahmed, and K. A. Mohamed, "Motor and visual cortical excitability in migraineurs patients with or without aura: transcranial magnetic stimulation," *Neurophysiol Clin,* vol. 36, pp. 13-8, Jan-Feb 2006.

[38] A. Judit, P. S. Sandor, and J. Schoenen, "Habituation of visual and intensity dependence of auditory evoked cortical potentials tends to normalize just before and during the migraine attack," *Cephalalgia,* vol. 20, pp. 714-9, Oct 2000.

[39] O. Bruni, P. M. Russo, C. Violani, and V. Guidetti, "Sleep and migraine: an actigraphic study," *Cephalalgia,* vol. 24, pp. 134-9, Feb 2004.

[40] V. Sakkalis, "Review of advanced techniques for the estimation of brain connectivity measured with EEG/MEG," *Computers in biology and medicine,* vol. 41, pp. 1110-1117, 2011.

[41] E. van Diessen, T. Numan, E. van Dellen, A. W. van der Kooi, M. Boersma, D. Hofman*, et al.*, "Opportunities and methodological challenges in EEG and MEG

resting state functional brain network research," *Clin Neurophysiol,* vol. 126, pp. 1468-81, Aug 2015.

[42] R. D. Pascual-Marqui, R. J. Biscay, J. Bosch-Bayard, D. Lehmann, K. Kochi, T. Kinoshita*, et al.*, "Assessing direct paths of intracortical causal information flow of oscillatory activity with the isolated effective coherence (iCoh)," *Frontiers in human neuroscience,* vol. 8, 2014.

[43] A. Russo, A. Tessitore, A. Giordano, D. Corbo, L. Marcuccio, M. De Stefano*, et al.*, "Executive resting-state network connectivity in migraine without aura," *Cephalalgia,* vol. 32, pp. 1041-8, Oct 2012.

[44] T. J. Schwedt, L. Larson-Prior, R. S. Coalson, T. Nolan, S. Mar, B. M. Ances*, et al.*, "Allodynia and descending pain modulation in migraine: a resting state functional connectivity analysis," *Pain Med,* vol. 15, pp. 154-65, Jan 2014.

[45] M. Costa, A. L. Goldberger, and C.-K. Peng, "Multiscale entropy analysis of biological signals," *Physical review E,* vol. 71, p. 021906, 2005.

[46] S. M. Pincus, "Approximate entropy as a measure of system complexity," *Proceedings of the National Academy of Sciences,* vol. 88, pp. 2297-2301, 1991.

[47] J. S. Richman and J. R. Moorman, "Physiological time-series analysis using approximate entropy and sample entropy," *American Journal of Physiology-Heart and Circulatory Physiology,* vol. 278, pp. H2039-H2049, 2000.

[48] M. de Tommaso, K. Ricci, E. Vecchio, D. Marinazzo, G. Trotta, and S. Stramaglia, "Migraine and functional connectivity: an innovative pathophysiological perspective," *The journal of headache and pain,* vol. 16, 2015.

[49] G. Coppola, F. Pierelli, P. M. Omland, and T. Sand, "Neurophysiology of Migraine," in *Pathophysiology of Headaches*, ed: Springer, 2015, pp. 155-174.

[50] R. Lev, Y. Granovsky, and D. Yarnitsky, "Enhanced Pain Expectation in Migraine: EEG-Based Evidence for Impaired Prefrontal Function," *Headache: The Journal of Head and Face Pain,* vol. 53, pp. 1054-1070, 2013.

[51] Y. S. Koo, D. Ko, G.-T. Lee, K. Oh, M.-S. Kim, K. H. Kim*, et al.*, "Reduced frontal P3a amplitude in migraine patients during the pain-free period," *Journal of Clinical Neurology,* vol. 9, pp. 43-50, 2013.

[52] T. Sand and J. V. Vingen, "Visual, long-latency auditory and brainstem auditory evoked potentials in migraine: relation to pattern size, stimulus intensity, sound and light discomfort thresholds and pre-attack state," *Cephalalgia,* vol. 20, pp. 804-20, Nov 2000.

[53] W. T. Chen, S. J. Wang, J. L. Fuh, C. P. Lin, Y. C. Ko, and Y. Y. Lin, "Peri-ictal normalization of visual cortex excitability in migraine: an MEG study," *Cephalalgia,* vol. 29, pp. 1202-11, Nov 2009.

[54] Z. Cao, C.-T. Lin, C.-H. Chuang, K.-L. Lai, A. C. Yang, J.-L. Fuh*, et al.*, "Resting-state EEG power and coherence vary between migraine phases," *The Journal of Headache and Pain,* vol. 17, p. 102, 2016.

[55] M. Siniatchkin, P. Kropp, W.-D. Gerber, and U. Stephani, "Migraine in childhood–are periodically occurring migraine attacks related to dynamic changes of cortical information processing?," *Neuroscience letters,* vol. 279, pp. 1-4, 2000.

[56] S. Evers, F. Quibeldey, K.-H. Grotemeyer, B. Suhr, and I. Husstedt, "Dynamic changes of cognitive habituation and serotonin metabolism during the migraine interval," *Cephalalgia,* vol. 19, pp. 485-491, 1999.

[57] R. Göder, G. Fritzer, A. Kapsokalyvas, P. Kropp, U. Niederberger, H. Strenge*, et al.*, "Polysomnographic findings in nights preceding a migraine attack," *Cephalalgia,* vol. 21, pp. 31-37, 2001.

[58] M. Steriade, P. Gloor, R. R. Llinas, F. L. Da Silva, and M.-M. Mesulam, "Basic mechanisms of cerebral rhythmic activities," *Electroencephalography and clinical neurophysiology,* vol. 76, pp. 481-508, 1990.

[59] R. R. Llinás, U. Ribary, D. Jeanmonod, E. Kronberg, and P. P. Mitra, "Thalamocortical dysrhythmia: a neurological and neuropsychiatric syndrome characterized by magnetoencephalography," *Proceedings of the National Academy of Sciences,* vol. 96, pp. 15222-15227, 1999.

[60] S. E. Lakhan, M. Avramut, and S. J. Tepper, "Structural and functional neuroimaging in migraine: insights from 3 decades of research," *Headache: The Journal of Head and Face Pain,* vol. 53, pp. 46-66, 2013.

[61] R. J. Barry, A. R. Clarke, S. J. Johnstone, C. A. Magee, and J. A. Rushby, "EEG differences between eyes-closed and eyes-open resting conditions," *Clinical Neurophysiology,* vol. 118, pp. 2765-2773, 2007.

[62] A. Delorme and S. Makeig, "EEGLAB: an open source toolbox for analysis of single-trial EEG dynamics including independent component analysis," *Journal of Neuroscience Methods,* vol. 134, pp. 9-21, 2004.

[63] J. C. Shaw, "Correlation and coherence analysis of the EEG: a selective tutorial review," *International Journal of Psychophysiology,* vol. 1, pp. 255-266, 1984.

[64] J.-P. Lachaux, E. Rodriguez, J. Martinerie, and F. J. Varela, "Measuring phase synchrony in brain signals," *Human brain mapping,* vol. 8, pp. 194-208, 1999.

[65] K. J. Blinowska, R. Kuś, and M. Kamiński, "Granger causality and information flow in multivariate processes," *Physical Review E,* vol. 70, p. 050902, 2004.

[66] L. A. Baccalá and K. Sameshima, "Partial directed coherence," in *Methods in Brain Connectivity Inference through Multivariate Time Series Analysis*, ed: CRC Press, 2014, pp. 57-73.

[67] L. A. Baccalá, K. Sameshima, and D. Takahashi, "Generalized partial directed coherence," in *Digital Signal Processing, 2007 15th International Conference on*, 2007, pp. 163-166.

[68] A. Delorme, T. Mullen, C. Kothe, Z. Akalin Acar, N. Bigdely-Shamlo, A. Vankov*, et al.*, "EEGLAB, SIFT, NFT, BCILAB, and ERICA: new tools for advanced EEG processing," *Comput Intell Neurosci,* vol. 2011, pp. 1-12, 2011.

[69] L. Zadeh, "Fuzzy Sets," *Information and Control,* vol. 8, pp. 338-353, 1965.

[70] W. Chen, J. Zhuang, W. Yu, and Z. Wang, "Measuring complexity using fuzzyen, apen, and sampen," *Medical Engineering & Physics,* vol. 31, pp. 61-68, 2009.

[71] K. Hu, P. C. Ivanov, Z. Chen, P. Carpena, and H. E. Stanley, "Effect of trends on detrended fluctuation analysis," *Physical Review E,* vol. 64, p. 011114, 2001.

[72] N. E. Huang, Z. Shen, S. R. Long, M. C. Wu, H. H. Shih, Q. Zheng*, et al.*, "The empirical mode decomposition and the Hilbert spectrum for nonlinear and non-stationary time series analysis," in *Proceedings of the Royal Society of London A: Mathematical, Physical and Engineering Sciences*, 1998, pp. 903-995.

[73] A. Moghtaderi, P. Flandrin, and P. Borgnat, "Trend filtering via empirical mode decompositions," *Computational Statistics & Data Analysis,* vol. 58, pp. 114-126, 2013.

[74] "The International Classification of Headache Disorders: 2nd edition," *Cephalalgia,* vol. 24 Suppl 1, pp. 9-160, 2004.

[75] G. H. Klem, H. O. Lüders, H. Jasper, and C. Elger, "The ten-twenty electrode system of the International Federation," *Electroencephalogr Clin Neurophysiol,* vol. 52, 1999.

[76] J. N. Acharya, A. J. Hani, P. D. Thirumala, and T. N. Tsuchida, "American Clinical Neurophysiology Society Guideline 3: A Proposal for Standard Montages to Be Used in Clinical EEG," *J Clin Neurophysiol,* vol. 33, 2016.

[77] A. Delorme and S. Makeig, "EEGLAB: An open source toolbox for analysis of single‐trial EEG dynamics including independent component analysis," *J. Neurosci. Methods,* vol. 134, pp. 9-21, 2004.

[78] S. S. Chung, P. Gerber, and K. A. Kirlin, "Ictal eye closure is a reliable indicator for psychogenic nonepileptic seizures," *Neurology,* vol. 66, pp. 1730-1731, 2006.

[79] D. A. Gusnard and M. E. Raichle, "Searching for a baseline: functional imaging and the resting human brain," *Nature Reviews Neuroscience,* vol. 2, pp. 685-694, 2001.

[80] B. Clemens, J. Bank, P. Piros, M. Bessenyei, S. Veto, M. Toth*, et al.*, "Three-dimensional localization of abnormal EEG activity in migraine: a low resolution electromagnetic tomography (LORETA) study of migraine patients in the pain-free interval," *Brain Topogr,* vol. 21, pp. 36-42, Sep 2008.

[81] T. Sand, "EEG in migraine: a review of the literature," *Funct Neurol,* vol. 6, pp. 7-22, Jan-Mar 1991.

[82] M. Siniatchkin, W. D. Gerber, P. Kropp, and A. Vein, "How the brain anticipates an attack: a study of neurophysiological periodicity in migraine," *Funct Neurol,* vol. 14, pp. 69-77, Apr-Jun 1999.

[83] Y. Sakai, C. Dobson, M. Diksic, M. Aubé, and E. Hamel, "Sumatriptan normalizes the migraine attack-related increase in brain serotonin synthesis," *Neurology,* vol. 70, pp. 431-439, 2008.

[84] F. H. Maniyar, T. Sprenger, T. Monteith, C. J. Schankin, and P. J. Goadsby, "The Premonitory Phase of Migraine–What Can We Learn From It?," *Headache: The Journal of Head and Face Pain,* vol. 55, pp. 609-620, 2015.

[85] R. Barry and A. Clarke, "Resting state brain oscillations and symptom profiles in attention deficit/hyperactivity disorder," *Supplements to Clinical neurophysiology,* vol. 62, pp. 275-287, 2012.

[86] C. Tas, M. Cebi, O. Tan, G. Hızlı-Sayar, N. Tarhan, and E. C. Brown, "EEG power, cordance and coherence differences between unipolar and bipolar depression," *Journal of affective disorders,* vol. 172, pp. 184-190, 2015.

[87] M. Gerwig, L. Niehaus, O. Kastrup, P. Stude, and H. C. Diener, "Visual cortex excitability in migraine evaluated by single and paired magnetic stimuli," *Headache: The Journal of Head and Face Pain,* vol. 45, pp. 1394-1399, 2005.

[88] M. Bjørk, L. Stovner, K. Hagen, and T. Sand, "What initiates a migraine attack? Conclusions from four longitudinal studies of quantitative EEG and steady-state visual-evoked potentials in migraineurs," *Acta Neurologica Scandinavica,* vol. 124, pp. 56-63, 2011.

[89] L.-D. Liao, I.-J. Wang, S.-F. Chen, J.-Y. Chang, and C.-T. Lin, "Design, Fabrication and Experimental Validation of a Novel Dry-Contact Sensor for Measuring Electroencephalography Signals without Skin Preparation," *Sensors,* vol. 11, pp. 5819-5834, May 2011.

[90] M. Costa, A. Priplata, L. Lipsitz, Z. Wu, N. Huang, A. L. Goldberger*, et al.*, "Noise and poise: enhancement of postural complexity in the elderly with a stochastic-resonance–based therapy," *EPL (Europhysics Letters),* vol. 77, p. 68008, 2007.

[91] F. Lotte, M. Congedo, A. Lécuyer, F. Lamarche, and B. Arnaldi, "A review of classification algorithms for EEG-based brain–computer interfaces," *Journal of neural engineering,* vol. 4, p. R1, 2007.

[92] R. O. Duda, P. E. Hart, and D. G. Stork, *Pattern classification*: John Wiley & Sons, 2012.

[93] C. M. Bishop, *Neural networks for pattern recognition*: Oxford university press, 1995.

[94] C. J. Burges, "A tutorial on support vector machines for pattern recognition," *Data mining and knowledge discovery,* vol. 2, pp. 121-167, 1998.

[95] R. A. Fisher, "The use of multiple measurements in taxonomic problems," *Annals of eugenics,* vol. 7, pp. 179-188, 1936.

[96] G. McLachlan, *Discriminant analysis and statistical pattern recognition* vol. 544: John Wiley & Sons, 2004.

[97] P. A. Lachenbruch, "Discriminant Analysis," in *Encyclopedia of Statistical Sciences*, ed: John Wiley & Sons, Inc., 2004.

[98] T. Cover and P. Hart, "Nearest neighbor pattern classification," *Information Theory, IEEE Transactions on,* vol. 13, pp. 21-27, 1967.

[99] P. Cheeseman, M. Self, J. Kelly, W. Taylor, D. Freeman, and J. C. Stutz, "Bayesian Classification," in *AAAI*, 1988, pp. 607-611.

[100] J. A. Suykens and J. Vandewalle, "Least squares support vector machine classifiers," *Neural processing letters,* vol. 9, pp. 293-300, 1999.

[101] C. Mainero, J. Boshyan, and N. Hadjikhani, "Altered functional magnetic resonance imaging resting-state connectivity in periaqueductal gray networks in migraine," *Annals of neurology,* vol. 70, pp. 838-845, 2011.

[102] D. Aderjan, A. Stankewitz, and A. May, "Neuronal mechanisms during repetitive trigemino-nociceptive stimulation in migraine patients," *Pain,* vol. 151, pp. 97-103, 2010.

[103] A. Russo, A. Tessitore, A. Giordano, D. Corbo, L. Marcuccio, M. De Stefano*, et al.*, "Executive resting-state network connectivity in migraine without aura," *Cephalalgia,* vol. 32, pp. 1041-1048, 2012.

[104] D. S. Bassett and M. S. Gazzaniga, "Understanding complexity in the human brain," *Trends in cognitive sciences,* vol. 15, pp. 200-209, 2011.

[105] F. H. Maniyar, T. Sprenger, T. Monteith, C. Schankin, and P. J. Goadsby, "Brain activations in the premonitory phase of nitroglycerin-triggered migraine attacks," *Brain,* vol. 137, pp. 232-241, 2014.

[106] H. Bolay, "The first phase of a migraine attack resides in the cortex," *Journal of neural transmission,* vol. 119, pp. 569-574, 2012.

[107] C.-T. Lin, L.-D. Liao, Y.-H. Liu, I.-J. Wang, B.-S. Lin, and J.-Y. Chang, "Novel dry polymer foam electrodes for long-term EEG measurement," *Biomedical Engineering, IEEE Transactions on,* vol. 58, pp. 1200-1207, 2011.

[108] B. C.-T. Lin, L.-W. Ko, J.-C. Chiou, J.-R. Duann, R.-S. Huang, S.-F. Liang*, et al.*, "Noninvasive neural prostheses using mobile and wireless EEG," *Proceedings of the IEEE,* vol. 96, pp. 1167-1183, 2008.

[109] L.-D. Liao, C.-T. Lin, K. McDowell, A. E. Wickenden, K. Gramann, T.-P. Jung*, et al.*, "Biosensor technologies for augmented brain–computer interfaces in the next decades," *Proceedings of the IEEE,* vol. 100, pp. 1553-1566, 2012.

Appendix

3-1

The white noise is usually used to analyse the performance of the entropy algorithms. When superimposed with trends, the simulated signal (white noise) can be applied to evaluate the effectiveness of the ApEn, SampEn, FuzzyEn and Inherent FuzzyEn algorithms. The added superimpose periodic trends $\{T_1\}$ and $\{T_2\}$ were showed as follows:

$$\{T_1\} = 1.2\sin\left(\frac{2\pi i}{720}\right) + 1.5\sin\left(\frac{2\pi i}{360}\right)$$

$$\{T_2\} = 0.8\sin\left(\frac{2\pi i}{240}\right)$$

Where N = 10,000 denotes the length of one signal, $i = 1,2,\ldots,N$.

As listed in the following Table, compared to the entropy value in the simulated signal, the entropy value in the simulated signal with trends has the smallest entropy error (0.053 and 0.033) by the Inherent FuzzyEn evaluation.

Entropy algorithm	**White noise (simulated signal)**	**White noise + Periodic trends $\{T_1\}$**	**White noise + Periodic trends $\{T_2\}$**	**Entropy error $\{T_1\}$**	**Entropy error $\{T_2\}$**
ApEn	2.435	2.067	2.134	0.368	0.301
SampEn	2.012	1.812	1.726	0.200	0.286
FuzzyEn	1.827	1.617	1.648	0.210	0.179
Inherent FuzzyEn	1.534	1.481	1.501	**0.053**	**0.033**

4-1

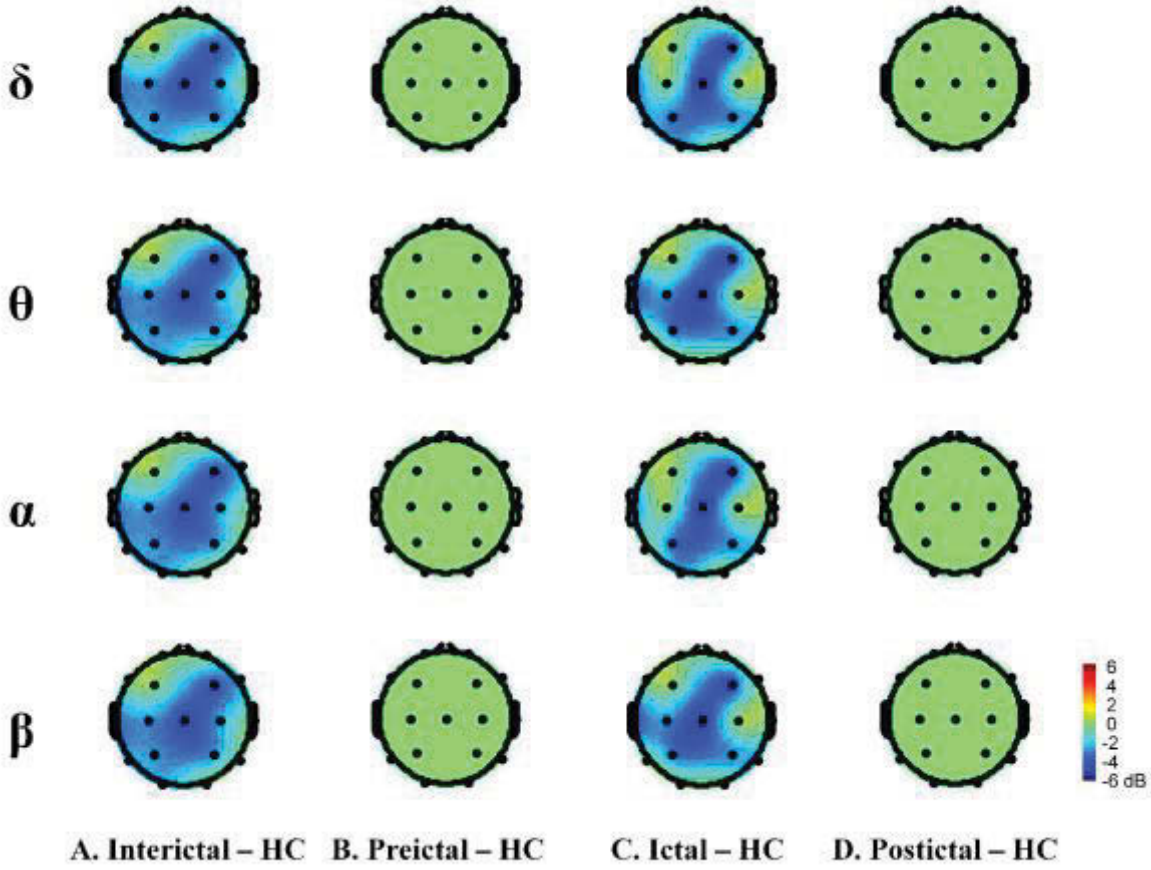

Appendix Figure 3-1. Topographical comparison of significant EEG power differences ($p < .05$) between migraine patients in different migraine phases and HCs during eyes-closed recording. Colour intensity indicates the magnitude of the power difference (red for increased power, blue for decreased power) in each channel.

4-2

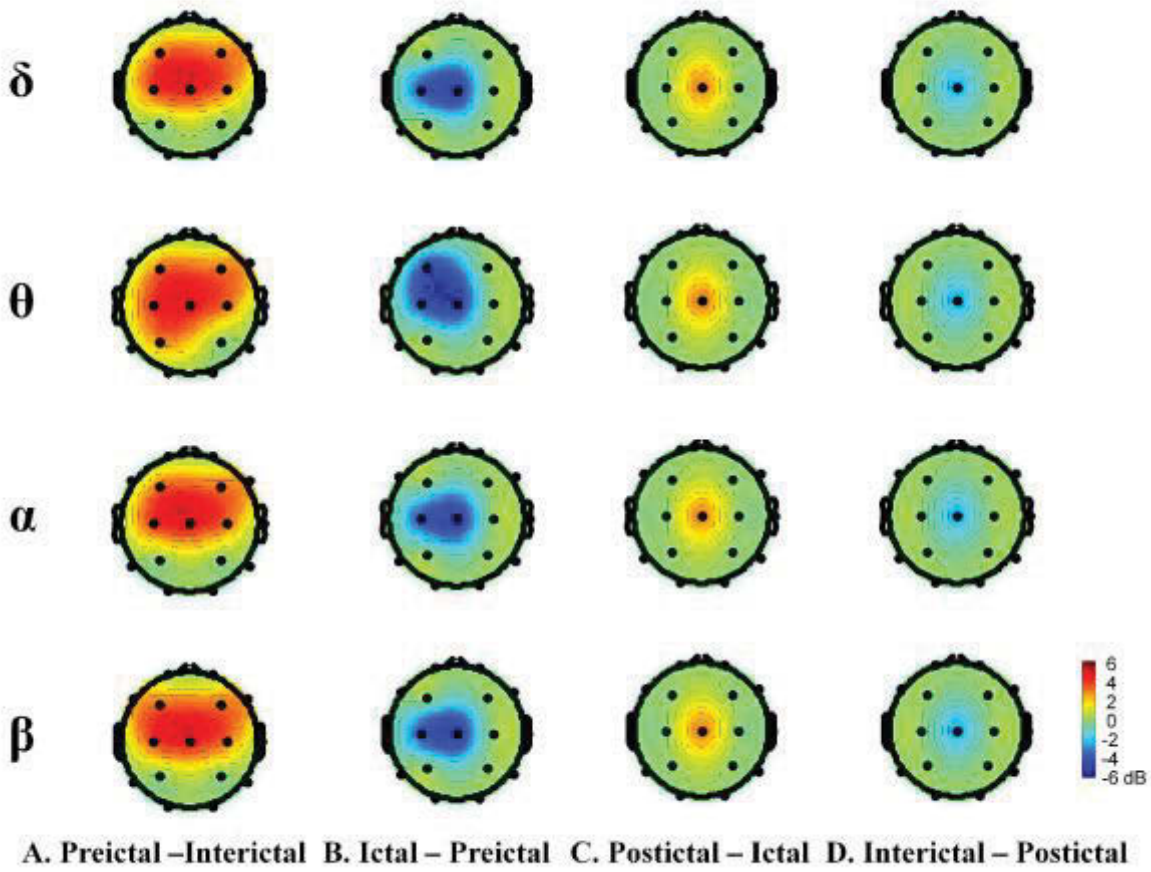

Appendix Figure 3-2. Topographical comparisons of significant EEG power differences ($p < .05$) between patients in each of the four migraine phases during eyes-closed recording. Colour intensity indicates the magnitude of the power difference (red for increased power, blue for decreased power) in each channel.

4-3

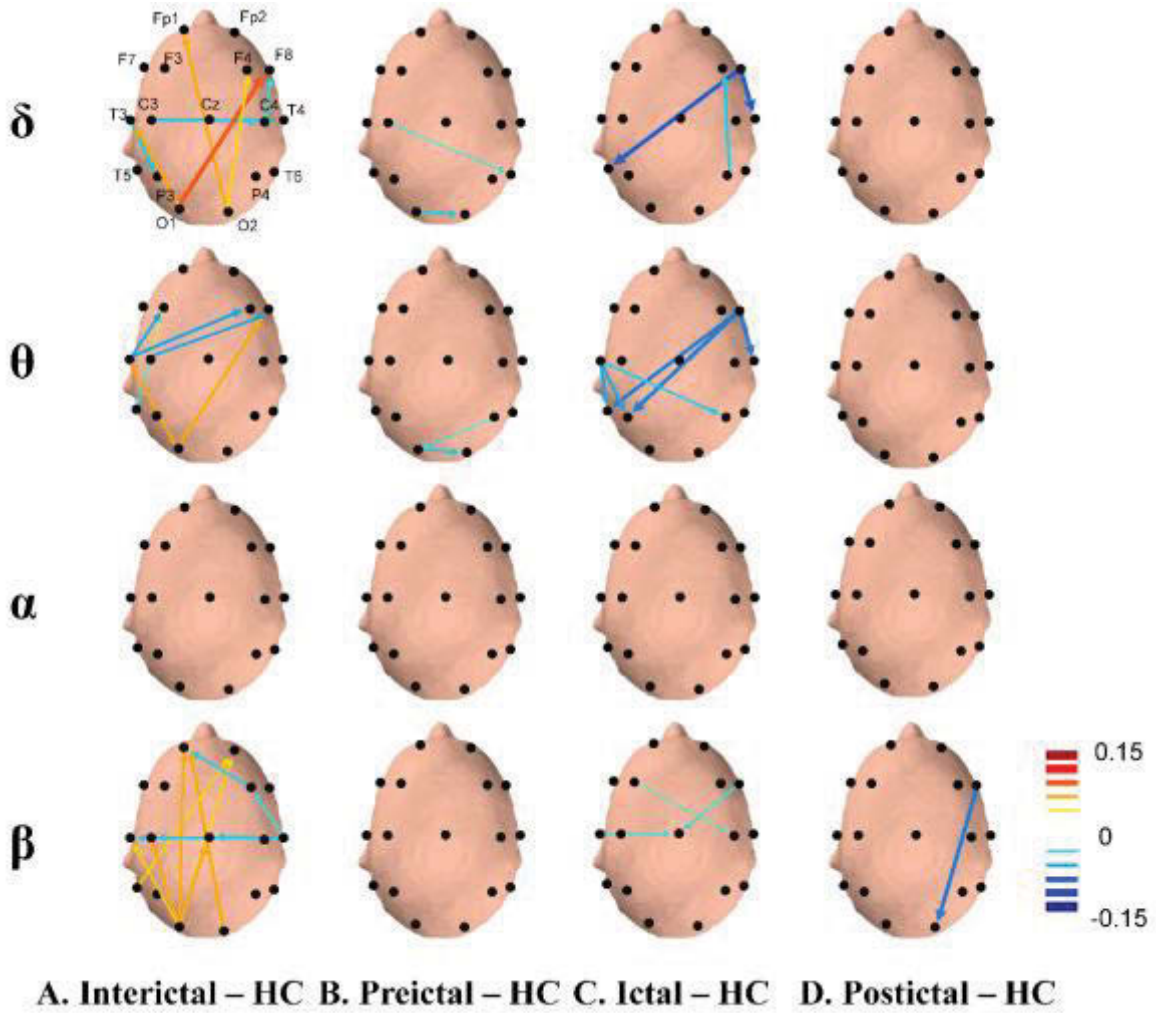

Appendix Figure 3-3. Topographical comparisons of significant EEG coherence differences ($p < .05$) between patients in different migraine phases and HCs during eyes-closed recording. Line sizes and colours reflect the magnitude of the difference in coherence intensity between electrode pairs, with red indicating positive differences (more coherent) and blue indicating negative differences (more independent). The directions of arrow represent the direct paths of inter-channel coupling.

4-4

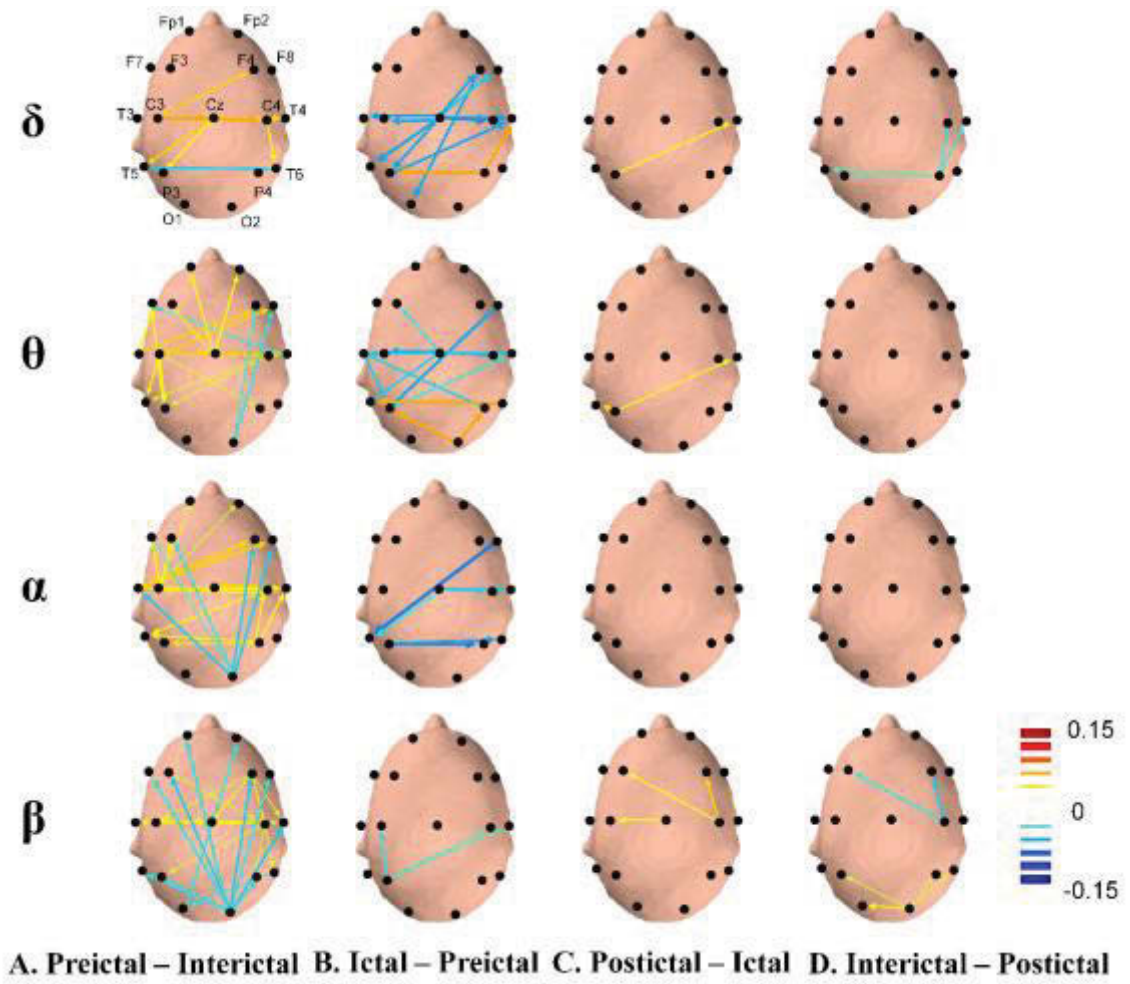

Appendix Figure 3-4. Topographical comparisons of significant EEG coherence differences ($p < .05$) between migraine patients in each of the four phases of the migraine cycle during eyes-closed recording. Line sizes and colours reflect the magnitude of the difference in coherence intensity between electrode pairs, with red indicating positive differences (more coherent) and blue indicating negative differences (more independent). The directions of arrow represent the direct paths of inter-channel coupling.

Appendix Table 5-1 Demographics, Headache Profile and Psychological Characteristics

Characteristics	HCs (N=40)	Patients Groups			*P*
		72-hours (N=40)	48-hours (N=30)	36-hours (N=25)	
Demographics					
Gender, F:M	32:8	30:10	24:6	19:6	0.935
Age, y	36.1 ± 9.8	38.1 ± 8.2	38.8 ± 8.0	38.0 ± 7.2	0.572
Headache Profile					
Disease duration, y	n/a	18.3 ± 7.8	18.7 ± 7.4	19.5 ± 7.7	0.824
Frequency, d/mo	n/a	4.7 ± 2.3	4.8 ± 2.4	4.8 ± 2.5	0.973
Onset Age	n/a	19.6 ± 8.9	19.8 ± 9.4	18.0 ± 7.4	0.726
MIDAS score[a]	n/a	13.4 ± 12.3	16.1 ± 13.0	16.6 ± 11.3	0.758
Psychometric Scores					
BDI	5.5 ± 5.9	9.5 ± 6.3*	9.7 ± 6.3*	9.2 ± 5.7*	**0.013**
HADS-A	5.3 ± 3.9	6.8 ± 4.0	7.1 ± 4.0	7.1 ± 3.6	0.202
HADS-D	3.2 ± 2.9	4.9 ± 3.6*	5.2 ± 3.8*	5.2 ± 3.7*	**0.049**

[a]0–270 range;

Abbreviations: HCs, healthy controls; F:M, ratio of females to males; MIDAS, Migraine Disability Assessment Scale; BDI, Beck Depression Inventory; HADS-A, Hospital Anxiety Depression Scale, Anxiety; HADS-D, Hospital Anxiety Depression Scale, Depression;

Of note, three or four group differences in clinical profiles were analyzed by the chi-square test for categorical variables, and one-way ANOVA for continuous variables.

*: After utilizing one-way ANOVA, the Turkey's post hoc test was performed for pair comparison (HCs vs. patients in different groups): $p < 0.05$.

Appendix: Experimental Protocol

1. Leverage wearable technology to aggregate biometric, psychological and ambient data and develop data streaming infrastructure to facilitate data recording

Rationale

Measuring daily changes in pain and stress intensity in patients with migraine disorders can facilitate the patient-doctor communication and pain management. Recently, advances in wearable technology offer promising and practical access to physiological and ambient data we are experiencing. Several wristbands featuring the state-of-the-art miniature sensors are able to aggregate multiple physiological data such as electroencephalography (EEG), electrocardiography (ECG), electrodermal activity (EDA)/skin conductance response (SCR), and actigraphy (ACT) at the same time, and meanwhile, record ambient temperature and pressure. These data with rich information have been demonstrated to have such potentials, and correlated with the different migraine phases.

Methods

a. Apply daily and regular sampling to collect data from patients before & after the treatment

These physiological recording devices have the advantage of greater availability and convenience to access, and thus make repeated or continuous measurements feasible. This project will try to record these multimodal physiological signals, and correlate them with subjective pain discomfort. At least 5 times sampling experiments lasting 6 months will be conducted to record patients' pain intensity, physiological signals, and environmental data in different migraine phases. The collected data will facilitate to calculate the average intensity of headache over the past months and on the study day. Additionally, EEG and ECG will be studied in clinical settings during a regular out-patient clinic visit (5 times).

b. Develop data streaming technology: from laboratory/clinical settings to at-home analysis

We plan to develop wearable stream mining infrastructure for at-home analysis. The data stream mainly composes of physiological and environmental data collected from patients on a daily basis. A mobile/PC APP will be developed to connect wearable devices to acquisition system, filter and receive data in a custom format, get real-time signals, as well as upload the data recorded to a cloud storage.

2. Analyze longitudinal data to identify key factors in triggering headache and correlate the objective parameters of migraine with subjective experience of migraine cycle.

Rationale

Since the cortical activiation can be significantly changed before and after migraine attacks, predicting the onset of intense migraine is desirable. Hence, investigating the fundamental patterns that can be used to distinguish the brain activity is critical. Based on the results of the Pilot Project, as compared to HC, patients with migraine had significant lower short- and long-term EEG and HRV, which varied with the upcoming headache. These promising findings, along with the subsequent implementation of advanced analyses and computation, will help to elucidate the significance of electrophysiological signatures in clinically setting.

Methods

a. Apply both time and frequency domain analysis to EEG and ECG to extract informative features

The multiscale entropy analysis, Granger causality analysis, and power spectral analysis will be used to explore EEG signatures of migriane. Regarding ECG, both linear and nonlinear dynamics will be investigated. The correlation between the EEG, ECG and other physiological signatures of migraine will be examined. The relationship between EEG and other physiological signatures and MEG/fMRI signatures of migraine will be investigated. The time-frequency cortical dynamics measured by MEG and EEG will be compared, so that we can extend the findings from MEG into wider applications.

b. Apply longitudinal data analysis to track changes in physiological states

To examine the correlation between different parameters (eg. subjective pain level and objective physiological data), a multilevel modeling approach using two-level hierarchical linear model (HLM) will be carried out. Level 1 measures the within-subject variability of the data recorded repeatedly over extended time periods, and Level 2 measures the variability across subjects over time.

Publication

Journal:

1. **Z. Cao** and C.-T. Lin, "Inherent Fuzzy Entropy for the Improvement of EEG Complexity Evaluation", *IEEE Transitions on Fuzzy Systems*. (in press) [Q1; IF 7.6, ranked in the top 1% of journals in Computer Science and Artificial Intelligence]

2. **Z. Cao**, C.T. Lin, C.H. Chuang, K.L. Lai, Albert C. Yang, J.L. Fuh and S.J. Wang, "Resting-state EEG Power and Coherence Vary between Migraine Phases", *The Journal of Headache and Pain*, 2016. [Q1; IF 3.5, ranked in the top 23.8% of journals in Clinical Neurology]

3. **Z. Cao**, K.L. Lai, C.-T. Lin, C.-H. Chuang and S.J. Wang "Exploring Resting-State EEG Complexity before Migraine Attacks ", *Cephalalgia* (in press) [Q1; IF 3.6, ranked in the top 20.1% of journals in Clinical Neurology]

4. C.T. Lin, C.H. Chuang, **Z. Cao**, A.K. Singh, C.S. Hung, Y.H. Yu, M. Nascimben, Y.T. Liu, J.T King, T.P Su, and S.J Wang, "Forehead EEG in Support of Future Feasible Personal Healthcare Solutions at Home", *IEEE Access*. (in press) [Q1; IF 3.3, ranked in the top 18.4% of journals in Computer Science and Information Systems]

5. W. Ding, C.T Lin, M. Prasad, **Z. Cao**, and J. Wang, "A Layered-Coevolution-Based Attribute-Boosted Reduction Using Adaptive Quantum Behavior PSO and Its Consistent Segmentation for Neonates Brain Tissue", *IEEE Transactions on Fuzzy Systems*. (in press) [Q1; IF 7.6, ranked in the top 1% of journals in Computer Science and Artificial Intelligence]

6. C.T. Lin, Y.T. Liu, S.L. Wu, **Z. Cao**, Y.K. Wang, C.S. Huang, J.T. King, S.A. Chen, S.W. Lu, and C.H. Chuang, "EEG-Based Brain-Computer Interfaces: A Novel Neurotechnology and Computational Intelligence Method", *IEEE Systems, Man, and Cybernetics Magazine*, 16-26, 2017.

Conference:

1. **Z. Cao**, L.W. Ko, K.L. Lai, S.B. Huang, S.J. Wang, and C.T. Lin, "Classification of Migraine Stages based on Resting-State EEG Power", *International Joint Conference on Neural Networks (IJCNN)*, Killarney, Ireland, 2015.

2. **Z. Cao** and C.-T. Lin "Estimation of SSVEP-based EEG Complexity using Inherent Fuzzy Entropy", *IEEE International Conference on Fuzzy Systems*, Naples, Italy, 2017.